Annexin A2
in membrane microdomain organisation
and influenza A infection

Sonja Schäfers

2010

Biologie

Annexin A2
in membrane microdomain organisation
and influenza A infection

Inaugural-Dissertation
zur Erlangung des Doktorgrades
der Naturwissenschaften im Fachbereich Biologie
der Mathematisch-Naturwissenschaftlichen Fakultät
der Westfälischen Wilhelms-Universität Münster

vorgelegt von

Sonja Schäfers

aus Rheine

- 2010 -

Dekan:	Prof. Dr. Christian Klämbt
Erster Gutachter:	Prof. Dr. Volker Gerke
Zweiter Gutachter:	Prof. Dr. Stephan Ludwig
Tag der mündlichen Prüfung:	17. März 2010
Tag der Promotion:	23. April 2010

Table of Contents

1 Abstract

Influenza A virus, the causative agent of the flu, is a widely spread pathogen in humans and some animal species. Membrane rafts have been shown to be the cellular budding sites of this enveloped virus. Rafts are dynamic sphingolipid and cholesterol-rich membrane microdomains that serve as platforms for multiple processes like membrane sorting, signal transduction, cell adhesion and pathogen entry by the recruitment and concentration of effectors. Annexin A2, a Ca^{2+}-regulated membrane- and actin-binding protein of the annexin family, is one of the few known structural components on the cytosolic site of such microdomains. It has been implicated in regulating the aggregation and stabilisation of rafts. Furthermore, it is involved in endo- and exocytotic processes and membrane-cytoskeleton organisation. Since all of these events play a role in influenza A virus replication the involvement of annexin A2 in this process was investigated.

siRNA mediated down-regulation of annexin A2 in A549 or HeLa cells revealed that influenza A virus replication efficiency was not dependent on cytosolic annexin A2 protein levels. Further, in MDCK the aggregation of annexin A2 by a dominant-negative construct does not influence influenza A replication and in an endothelial cell line from the annexin A2 knockout mouse this virus efficiently replicates.

Next, the surface localisation of the raft-associated influenza protein hemagglutinin was analysed and found to be not affected by annexin A2 depletion in non-polarised A549. Furthermore, real-time PCR analysis did not reveal a difference in the mRNA level of annexin A2 between influenza infected in comparison to uninfected A549, HeLa and HepG2 cells.

However, although no colocalisation of annexin A2 with virus particles in influenza A infected A549 could be detected, annexin A2 was found to be associated with purified influenza A virus particles. Whether this incorporation is of critical importance for influenza A infectivity remains to be determined.

Collectively, the experimental data obtained in this thesis implicate that annexin A2 is not actively involved in influenza A replication.

Influenza A virus induces apoptosis in infected cells. The role of annexin A2 in this process was analysed in the second part of this thesis. Cells with reduced annexin A2 were found to be more susceptible to influenza A-induced apoptosis, as revealed by apoptotic morphological changes and enhanced PARP cleavage. An increased sensitivity towards apoptosis upon annexin A2 depletion was also observed when apoptosis was induced with other agents, like staurosporine and TNFα, in A549 and HeLa cells. Not only PARP is cleaved to a greater extent but also the activation of the initiator caspases 8 and 9 is enhanced in annexin A2 depleted HeLa. However, the mechanism of action of annexin A2 in the apoptotic pathways could not be resolved.

The lateral organisation of cellular membranes in rafts does not only play a role in influenza A infection but also in various other host-pathogen interactions. Since annexin A2 is involved in the aggregation and stabilisation of membrane rafts the binding of annexin A2 to these membrane microdomains was studied in more detail in the third part of this thesis. The aim was to elucidate which functions of this protein are involved in raft association and thereby possibly are of importance for the organisation and function of membrane rafts in living cells.

Annexin A2 not only exists as a monomer but also in a heterotetrameric form, where two annexin A2 molecules are bridged via a dimer of the S100 protein p11. Thus, the impact of this p11-binding for raft association was investigated. Furthermore, the effects of phosphorylation on Tyr23, $PI(4,5)P_2$-binding and Ca^{2+}-binding of annexin A2 were analysed by employing the respective annexin A2 mutants.

Raft association of these annexin A2 derivatives was revealed by binding to detergent resistant membranes, by segregation with raft lipids in plasma membrane spheres and by colocalisation with lipid ordered domains identified by Laurdan 2-photon microscopy. While the latter techniques did not reveal any conclusive results yet, the analysis of plasma membrane spheres indicates a raft association of all annexin A2 derivatives at elevated Ca^{2+} concentrations. The detergent extraction showed that only p11-binding deficient monomeric mutants of annexin A2 show reduced binding to rafts. All other mutations had no effect. From these data it could be concluded that binding to p11 is of regulating importance for the association of annexin A2 with membrane rafts *in vivo*.

2 Introduction

2.1 The influenza A virus

2.1.1 Pathogen-host interactions

Infectious diseases provoke 25 % of deaths worldwide and therewith are the second most common cause of death (World Health Organization, 1999). These diseases result from the presence of pathogenic microbial agents in the host organism. Infection with some of these agents might also result in other secondary causes of death like cardiovascular diseases or cancer.

The interactions between a pathogen and its host are complex and dynamic. All pathogenic organisms (bacteria, viruses, fungi and parasites) initially contact surfaces of cellular barriers. This is followed by the induction of specific signal transduction pathways resulting in host responses. Fundamental understanding of the molecular mechanisms underlying these interactions can help eradicate life threatening diseases and improve life quality and expectancy.

2.1.2 General properties of the influenza A virus

Influenza A viruses (IAV) are important worldwide pathogens for humans and different animal species. They are the infectious agent of the flu and still cause thousands of deaths and an enormous economic loss every year.

IAV belong to the family orthomyxoviridae which are characterised by a segmented linear negative-sense single-stranded RNA genome. These viruses can further be classified based on the antigenic properties of the surface glycoproteins hemagglutinin (HA) and neuraminidase (NA). Sixteen HA subtypes and nine NA subtypes of IAV have been identified so far.

This virus possesses eight genome segments encoding for eleven proteins. These proteins include the three components of the viral RNA-dependent RNA polymerase complex (PB2, PB1 and PA), two surface glycoproteins (HA and NA), two matrix proteins (M1 and M2), one nucleoprotein (NP) and a nuclear export protein (NEP). The PB1 genome segment of many but not all IAV strains also contains a +1 reading frame encoding the PB1-F2 protein (Chen et al., 2001). This protein as well as the non-structural protein 1 (NS1) are not incorporated into the virion. Therefore, the virion consists of nine structural proteins, eight genome segments and an envelope which originates from the host cell. A schematic presentation of IAV structure is depicted in Figure 2-1. For a detailed review see Cheung and Poon, 2007.

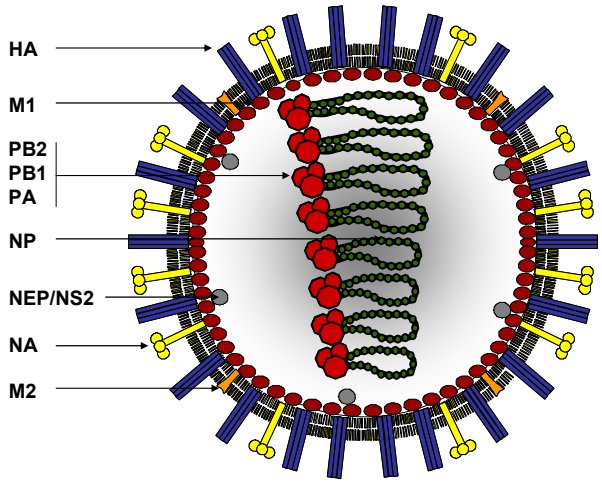

Figure 2-1: Structure of the influenza A virion
The eight viral RNA segments are surrounded by a membrane which originates from the host cell. The localisation of the different viral structural proteins within the virus particle is indicated. NP (green) binds to the vRNA segments to form ribonucleoprotein (RNP) complexes. PB1, PB2 and PA (red) are also associated with the RNPs. The viral glycoproteins HA (blue) and NA (yellow) are exposed on the virus surface. M1 (dark red) forms the inner layer of the virion whereas M2 (orange), which is a pH dependent ion channel, is a transmembrane protein. NEP (grey) is also incorporated into the virus particle. From Ludwig et al., 2003.

2.1.3 The influenza A replication cycle

Viruses need a cell of their host to propagate. A schematic presentation of the IAV replication cycle is depicted in Figure 2-2. As a first step HA of influenza A binds to sialic-acid containing receptors on the apical side of polarised epithelial cells (Dimmock, 1982). Subsequently the virus enters the cell via multiple endocytotic pathways (Lakadamyali et al., 2004) and reaches endosomal compartments. Acidification of the endosome environment induces conformational changes in the HA, mediating fusion between the viral envelope and the endosomal membrane. For this event as well as for the receptor binding a cleaved form of HA (into HA1 and HA2) is essential. This proteolytic activation is mediated by proteases of the host and is a prime determinant of influenza pathogenicity. HA of low pathogenic avian influenza strains have a single arginine at the cleavage site and are activated by trypsin-like proteases restricted to enteric or respiratory epithelia. In contrast the HA of highly pathogenic avian influenza strains posses a series of basic amino acids at the cleavage site, which are cleaved by ubiquitous proteases such as furin (Horimoto and Kawaoka, 2005).

After the fusion event the viral RNA is released into the cytoplasm and transported into the nucleus where amplification of the genome and transcription take place. Viral mRNA is translated in the cytoplasm. At late time points of the viral infection cycle the viral genome is transported out of the nucleus in the form of RNP complexes. The influenza surface glycoproteins HA and NA are post-translationally modified in the Golgi network and transported to the cell surface for integration into the cellular membrane. In this membrane these proteins preferentially localise to membrane microdomains called rafts. The local concentration of the cytoplasmic tails of HA and NA leads to the recruitment of the influenza matrix protein M1 and RNPs (Suomalainen, 2002). Hence, the virus assembles and buds from the cell surface at sites of membrane rafts. The replication cycle is completed within 6 - 16 h, depending on the particular virus strain and the cell type.

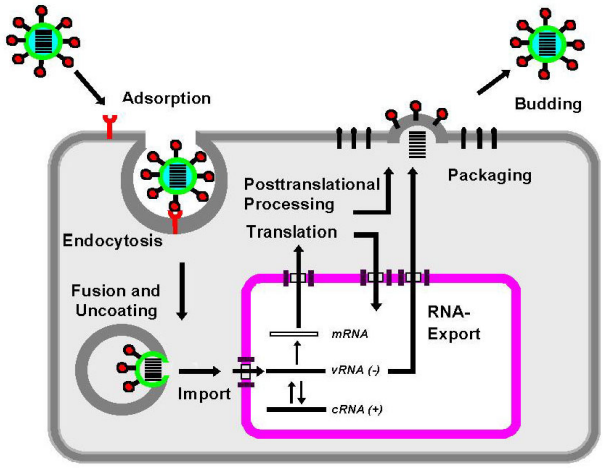

Figure 2-2: The lifecycle of influenza A
IAV binds to receptors on the cell surface and is endocytosed. The viral and endosomal membrane fuse thereby releasing the viral genome into the cytoplasm. The genome is transported into the nucleus where it is transcribed and replicated. Viral proteins are synthesised in the cytoplasm. The vRNAs as well as the viral proteins assemble at the plasma membrane from where new virions finally bud. For a detailed explanation see text. From Ludwig et al., 2003.

Taking into account that the genome of influenza A is relatively small - coding only for up to eleven viral proteins - it is not surprising that a whole range of cellular proteins and cellular processes are employed and manipulated by the virus to efficiently replicate. This includes numerous interactions of viral proteins with cellular proteins. The virus thereby manipulates e.g. the cellular protein expression machinery, intracellular transport processes or the host cell defence (Ludwig et al., 1999). The role of cellular proteins involved in IAV replication is only beginning to emerge and an understanding of these processes could help in developing strategies for fighting the infectious agent of the flu.

2.1.4 Influenza A and apoptosis

Influenza virus causes apoptosis of the infected cells at late stages of infection (Hinshaw et al., 1994). Apoptosis is a morphologically and biochemically defined form of cell death (Kerr et al., 1972) and it results in changes like chromatin condensation, DNA fragmentation, cell shrinkage, externalisation of phosphatidylserine, membrane blebbing or budding and formation of apoptotic bodies (Earnshaw, 1995; Martin et al., 1995). The most important cellular proteins for the onset of apoptosis belong to a family of cysteine proteases called caspases that exist as inactive zymogens in normal cells (Salvesen and Dixit, 1997). Apoptosis relies on a complex interplay of a whole range of proteins and can be induced in response to various signals from inside and outside of cells.

Internal stimuli frequently have their origin within the nucleus. E.g. DNA damage induced by irradiation, drugs or other sort of stress in most cases results in the activation of the p53 transcription factor which promotes expression of proapoptotic Bcl-2 members (Chipuk et al., 2004) and suppresses antiapoptotic Bcl-2 and Bcl-XL (Wu et al., 2001). Proapoptotic members of the Bcl-2 family regulate the exit of cytochrome c and other proapoptotic molecules from the mitochondria into the cytosol (Green and Reed, 1998). In the cytosol cytochrome c forms a multimeric complex with the adaptor protein Apaf-1, procaspase-9 and dATP, the apoptosome (Adams and Cory, 2002). This complex formation results in the activation of caspase-9 which is an initiator caspase and thus is able

to trigger the caspase cascade including the effector caspases-3, -6 and -7. Cleavage of caspase substrates eventually leads to the characteristic morphological and biochemical features of apoptosis.
Extracellular apoptosis-inducing signals involve a whole range of soluble and membrane bound molecules, especially those of the family of tumour necrosis factors (TNF) (Locksley et al., 2001). When a death ligand, such as the Fas ligand (FasL), interacts with its cell surface receptor (i.e., Fas, a member of the TNF receptor family) a death-inducing signal complex (DISC) is formed (Nagata, 1999). The initiator caspase-8 is activated which results in the activation of a caspase cascade and subsequently in the induction of apoptosis.
Activated caspase-8 also cleaves Bid, which translocates from the cytosol into the mitochondrial membrane, where it stimulates cytochrome c release and subsequent caspase-9 activation. Thus, the extrinsic and intrinsic apoptotic pathways converge through Bid (Li et al., 1998).

There are also negative regulators of apoptosis. Members of the IAP (inhibitor of apoptosis) family directly inhibit caspases. IAP expression can be up-regulated in response to survival signals (Budihardjo et al., 1999). Of central importance are also the antiapoptotic Bcl-2 family members such as Bcl-2 and Bcl-XL which counteract the action of proapoptotic Bcl-2 proteins and thus can inhibit mitochondrial proapoptotic events.

An overview of the major apoptotic pathways is given in Figure 2-3. Aside from these pathways also caspase-independent apoptotic pathways have been described. E.g. apoptosis inducing factor (AIF) is a caspase-independent mitochondrial death effector (Daugas et al., 2000). Furthermore, other organelles besides mitochondria and the nucleus, such as the ER and lysosomes, also have been implicated in apoptotic signalling pathways (Ivanova et al., 2008; Mund et al., 2003), which stresses the fact that the regulation of apoptosis is a fine-tuned mechanism involving presumably hundreds of proteins.

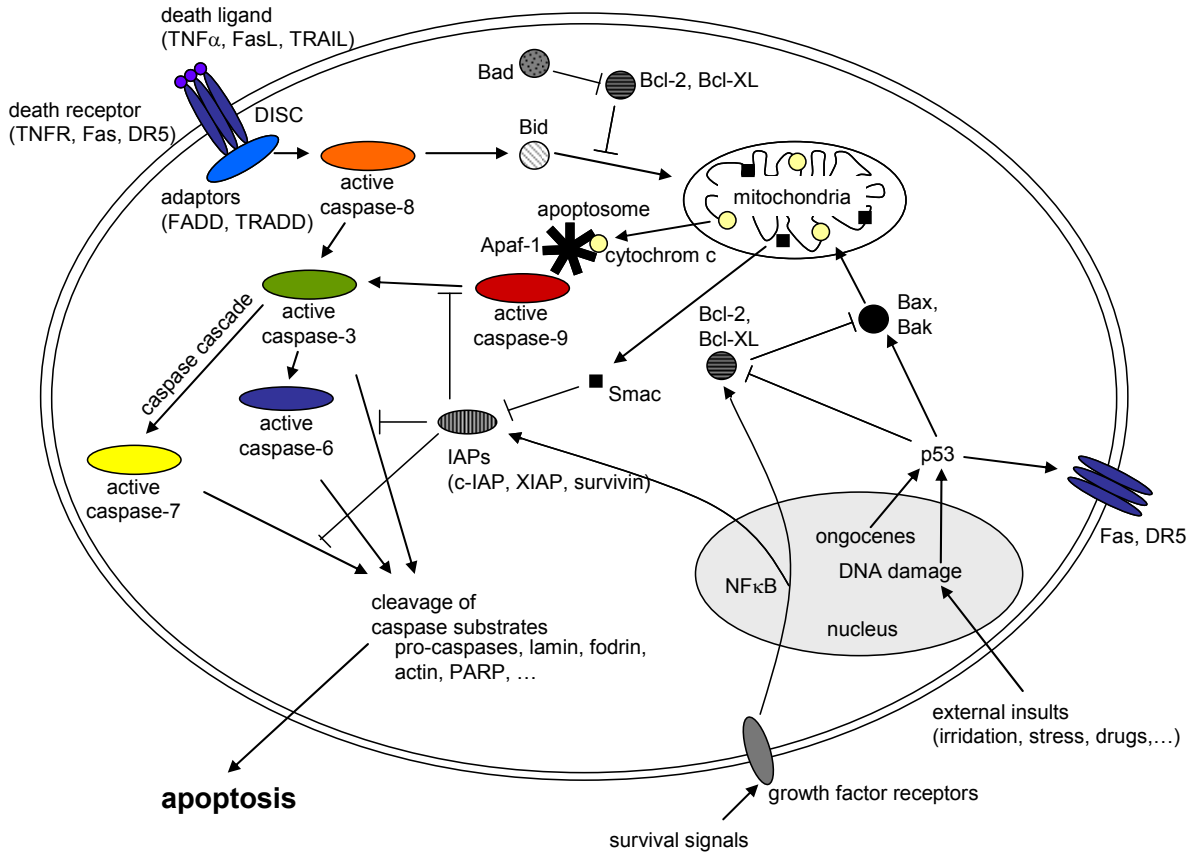

Figure 2-3: Schematic representation of the major apoptotic signalling pathways
Apoptosis-inducing mechanisms can be classified into two major groups: an extrinsic receptor mediated pathway and an intrinsic mitochondria mediated pathway. These pathways are explained in detail in the text. From Gewies, 2003.

Apoptosis is thought to play an important role in the pathogenesis of many infectious diseases including those caused by viruses (Collins, 1995). The mechanisms involved in the process of influenza-induced apoptosis are only partly understood. Cellular as well as viral factors are of importance for this process.

One influenza protein that has been shown to be involved in apoptosis induction is the NA, which activates latent transforming growth factor β. This protein is a multifunctional growth-regulatory protein that induces apoptosis in many cell types (Schultz-Cherry and Hinshaw, 1996). There is evidence that the non-structural viral protein NS1 is able to initiate apoptosis when it is expressed in the cells alone (Schultz-Cherry et al., 2001) but on the other hand an interferon-dependent antiapoptotic potential of this protein has also been described (Zhirnov et al., 2002). Furthermore, the PB1-F2 protein has been shown to induce cell death by influencing the mitochondrial permeability during apoptosis (Chen et al., 2001; Zhirnov et al., 2002).

Induction of apoptosis at first seems to be disadvantageous for virus replication because it is a host mechanism to limit virus production. But it has been shown that the activation of caspase-3 is important in replication and propagation of IAV (Wurzer et al., 2003) and expression of antiapoptotic Bcl-2 reduces the level of infectious virus production (Olsen et al., 1996). Furthermore, the induction of apoptosis by influenza virus has been shown to limit the release of proinflammatory cytokines (Brydon et al., 2003).

2.2 Annexin A2

2.2.1 The annexin protein family

Annexins are a family of Ca^{2+}-regulated phospholipid-binding proteins. The name annexin originates form the Greek word *annex*, meaning “to bring/hold together”. This reflects the principle property of nearly all annexins, i.e. the binding to and possibly holding together of certain biological structures, in particular membranes (Gerke and Moss, 2002).

Annexins were identified in all eukaryotic phyla (Morgan et al., 2004). In vertebrates there are twelve annexin subfamilies (annexin A1 - annexin A11 and annexin A13). Annexins outside vertebrates are classified into families B (in invertebrates), C (in fungi and some groups of unicellular eukaryotes), D (in plants) and E (in protists). This protein family is absent from prokaryotes (Moss and Morgan, 2004).

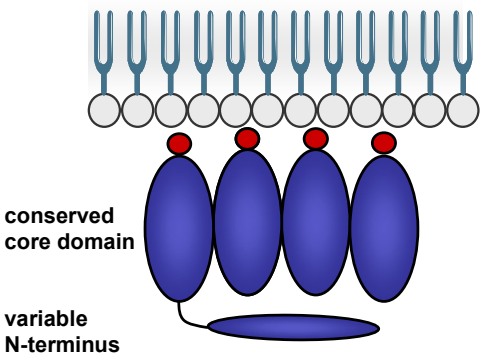

Figure 2-4: Schematic presentation of an annexin associated with a membrane
This drawing shows an annexin that is peripherally attached to a membrane surface through bound Ca^{2+} ions (red). Annexins possess a conserved core domain which consists of four annexin repeats. The variable N-terminal domain harbours sites for posttranslational modifications and protein-protein interactions.

All annexin family members share a homologous molecular structure which is depicted in Figure 2-4. They consist of two domains: a highly conserved protein core and a regulatory N-terminal domain. The core domain is composed of four homologous segments (exception: annexin A6 has 8 segments), the so-called annexin repeats. Each repeat spans 70 - 80 amino acids and is made up of five α-helices which are connected by turns or short loops. The annexin core domain forms a slightly curved disc. The convex side of this disc faces the membrane when an annexin is associated peripherally with phospholipids. This side also contains characteristic types of Ca^{2+}-binding sites, the so-called type II and type III sites differing in their architecture and Ca^{2+} affinity (Jost et al., 1994). Although the general folding of the annexin core domain is highly similar for the members analysed so far, annexins show differences in the number and location of the individual Ca^{2+}-binding sites. This might explain the differences in Ca^{2+} sensitivity and phospholipid specificity observed within this protein family.

The N-terminal annexin domain is diverse in sequence and length. It mediates the interaction with specific target proteins and regulates the annexin-membrane association (for a review, see Gerke and Moss, 2002). The N-terminus is located on the concave side of the annexin core opposite the membrane-binding surface and forms a separate entity. It harbours sites for posttranslational modifications.

Annexins are able to interact with a whole range of proteins. Ligand-binding sites are mainly localised in the N-terminus which in some cases also harbours a binding site for S100 proteins. S100 proteins are members of the EF-hand superfamily of Ca^{2+}-binding proteins. They have a size of about 10 - 14 kDa and transmit Ca^{2+}-dependent cell-regulatory signals. For a review on S100 proteins see Donato, 1999 or Schafer and Heizmann, 1996. S100 proteins appear intracellularly as dimers. Upon Ca^{2+} binding, S100 dimers are able to crossbridge two homologous or heterologous target proteins (Donato, 2001). Therefore, some S100 proteins are also able to form symmetric heterotetramers with annexins.
In addition to the interaction partners of the S100 family some annexins also were shown to bind cytoskeletal proteins like F-actin and spectrin (Hayes et al., 2004). Furthermore, binding to other ligands, ranging from proteins to RNA, has been described (for a review see Gerke and Moss, 2002; Raynal and Pollard, 1994).

Annexins are generally cytosolic proteins, but several members of this family are also stably or transiently associated with the cytoskeleton or cellular membranes. The expression level and tissue distribution of annexins varies extremely, probably reflecting the importance of gene regulation in the context of cell-type specific functions. Some annexins, such as annexin A1, A2, A4, A5, A6, A7 and A11 show a rather ubiquitous expression (Gerke and Moss, 1997), whereas e.g. annexin A3 is mainly expressed in neutrophils (Le Cabec and Maridonneau-Parini, 1994).
Some annexins have been found in the nucleus. E.g. In this compartment annexin A11 seems to be involved in the progression of cytokinesis (Tomas et al., 2004). Furthermore, annexin A2 has been shown to bind RNA {{261 Vedeler,A. 2000}}.
Even though this protein family lacks an export signal several members were identified extracellularly. These include annexin A1, an important endogenous modulator of inflammation (Perretti and Gavins, 2003), annexin A5 that has been suggested to play an antithrombotic role (Raynal and Pollard, 1994) and annexin A2 which is found on the surface of vascular endothelial cells where it functions in the regulation of blood clotting (Brownstein et al., 2001).

Some of the posttranslational modifications of annexins implicate a role of this protein family in signal transduction. Annexin A1 is phosphorylated by the epidermal growth factor (EGF) receptor tyrosine kinase (Fava and Cohen, 1984; Pepinsky and Sinclair, 1986) and annexin A2 was identified as a substrate for protein tyrosine kinase of Rous sarcoma virus pp60src (Erikson and Erikson, 1980; Radke et al., 1980). Furthermore, almost all annexins are both *in vitro* and *in vivo* substrates for protein kinase C (PKC) (Dubois et al., 1996). Since protein kinases play an important role in cancer development and progression an involvement of annexins in cancer related processes has been suggested (Bastian, 1997; Hayes et al., 2004).

The physiological functions of annexins are only beginning to emerge since they are very diverse (Rescher and Gerke, 2004). A central feature that can be related to a range of cellular functions is the regulated binding to negatively charged phospholipids. The ability to bind to lipids argues for a role of annexins in membrane transport processes. Annexins have been implicated to be involved in diverse endocytotic processes, as reviewed in Futter and White, 2007. And it has also been shown that they are of importance for exocytotic processes (Creutz, 1992).

2.2.2 Specific properties and functions of annexin A2

2.2.2.1 The annexin A2/p11 complex

Annexin A2 is one of the best characterised members of the annexin protein family. It is able to bind the S100 protein S100A10, also called p11. This binding leads to the formation of a symmetric heterotetramer consisting of two annexin A2 molecules that are bridged by a p11 homodimer. The interaction site for p11 is localised in the amino acids 1 - 14 in the N-terminus of annexin A2 (Johnsson et al., 1988).

In contrast to other S100 proteins p11 is unable to bind Ca^{2+}. It harbours mutations in the EF-hand Ca^{2+}-binding motif (Gerke and Weber, 1985) and therefore is locked in an active state with respect to annexin A2 binding (Johnsson et al., 1990). So far, endogenous p11 has not been purified from tissues or cells in the absence of annexin A2, indicating that the unbound protein is metabolically instable (He et al., 2008; Puisieux et al., 1996). Annexin A2 not only interacts with p11 but also with other members of the S100 family, like S100A11 (Rintala-Dempsey et al., 2006), S100A4 (Semov et al., 2005) and S100A6 (Filipek et al., 1991).

Intracellular annexin A2 predominantly exists in complex with p11. This complex formation alters some of the biophysical properties of annexin A2. The tetramer can aggregate vesicles at micromolar Ca^{2+} levels, whereas the subunits of this complex are inactive in promoting granule aggregation at low Ca^{2+} concentrations (Drust and Creutz, 1988). Furthermore, monomeric annexin A2 needs higher Ca^{2+} levels for binding to phospholipids and membranes (Evans and Nelsestuen, 1994). On the other hand the p11 binding is dispensable for the association of annexin A2 with endosomal membranes. This process is independent of Ca^{2+} ions but requires an N-terminal binding site (Jost et al., 1997).

2.2.2.2 Annexin A2 localisation

Like other members of the annexin family annexin A2 is cytosolic but it is also bound to cytoskeletal components and membranes. Annexin A2 binds membranes in a Ca^{2+}-dependent manner. It harbours different Ca^{2+}-binding sites at the convex surface of the core domain. Three so-called type II sites are found in annexin repeats 2, 3 and 4, respectively. Two so-called type III sites are located in the first repeat. The type II binding sites have a much higher affinity for the divalent cation than the type III sites and are thought to be essential for the intracellular association of annexin A2 with the submembraneous cytoskeleton (Jost et al., 1994). But also a Ca^{2+}-independent membrane association of annexin A2 has been described which depends on cholesterol (Harder et al., 1997).

In addition to the cytoplasmic and membrane-bound localisation annexin A2 has been detected in the nucleus. Annexin A2 harbours a nuclear export sequence in the N-terminus and is actively exported after entering the nucleus. This nuclear exclusion might be modulated by phosphorylation (Eberhard et

al., 2001). Furthermore, annexin A2 is associated to cytoskeleton-associated polysomes and is capable of binding specific mRNAs (Vedeler et al., 2000).
Although it lacks a signal peptide and its mechanism of secretion is unknown, extracellular annexin A2 has been found in several tissues as both soluble and membrane-bound protein (Siever and Erickson, 1997). Extracellular annexin A2 is involved in the activation of plasminogen by tissue plasminogen activator and therefore plays a role in fibrinolysis (Hajjar et al., 1994). The extracellular form of this protein might also be important for other biological processes, such as cell adhesion (Tressler et al., 1993), ligand-mediated cell signalling (Chung et al., 1996) and virus infection (Wright et al., 1995).

2.2.2.3 Binding of annexin A2 to membrane microdomains and the cytoskeleton

The cytoskeletal scaffolding protein spectrin has been defined as an interaction partner of annexin A2 (Gerke and Weber, 1984). Furthermore, annexin A2 binds F-actin and displays a Ca^{2+}-dependent actin filament bundling activity which is more pronounced for the heterotetrameric annexin A2/p11 complex (Waisman, 1995). The F-actin-binding site is located in the annexin core (Filipenko and Waisman, 2001). Annexin A2 is not a general bundling factor for F-actin because it needs cellular membranes for its recruitment to sites of actin rearrangement (Hayes et al., 2004). This is supported by the observation that annexin A2 is involved in the formation of actin comet tails of moving pinosomes, whereas it is not involved in the formation of actin tails propelling the pathogen *Listeria monocytogenes* (Merrifield et al., 2001).

Annexin A2 is involved in a whole range of membrane transport process like endocytosis and exocytosis (Gerke et al., 2005; Futter and White, 2007), including the apical transport of vesicles in polarised cells, specifically vesicles that carry membrane raft-associated proteins (Jacob et al., 2004).

Annexin A2 is one of the few known structural proteins on the cytosolic site of membrane microdomains enriched in sphingolipids and cholesterol, termed lipid rafts. These rafts provide a means for cellular membranes to locally concentrate effectors to form platforms that function e.g. in signal transduction, membrane trafficking, cell polarisation and pathogen entry (Simons and Ikonen, 1997; Simons and Toomre, 2000). A key feature that is thought to contribute to raft assembly is the fact that cholesterol packs tightly with saturated acyl chains of lipids causing them to adopt an extended conformation in model membranes (Ipsen et al., 1987). This results in the induction of different phases which have a different degree of packing order. Therefore, cholesterol containing microdomains can be referred to as liquid ordered (l_o) in contrast to liquid disordered (l_d) membrane phases. Originally defined biochemically as detergent resistant membrane (DRM) fractions, rafts are proposed to be highly dynamic, submicroscopic assemblies that float freely within the liquid disordered bilayer in cell membranes and can coalesce upon clustering of their components.
Several mammalian viruses like influenza, human immunodeficiency virus (HIV), measles and ebola bud from lipid rafts (Suomalainen, 2002). But these microdomains also serve as preferential sites for other host-pathogen interactions. E.g. the pore forming toxin aerolysin from *Aeromonas hydrophila* directly binds a GPI-anchored protein localised in rafts (Abrami et al., 1998). CD48 is also a GPI-linked raft resident protein that serves as a receptor for the FimH protein of some *E. coli* strains. This binding

triggers the internalisation of the pathogen (Baorto et al., 1997). For a review on membrane rafts in pathogen infection, see van der Goot and Harder, 2001 or Rosenberger et al., 2000.

As mentioned above annexin A2 localises to membrane rafts. It plays an important role for the aggregation and stabilisation of these domains and probably functions by stabilising a lateral membrane segregation, i.e. that of raft and non-raft lipids (Gerke et al., 2005). Phosphatidylinositol-4,5-bisphosphat ($PI(4,5)P_2$) is a phospholipid component of cellular membranes which is localised to rafts (Pike and Casey, 1996). It has been reported that annexin A2 monomer and heterotetramer bind to $PI(4,5)P_2$ with high specificity and affinity. This attachment is mediated by cationic residues at the convex side of the annexin A2 core domain, Lys279, Lys281 and Arg284 (Gokhale et al., 2005). The binding of annexin A2 to $PI(4,5)P_2$ is linked to the organisation of actin at membrane sites that are enriched in this phospholipid (Rescher et al., 2004). Annexin A2 has also been described to be involved in the stabilisation and regulation of membrane microdomains at sites of dynamic actin rearrangement (Merrifield et al., 2001; Zobiack et al., 2002).
In the presence of Ca^{2+} annexin A2 binds to and possibly promotes the lateral association of glycosphingolipid- and cholesterol-rich membrane microdomains (Babiychuk and Draeger, 2000; Harder and Gerke, 1994). Annexin A2 forms a monolayer of protein clusters when bound to a lipid bilayer (Menke et al., 2004). This lateral aggregation could promote the aggregation of membrane microdomains. Expression of a mutant annexin A2 protein causing the submembraneous aggregation of annexin A2 and its ligand p11 results in the simultaneous aggregation of a transmembrane raft protein (CD44) and a redirection of actin bundles towards these clusters (Oliferenko et al., 1999). Thus, due to its Ca^{2+}-dependent membrane- and F-actin-binding and its intracellular location at sites of membrane rafts, annexin A2 could serve as an organiser of these membrane microdomains and their connection to the actin cytoskeleton (Gerke and Moss, 2002).
A schematic model of the involvement of annexin A2 in membrane binding and membrane domain stabilisation is depicted in Figure 2-5. Annexin A2 might first be targeted to membranes by a general binding to negatively charged phospholipids and is then recruited to raft structures by the specific interaction with $PI(4,5)P_2$. By engaging homophilic lateral interactions annexin A2 could then induce and/or stabilise raft clustering which is likely to be a prerequisite for actin assembly at such sites (Rescher et al., 2004).

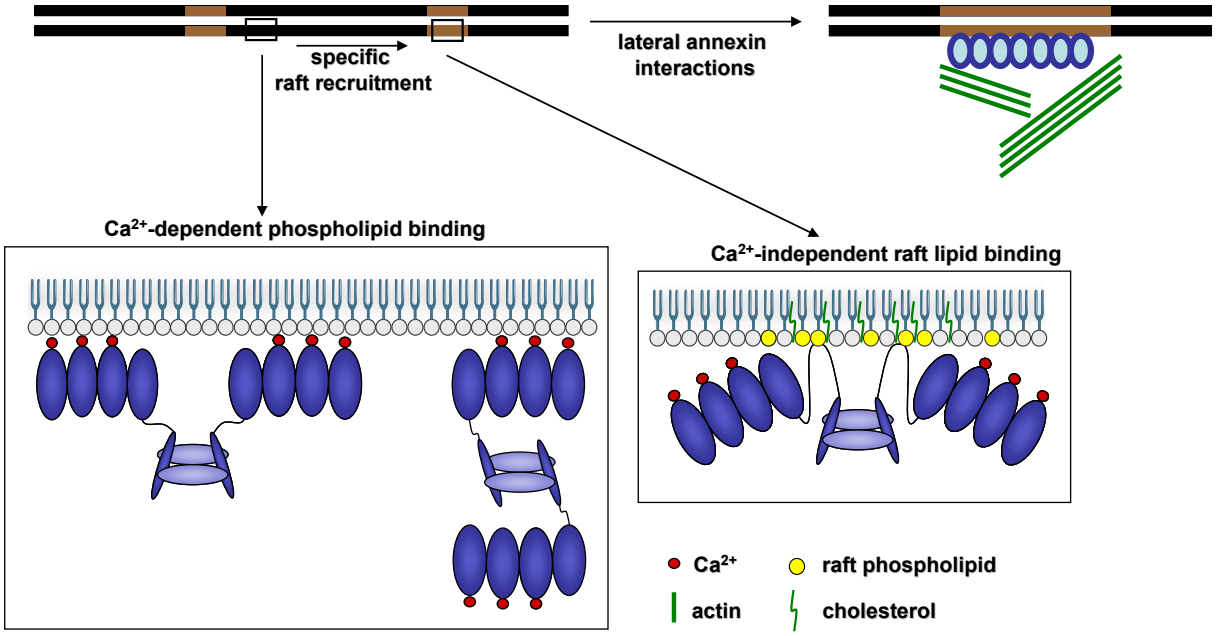

Figure 2-5: Model of membrane domain stabilisation mediated by annexin A2
The interaction of the heterotetrameric complex of annexin A2 (dark blue) and a p11 dimer (light blue) with membrane phospholipids might be mediated via the Ca^{2+}-binding sites of the annexin A2 core domain (left). Lateral diffusion could then direct the complex to raft membrane domains enriched in cholesterol, glycosphingolipids and certain phosphatidylinositol phosphates, in particular $PI(4,5)P_2$. Another fraction of annexin A2 heterotetramer might bind to raft lipids independently of Ca^{2+} (right). Lateral annexin-annexin interactions could lead to the formation of a protein scaffold beneath the membrane and the concomitant clustering of rafts and recruitment of F-actin. From Rescher and Gerke, 2004.

2.2.2.4 Posttranslational modifications of annexin A2

Annexin A2 was initially identified in 1980 as a substrate of the src kinase of Rous sarcoma virus (see 2.2.1). The phosphorylation site has been localised to Tyr23 in the N-terminus. This phosphorylation alters some of the properties of the annexin A2 monomer and also of the heterotetramer. Phosphorylation on Tyr23 reduces the affinity of annexin A2 to phospholipids in liposome binding experiments (Powell and Glenney, 1987). *In vitro* phosphorylation of the annexin A2/p11 complex inhibits the ability of the protein to bind and bundle F-actin and to form a higher order complex together with the plasma membrane and secretory vesicles. Furthermore, an increased Ca^{2+} concentration is needed for vesicle aggregation by the phosphorylated complex (Hubaishy et al., 1995). Annexin A2 is also phosphorylated on Tyr23 by the insulin receptor tyrosine kinase (Karasik et al., 1988) and by kinases associated with the platelet-derived growth factor (PDGF) (Brambilla et al., 1991).

Other phosphorylation sites of annexin A2 are Ser11 and Ser25 which are targeted by PKC (Johnsson et al., 1986; Jost and Gerke, 1996). Modification of Ser25 does not have an effect on the binding to lipids but it appears to be essential for annexin A2 function in Ca^{2+}-regulated exocytosis (Sarafian et al., 1991). *In vitro* experiments suggest that phosphorylation of Ser11 can inhibit the formation of a complex between annexin A2 and p11 (Jost and Gerke, 1996). The phosphorylation of Ser11 and a resulting inhibition of complex formation can also be achieved by calmodulin- or cAMP-dependent kinases *in vitro* (Johnsson et al., 1986).

Another posttranslational modification is the N-acetylation of annexin A2 which is of importance for the binding to p11 (Becker et al., 1990; Johnsson et al., 1988).

2.2.2.5 Annexin A2 and pathogens

Annexins have been shown to be involved in the replication of several pathogens. It has been demonstrated that annexin A2 is incorporated into viral particles of the human immunodeficiency virus-1 (HIV-1) (Harrist et al., 2009). Further, there are several other enveloped viruses that incorporate annexin A2 as one of several host cell proteins into the virion. Annexin A2 was detected in extracellular and primary enveloped virions of herpes simplex virus 1 (Loret et al., 2008; Padula et al., 2009) and in virions of vesicular stomatitis virus (Moerdyk-Schauwecker et al., 2009). Furthermore, this protein was identified in the viral particles of vaccinia virus (Chung et al., 2006), alcelaphine herpesvirus-1 (Dry et al., 2008; Zhu et al., 2005) and Kaposi's sarcoma-associated herpesvirus (Zhu et al., 2005). Host cellular annexin A2 was also found to be associated with human cytomegalovirus (HCMV) (Wright et al., 1995).

In most cases only the incorporation of annexin A2 and also other annexins was reported in the literature. Because annexins are calcium-dependent phospholipid-binding proteins and are proposed to act as scaffolding proteins at certain membrane domains their incorporation into virions might not just be accidental but those proteins might be important for viral infection cycles. The role of annexins in the viral replication remains rather elusive albeit a few exceptions. In HCMV annexin A2 is not only incorporated but it is also thought to act as a receptor for this virus on the surface of endothelial cells (Wright et al., 1994). Furthermore, this annexin has been shown to be a receptor for respiratory syncytial virus on epithelial cells (Malhotra et al., 2003). Annexin A2 plays a role in virus assembly in the case of HIV-1 (Ryzhova et al., 2006) and it facilitates HIV-1 binding to and entry into macrophages (Ma et al., 2004). A direct interaction of annexin A2 with HIV-GAG at GM1 containing membrane rafts in the plasma membrane of 293T cells has been demonstrated and in this cell line annexin A2 increases the production of HIV-1 virus particles (Harrist et al., 2009).

Enveloped viruses may use similar cellular pathways for their assembly and exit from the cell. But annexin A2 has also been described in the context of replication of other viruses. E.g. non-enveloped rabbit vesivirus particles have been shown to bind annexin A2. A monoclonal anti-annexin A2 antibody and siRNA-mediated knock-down of annexin A2 expression reduced the infection of this virus significantly (Gonzalez-Reyes et al., 2009). The non-structural protein 3 of bluetongue virus has been described to bind the annexin A2 binding partner p11. This interaction probably links the assembled virions to the cellular exocytic machinery (Beaton et al., 2002).

Other annexins have also been reported to be essential for the pathogenesis of viruses. E.g. annexin A5 has been shown to specifically bind to a surface antigen of hepatitis B virus (HBV) and it was demonstrated that this protein is important for the susceptibility of cells to HBV infection (Gong et al., 1999; Hertogs et al., 1993). In a fish cell line salmon annexin A1 transcription is induced after infection of the cells with the non-enveloped RNA virus infectious pancreatic necrosis virus and the depletion of this annexin leads to a reduction of the virus titre (Hwang et al., 2007).

Involvements of annexins in pathogen replication are very diverse and are not limited to viruses. E.g. annexin A2 has been described to act as a receptor for *Pseudomonas aeruginosa* (Kirschnek et al., 2005) and it is of importance for the F-actin aggregation underneath some *E. coli* strains during the course of infection (Miyahara et al., 2009; Zobiack et al., 2002). Furthermore, annexin A2 is involved in microbial clearance by macrophages (Swisher et al., 2007).

2.3 Aim of this thesis

The cellular mechanisms that are important for IAV replication are rather nondistinctive and a better understanding could help in finding strategies to fight this pathogen. The focus of this work thereby was to elucidate a possible role of host cell annexin A2 in influenza A infection. Annexin A2 as a candidate host factor in IAV replication was chosen for several reasons. First, annexin A2 was identified as a structural component of membrane rafts that is involved in the aggregation and stabilisation of these domains. Since membrane rafts have been defined as the budding site of IAV, annexin A2 could be involved in IAV replication, specifically virus budding. Second, annexin A2 is involved in several endo- and exocytotic processes and is especially important for the apical transport of raft associated proteins. Such annexin A2-regulated transport processes might also be crucial for efficient influenza A replication. Third, annexin A2 is involved in actin dynamics and the organisation of the actin cytoskeleton is of importance for influenza A replication.
To elucidate a possible role of annexin A2 in influenza A infection the replication of IAV and the surface localisation of influenza HA were determined in annexin A2 manipulated cells. Furthermore, a possible incorporation of this protein into the virion was analysed and the localisation of IAV in infected host cells was visualised with respect to a possible colocalisation with annexin A2.

A second focus of this work was placed on the association of annexin A2 with membrane rafts. Particularly the effects of posttranslational modifications and ligand binding to annexin A2 on the raft association of this protein were investigated. Therefore, cellular annexin A2 phosphorylated on Tyr23 as well as ectopically expressed phospho-deficient and phospho-mimicking mutants of annexin A2 were analysed for the association with detergent resistant membranes (DRMs) as a defining criterion for membrane rafts. Furthermore, ectopically expressed proteins harbouring mutations in either the $PI(4,5)P_2$-binding site, the high affinity Ca^{2+}-binding sites or the p11-binding site were analysed. This analysis included the recruitment of the different annexin A2 variants to GM1 membrane phases and the recording of membrane order in regions of annexin A2 localisation with the help of Laurdan 2-photon microscopy.

3 Materials and Methods

3.1 Materials

3.1.1 Virus strains

FPV: avian influenza virus A/Bratislava/79 (H7N7); from Stephan Pleschka, Gießen, Germany

PR8: human influenza A/Puerto-Rico/8/34 (H1N1); from Thorsten Wolff, Berlin, Germany

3.1.2 Bacterial strains

E. coli DH5α: a chemically competent derivative of the *E. coli* strain K-12 used for plasmid amplification

3.1.3 Eukaryotic cell lines

A431: human epithelial skin cells from an epidermoid carcinoma, enriched in GM1; from Daniel Lingwood, Dresden, Germany

A549: human epithelial lung carcinoma cell line; from Stephan Ludwig, Münster, Germany

BHK-IR: baby hamster kidney cells stably overexpressing the human insulin receptor (IR); from Axel Ullrich, Martinsried, Germany

CMEC: cardiac microvascular endothelial cells isolated from a wt mouse (C57Bl/6J) (anxA2$^{+/+}$) or the annexin A2 knockout mouse (anxA2$^{-/-}$); from Katherine A. Hajjar, New York, USA (Ling et al., 2004)

HeLa: human epithelial cell line derived from a cervical cancer

HepG2: human epithelial cell line derived from a hepatocellular carcinoma

MDCK II: Madin Darby canine kidney: epithelial cell line derived from a kidney of a female cocker spaniel by S.H. Madin and N.B. Darby

- MDCK-anxA2-GFP: MDCK II cell line stably expressing GFP labelled annexin A2; from Fernando Martín-Belmonte, San Francisco, USA (Martin-Belmonte et al., 2007)
- MDCK-IMV: MDCK II cell line used for virus infections and plaque assays; from Stephan Ludwig, Münster, Germany
- MDCK-Tet: MDCK II cell line able to polarise on filters and form cysts; this cell line was used for the DRM association analysis of annexin A2 mutants
- MDCK-TG: MDCK II cell line used in the lab of Thomas Grewal, Sydney, Australia
- MDCK-XM: MDCK II cell line expressing the XM protein. The expression of this protein is regulated by a tet-off transactivator type II (Clontech, Germany) (Harder and Gerke, 1993)

3.1.4 Plasmids

anxA2-GFP: pEGFP-N3 vector (Clontech) coding for human annexin A2 fused with GFP under the control of a CMV promoter. The sequence of annexin A2 contains the aa exchange A65E allowing the specific detection of this ectopically expressed protein with the monoclonal antibody H28.

anxA2 YE-GFP: pEGFP-N3 vector coding for human annexin A2 fused with GFP under the control of a CMV promoter. The sequence of annexin A2 contains the aa exchange Y23E. The addition of negative charge mimics the phosphorylation of Tyr23 (Rescher et al., 2008). The sequence also contains the aa substitution A65E (see above).

anxA2 YF-GFP: pEGFP-N3 vector coding for human annexin A2 fused with GFP under the control of a CMV promoter. The sequence of annexin A2 contains the aa exchange Y23F. This exchange makes the phosphorylation of aa 23 impossible (phosphorylation deficient). The sequence also contains the aa substitution A65E (see above).

anxA2 KA-GFP: pEGFP-N3 vector coding for human annexin A2 fused with GFP under the control of a CMV promoter. The sequence of annexin A2 contains the aa exchange K281A. This exchange leads to a deficiency in binding to $PI(4,5)P_2$ *in vitro* (Gokhale et al., 2005). The sequence also contains the aa substitution A65E (see above).

anxA2 PM-GFP: pEGFP-N3 vector coding for human annexin A2 fused with GFP under the control of a CMV promoter. The sequence of annexin A2 contains the aa exchanges I6E and L7E in the p11-binding site, rendering this protein unable to bind p11 (Thiel et al., 1992). The sequence also contains the aa substitution A65E (see above).

anxA2 CM-GFP: pEGFP-N3 vector coding for human annexin A2 fused with GFP under the control of a CMV promoter. The sequence of annexin A2 contains the aa exchanges D161A, E246A and D321A which inactivate the type II Ca^{2+}-binding sites (Jost et al., 1992). The sequence also contains the aa substitution A65E (see above).

anxA2 PMCM-GFP: pEGFP-N3 vector coding for human annexin A2 fused with GFP under the control of a CMV promoter. The sequence of annexin A2 contains the aa exchanges I6E, L7E, D161A, E246A and D321A. So this protein harbours inactive p11- and type II Ca^{2+}-binding sites (Jost et al., 1997). The sequence also contains the aa substitution A65E (see above).

GFP: pEGFP-N3 vector coding for the GFP-tag under the control of a CMV promoter.

pRSET-B mCherry: pRSET-B vector (Invitrogen) coding for an mCherry tag. From Roger Y. Tsien, San Diego, USA.

anxA2 xx-mCherry: pEGFP-N3 vector coding for annexin A2 constructs (xx: wt, YE, YF, KA, PM, PMCM) under the control of a CMV promoter. The GFP-tag has been substituted by mCherry (see 3.4.4).

mCherry: pEGFP-N3 vector coding for mCherry instead of EGFP under the control of a CMV promoter.

H7-HA: pCAGGS vector expressing the HA of IAV A/FPV/Rostock/34 (H7N1) (Marjuki et al., 2006). From Stephan Pleschka, Giessen, Germany.

PHD-YFP: pEYFP-N1 vector (Clontech) coding for the PHD of human PLC-δ1 (Rescher et al., 2004).

3.1.5 Oligonucleotides

Oligonucleotides were purchased from Sigma Proligo, if not indicated otherwise.

Oligonucleotides for siRNA mediated knock-down of proteins

anxA2 (2.3)	fwd: 5' CUUUGAUGCUGAGCGGGAU 3' rev: 5´ AUCCCGCUCAGCAUCAAAG 3´	siRNA duplex corresponding to nucleotides 94 - 113 of the coding sequence from human annexin A2
control		non-targeting siRNA (Dharmacon)

Oligonucleotides for real-time PCR analysis

M1	fwd: 5' AGATGAGTCTTCTAACCGAGGTCG 3' rev: 5' TGCAAAAACATCTTCAAGTCTCTG 3'
annexin A1	Hs_ANXA1_1_SG QuantiTect Primer Assay (Qiagen)
annexin A2	Hs_ANXA2_1_SG QuantiTect Primer Assay (Qiagen)
GAPDH	Hs_GAPDH_2_SG QuantiTect Primer Assay (Qiagen)

Oligonucleotides for sequencing

pEGFP-N.3'.2	5' CGCTGAACTTGTGGCCGT 3'

Oligonucleotides for PCR amplification

mCherry	fwd: 5' GATCGCGGCCGCTTACTTGTACAGCTCGTC 3' rev: 5' GATCGGATCCGCCACCATGGTGAGCAAG 3'

3.1.6 Enzymes

*Bam*H I	MBI Fermentas
GoTaq®	Promega
Not I	MBI Fermentas
Pfu Turbo DNA polymerase	Stratagene
Sac I	MBI Fermentas
T4 DNA ligase	MBI Fermentas

3.1.7 Antibodies

Primary antibodies

antigen	host	origin	dilution		
			WB	IF	FACS
annexin A2 (HH7)	Ms	Thiel et al., 1992	1:5000	1:100	
annexin A2 (H28)	Ms	Osborn et al., 1988		1:100	
annexin A2	Ms	BD Transduction Lab	1:5000		
caveolin	Rb	BD Transduction Lab	1:5000		
cleaved caspase-8	Rb	Cell Signaling	1:1000		
cleaved caspase-9	Rb	Cell Signaling	1:1000		
GFP	Ms	Clontech	1:1000		
H7-HA	Ms	Marjuki et al., 2006			1:100
H7-HA (2KP 96/11)	Rb	Marjuki et al., 2006		1:200	
M1	Ms	AbD Serotech	1:1000		
NS1 (23-1)	Ms	Ehrhardt et al., 2007	1:500		
p11 (H21)	Ms	Osborn et al., 1988	1:1000	1:300	
PARP	Ms	BD Transduction Lab	1:500		
pTyr (4G10® platinum)	Ms	Millipore	1:1000		
human transferrin receptor (H68.4)	Ms	Zymed	1:3000		
vimentin	Ms	Dianova	1:500		

Secondary antibodies

antigen	species	label	origin	dilution		
				WB	IF	FACS
Ms	Rb	POX	Dako	1:2000		
Ms	G	TxRed	Dianova		1:200	
Ms	G	Cy2	Dianova		1:300	
Rb	G	POX	Dako	1:5000		
Rb	G	Alexa568	Invitrogen		1:500	
Rb	G	FITC	Dianova			1:300

3.1.8 Kits

BigDye® Terminator Cycle Sequencing Kit	Applied Biosystems
Gene Elute Plasmid Miniprep Kit	Sigma
High-Capacity cDNA Reverse Transcription Kit	Applied Biosystems
JetStar Maxi Kit	Genomed
PCR Purification Kit	Qiagen
Platinum® SYBR® Green qPCR SuperMix UDG with ROX	Invitrogen
QIAquick Gel Extraction Kit	Qiagen
RNeasy Mini Kit	Qiagen

3.1.9 Chemicals and reagents

10 x MEM	Gibco
2-mercaptoethanol	Roth
7.5 % $NaHCO_3$	Gibco
acrylamid / methylenbisacrylamid (30 % / 0.8 %)	Roth
agar	Oxoid
agarose	Biozym Diagnnostic GMBH
Amersham ECL Plus™ Western Blotting Detection Reagent	GE healthcare
ampicillin	Sigma-Aldrich
APS	Roth
blasticidin	Invitrogen
bovine albumin 35%	MP Biomedicals
bromophenol blue	Amresco
BSA fraction V	Roche
CtxB Alexa Fluor® 594 conjugate	Molecular Probes
Coomassie (Bradford) Protein Assay Kit	Thermo Scientific
cycloheximide	Fluka
DEAE dextran	Roth
DNA molecular weight standard: 1 kb DNA ladder	MBI Fermentas
dNTPs	MBI Fermentas
Dulbecco's MEM	PAA Laboratories GmbH
Dulbecco's PBS	PAA Laboratories GmbH
EDTA	AppliChem
ethidiumbromide	Sigma
FCS	PAA Laboratories GmbH
glucose	Sigma
insulin	Sigma-Aldrich
kanamycin	AppliChem
L-glutamine	Cambrex
Laurdan	Invitrogen
Lipofectamine™ 2000	Invitrogen
loading dye	MBI Fermentas
luminol	Roth
MEM	PAA Laboratories GmbH
Mowiol® 4-88	Calbiochem
neutral red	Sigma
n-propyl gallate	Sigma
Oligofectamine™	Invitrogen
Opti-MEM®	Invitrogen
p-coumaric acid	Roth
penicillin / streptomycin	Cambrex
PFA	Merck
PIC (complete, EDTA-free)	Roche
prestained protein marker, broad range	NEB
saccharose	AppliChem
SDS pellets	Roth
skimmed milk powder	AppliChem
staurosporine	Sigma
Surfact-Amps X-100	Thermo Scientific
TEMED	Sigma
TNFα	PeproTech (tebu-bio)
transferrin FITC	Invitrogen
trypsin/EDTA	Biochrom
trypsin SOLO	Gibco BRL
trypan blue	Sigma

All other chemicals were purchased from Roth, Merck or Sigma-Aldrich.

3.1.10 Other materials and equipment

ABIPrism® 7900 HT	Applied Biosystems
BioPhotometer	Eppendorf
blotting paper	Hartenstein
Branson Sonifier® 250	G. Heinemann
cell culture dishes	Greiner Bio-One
centrifuges and rotors	
Biofuge Fresco	Heraeus
Biofuge Pico	Heraeus
Megafuge 1.0R	Heraeus
Centrifuge C5810R	Eppendorf
Centrifuge 5417R	Eppendorf
Optima™ L-70K ultracentrifuge	G. Heinemann
rotor SW60 Ti	Beckman
rotor SW41 Ti	Beckman
confocal microscope LSM510 Meta	Zeiss
heating insert P	Zeiss
objective heater	Zeiss
confocal microscope TCS SP5	Leica
Mai Tai®, mode-locked Ti:Sapphire laser	Spectra-Physics
developing machine CURIX60	Agfa
developing reagents: developer and rapid fixer	Agfa
electrophoresis chamber	PeqLab
EOS 350D	Canon
FACSCalibur™	BD
FACSFlow™	BD
Immobilon™-P PVDF membrane	Millipore
incubators	Memmert
incubators for cell culture	Heraeus
inverted microscope Axiovert 40 C	Zeiss
inverted microscope Leica DM IL	Leica
Lab-Tek™ chamber coverglass	Nunc
laboratory shaker Innova 4000	New Brunswick Scientific
laminar flow	BDK
Mini-Trans-Blot chamber	BioRad
Multiphor™ II Electrophoresis unit	Amersham Biosciences
petri dishes	Corning
refractometer	Zeiss
spectrophotometer DU®-640	Beckman
thermocycler TRIO heated lid	Biometra
UV-transluminator	Biometra
X-ray films Fuji Super RX, 13 x 18 cm	Fischer-Sehner

3.2 Cellbiological methods

3.2.1 Cell culture

MDCK-IMV were cultivated in MEM supplemented with 10 % heat inactivated FCS, penicillin, streptomycin and glutamine at 37 °C and 5 % CO_2. All other cell lines were grown in supplemented DMEM at 7 % CO_2. For the cultivation of MDCK-XM tetracycline (1 µg/ml) was added unless the expression of the XM protein was desired. When cultivating MDCK-anxA2-GFP the medium was supplemented with blasticidin (50 µg/ml).

When reaching confluency the cells were washed with PBS without Ca^{2+} and Mg^{2+} and detached from the cell culture dish by incubating with trypsin/EDTA solution (0.05 % trypsin, 0.2 % EDTA) at 37 °C for several minutes. When using MDCK cells after the first wash step PBS was added and the cells were incubated for 10 min at 37 °C before trypsinisation. As soon as the cells detached from the cell culture dish they were collected in fresh medium to inactivate trypsin and centrifuged at 800 rpm for 4 min (Megafuge 1.OR; rotor 7750). The resulting pellet was resuspended in fresh supplemented medium and the cell number and viability were determined by counting trypan blue stained cells in a haemocytometer. The cells were seeded in an appropriate ratio onto new cell culture dishes.

3.2.2 Freezing cells

To freeze cells for long term storage the cells of a subconfluent 10 cm cell culture dish were trypsinised and afterwards pelleted via centrifugation. The pellet was resuspended in 1 ml of chilled freezing-medium (10 % DMSO in FCS). The cells were frozen at -80 °C for several days before transferring them into liquid nitrogen.

3.2.3 Thawing cells

Cells were thawed quickly at 37 °C and transferred into pre-warmed media. After centrifugation the supernatant was discarded and the cells were resuspended in 1 ml medium before being transferred into a culture dish containing the appropriate amount of media. The cells were cultivated as described above (see 3.2.1).

3.2.4 Transient transfection of eukaryotic cells

3.2.4.1 Plasmid transfection

To deliver plasmid DNA into A431 cells transient transfections were carried out using Lipofectamine 2000 according to the manufacturer's protocol. MDCK and A549 were transfected by means of a modified transfection protocol using Lipofectamine 2000 to yield higher transfection efficiencies. For this protocol the adherent cell lines were transfected in suspension. The transfection of one 35 mm dish is depicted in the following.

Cells were detached from the cell culture dish via trypsinisation and counted. $2*10^6$ cells were resuspended in 1.5 ml DMEM without antibiotics. In the meantime 2 µg DNA were diluted in 50 µl OptiMEM and 10 µl Lipofectamine 2000 in 200 µl OptiMEM. After vortexing and 5 min incubation at RT the two dilutions were mixed, vortexed and incubated for additional 15 min. The cells were transferred to a cell culture dish and the DNA/Lipofectamine mixture was added. After incubation for 4 - 6 h at 37 °C and 7 % CO_2 the medium was changed.

3.2.4.2 siRNA transfection

siRNA transfection of A549 was performed using Lipofectamine 2000 according to the manufacturer's instructions.

When transfecting siRNA into HeLa cells Oligofectamine was used. Cells were seeded in a 35 mm cell culture dish and grown to about 50 % confluency. 100 pmol siRNA were diluted in 175 µl DMEM without antibiotics and 4 µl Oligofectamine was mixed with 11 µl antibiotic-free medium. After incubation for 5 - 10 min at RT the two dilutions were mixed and incubated for 20 min. In the meantime 800 µl of fresh antibiotic-free DMEM was added to the cells. The siRNA/Olicofectamine mixture was added and the cells were cultivated for 3 - 4 h. 1 ml of complete DMEM was added and the cells were further cultivated at 37 °C and 7 % CO_2 for 48 h.

3.2.5 Immunofluorescence

Cells cultivated on coverslips were washed with PBS before being fixed with 10 % FA in PBS for 10 min at RT. The cells were washed for 5 min with PBS under gentle rocking and permeabilised by incubation with 0.2 % Triton X-100 in PBS for 2 min. After a washing step the free aldehyde groups of FA were quenched by incubation with 50 mM NH_4Cl for 7 min.

Before antibody incubation the fixed cells were blocked for 30 - 60 min with 2 % BSA in PBS. Incubation with the primary antibody was performed for 1 h at RT. After washing the cells with PBS they were incubated with an appropriate fluorophore labelled secondary antibody for 1 h. The antibodies were diluted in 2 % (w/v) BSA in PBS. After extensive washing the coverslips were rinsed in dist. H_2O and mounted onto microscope slides in Mowiol containing 4 % n-propyl gallate as anti-fading reagent. Microscopy images were obtained with an LSM510 Meta confocal microscope equipped with a Plan-Apochromat 63x/1.4 oil immersion objective.

PBS
137 mM NaCl
2.68 mM KCl
8.1 mM Na_2HPO_4
1.47 mM KH_2PO_4
pH 7.4

3.2.6 Induction and microscopy of PMSs

Plasma membrane spheres (PMSs) were prepared according to Lingwood et al., 2008. A431 cells were seeded on Lab-Tek chamber slides and transfected with GFP labelled constructs one day afterwards (3.2.4.1). Two days after seeding the cells were washed with PBS and incubated overnight with PMS buffer. Phase separation of the PMSs was induced by clustering GM1 with 1 µg/ml CtxB Alexa Fluor 594 conjugate for at least 2 h at 37 °C. The distribution of transferrin receptor was evaluated by the incubation of the phase separated PMSs of untransfected cells with 10 µg/ml FITC labelled transferrin for 1 h at 37 °C. Excess transferrin was removed by changing the PMS buffer to reduce background staining. For imaging the PMSs using the LSM510 Meta confocal microscope a life cell setup was used. The temperature was maintained at 37 °C by using a heating chamber, an objective heater and temperature controllers.

PMS buffer
1.5 mM $CaCl_2$
1.5 mM $MgCl_2$
5 mM Hepes
1 mg/ml Glucose
in PBS pH 7.4

3.2.7 Laurdan 2-photon microscopy

3.2.7.1 Tissue culture for microscopy

$0.2*10^6$ MDCK-TG were plated on coverslips in a 35 mm tissue culture dish. The next day the cells were transfected with mCherry-tagged annexin A2 constructs using Lipofectamine 2000 according to the manufacturer's instructions. 24 h afterwards the cells were washed once with warm PBS and incubated with 5 µM Laurdan in 1 ml serum-free medium for 30 min at 37 °C. After washing the cells twice with warm PBS they were fixed with 4 % PFA for 20 min at RT. After washing with PBS the coverslips were rinsed in dist. H_2O and mounted in Mowiol.

3.2.7.2 Microscopy

Microscopy images were obtained with a TCS SP5 microscope using a 63 x oil immersion objective. Laurdan fluorescence was excited at 800 nm with a Mai Tai, mode-locked Ti:Sapphire laser and intensity images were recorded simultaneously in the range of 400 - 460 nm and 470 - 530 nm for the two channels, respectively. For confocal microscopy, mCherry fluorescence was excited at 561 nm and the emission was recorded at 570 - 630 nm. The microscopy was performed in the laboratory of Katharina Gaus, University of New South Wales, Sydney, Australia.

3.2.7.3 Image analysis

Using the two Laurdan intensity images GP values were calculated for each pixel with the software Image J using a plug-in written by Carles Rentero, Sydney, Australia. GP values were corrected by using the G-factor obtained for Laurdan in DMSO. GP images were pseudo-coloured in Adobe Photoshop.
The confocal fluorescence images of mCherry tagged annexin A2 wt and mutant proteins were used to identify the localisation of these proteins in liquid-disordered / liquid-ordered (low / high GP value) regions, respectively. To do so, areas of high mCherry fluorescence were used to define a mask in Adobe Photoshop. This mask was layered onto the GP image to selectively determine the GP values of the regions of fluorophore localisation.

3.2.8 Flow cytometry

The hemagglutinin surface localisation in A549 was determined via flow cytometric measurements (Marjuki et al., 2006). For each measurement the cells of one 35 mm dish were used and samples were prepared in duplicate. A549 were transfected with an HA expressing plasmid (3.2.4.1). 24 h later the cells were detached with trypsin/EDTA, transferred into DMEM and centrifuged at 5 000 rpm for 4 min at 4 °C (Biofuge Fresco). After washing with PBS the cell pellet was fixed with 4 % FA in PBS for 1 h at RT. The cells were washed with PBS and stepwise incubated with MsαH7-HA (1:100) and then with RbαMs FITC-conjugated antibody for 30 min on ice each. The cells were washed between

and after the antibody incubation steps with cold PBS and finally resuspended in PBS to determine the HA surface localisation by FACS analysis.

3.3 Proteinbiochemical methods

3.3.1 Preparation of cellular protein extracts

Cells were washed with cold PBS, scraped off the cell culture dish in PBS and transferred into a reaction tube. After centrifugation at 13 000 rpm for 1 min at 4 °C (Biofuge Fresco) the cell pellet was resuspended in an appropriate volume of 8 M urea and sonified on ice (2 pulses, output control: 50 %, amplitude control: 5).

3.3.2 Triton solubilisation

The isolation of detergent resistant membranes (DRMs) was performed according to Brown and Rose, 1992. The cells of one 80 - 90 % confluent 35 mm cell culture dish were washed once with ice cold PBS, scraped in 1 ml PBS and transferred into a reaction tube. The tube was spun for 5 min at 2 000 rpm at 4 °C (Biofuge Fresco) and the cell pellet was resuspended in 200 µl cold MES buffer. The cells were homogenised by squeezing them through a 22-gauge needle ten times on ice. After incubation for 20 min on ice the homogenised cells were centrifuged for 20 min at 14 000 rpm and 4 °C. The supernatant contains the Triton soluble proteins and was transferred into a new reaction tube. The Triton insoluble pellet was solubilised in 50 µl HEPES buffer for 30 min at RT. The $CaCl_2$ concentrations added to the buffers varied in the different experiments and are indicated in the respective captions.

MES buffer	HEPES buffer
25 mM MES pH 6.5	25 mM HEPES pH 7.4
0.15 M NaCl	0.15 M NaCl
1 % (v/v)Triton X-100 final (Surfact-Amps X-100)	1 % (v/v) Triton X-100 final (Surfact-Amps X-100)
PIC	PIC

3.3.3 DRM flotation gradient

The cells of one 80 - 90 % confluent 10 cm dish were washed with ice cold PBS and scraped in 1 ml PBS into a reaction tube. The cells were spun down for 5 min at 2 000 rpm at 4 °C (Biofuge Fresco), resuspended in 1 ml lysis buffer and disrupted by sonification on ice (20 pulses, output control: 50 %, amplitude control: 5). Nuclear remnants and ER were removed with a centrifugation step (10 min, 2 000 rpm, 4 °C). The supernatant was adjusted to 7 ml and transferred into an ultracentrifugation tube. Membranes were sedimented by centrifugation for 30 min, 150 000 g at 4 °C (rotor SW41 Ti) and homogenised in 1 ml Triton buffer by squeezing through a 20-gauge needle twenty times on ice. After incubation for 30 min at 4 °C the pellet was homogenised again with a 20-gauge needle. Following 30 min incubation on ice the homogenisation step was repeated a third time. After another 30 min incubation step on ice the resuspended membranes were brought to 42 % saccharose by the addition of 85 % saccharose. The percentage of the saccharose was checked in a refractometer. The membrane dilution was overlayed with 8 ml 30 % saccharose solution and 2 ml 5 % saccharose solution and centrifuged at 200 000 g for 19 h at 4 °C. 1.5 ml fractions were collected from the top. The proteins were concentrated via TCA precipitation (3.3.5).

lysis buffer
10 mM HEPES pH 7.4
42 mM KCl
5 mM $MgCl_2$
50 µM $CaCl_2$
PIC

TN
10 mM Tris pH 7.5
150 mM NaCl
50 µM $CaCl_2$

Triton buffer
1 % (v/v) Triton X-100 final (Surfact-Amps X-100) in TN

saccharose solutions
85% (w/v) saccharose in TN
30% (w/v) saccharose in TN
5% (w/v) saccharose in TN

3.3.4 Protein quantification

Protein concentrations were determined with the Bradford protein assay (Bradford, 1976). The protein solution was diluted 1:500 in 500 µl dist. H_2O and incubated with 500 µl Coomassie Plus Protein Assay Reagent for 15 min at RT. The absorbance was measured at 595 nm with a spectrophotometer (DU®-640). A BSA standard curve (0 - 10 µg) was used to calculate the unknown protein concentration.

3.3.5 Protein precipitation with TCA

To concentrate proteins they were precipitated with TCA. 100 % TCA was added to the protein solution to give a final TCA concentration of 15 % and the solution was frozen at -20 °C for 1 h. After thawing on ice the proteins were precipitated by a 20 min centrifugation step at 13 000 rpm at 4 °C (Biofuge Fresco). The resultant protein pellet was washed with 2 % (w/v) sodium acetate in 70 % ethanol and after centrifugation the pellet was air-dried. The proteins were resuspended in SDS sample buffer and used for western blot analysis (3.3.7).

3.3.6 SDS-PAGE

Separation of proteins according to their apparent molecular mass was performed by denaturing sodium dodecyl sulfate polyacrylamide gel electrophoresis (SDS-PAGE) according to Laemmli, 1970. Depending on the molecular weight of the proteins resolving gels with polyacrylamide concentrations of 10 % or 12 % (v/v) were used. For each sample 30 µg protein was denatured in SDS sample buffer by boiling for 5 min at 95 °C prior to loading on an SDS-polyacrylamide gel (SDS-PAG). As a molecular weight standard Prestained Protein Marker was used. Separation was performed with 15 mA in the stacking gel and 30 mA in the resolving gel until the bromophenol blue dye front reached the desired height. The proteins were visualised via western blot analysis (3.3.7).

10 % / 12 % resolving gel
33 % / 40 % (v/v) acrylamid / methylenbisacrylamid
375 mM Tris pH 8.8
0.1 % (w/v) SDS
0.1 % (w/v) APS
0.0004 % (v/v) TEMED

5 % stacking gel
17 % (v/v) acrylamid / methylenbisacrylamid
125 mM Tris pH 6.8
0.1 % (w/v) SDS
0.1 % (w/v) APS
0.001 % (v/v) TEMED

running buffer
25 mM Tris
0.1 % (w/v) SDS
192 mM glycine

4 x SDS sample buffer
250 mM Tris pH 6.8
40 % (v/v) glycerine
1.5 % (w/v) SDS
2 % (v/v) 2-mercaptoethanol
0.3 mM bromophenol blue

3.3.7 Western blotting

For immunoblot analysis the proteins were first separated on an SDS-PAG (3.3.6) and afterwards transferred onto a PVDF membrane where they could be detected by means of specific antibodies. The membrane was activated and equilibrated according to the manufacturer's instructions. The PAG and the membrane were arranged in a tank blot chamber filled with transfer buffer. The proteins were transferred onto the membrane in an electric field of 300 mA for 1 h while cooling with ice.

To reduce unspecific antibody binding the PVDF membrane was blocked for 1 h with blocking buffer (either 5 % BSA in TBS-T or 5 % skim milk powder in TBS-T, depending on the primary antibody) at RT. The membrane was washed with TBS-T before being incubated with the primary antibody overnight at 4 °C under gentle rocking. After washing three times for 10 min with TBS-T the membrane was incubated with the appropriate peroxidase coupled secondary antibody for 1 h at RT. The primary as well as the secondary antibody was diluted in blocking buffer. Afterwards the membrane was washed three times with TBS-T. For the detection of the proteins the blot was incubated with self made ECL solution for 2 min. For the detection of weak signals Amersham ECL Plus™ Western Blotting Detection Reagent was used according to manufacturer's protocol. The incubation with the ECL reagent was followed by immediate exposure of the blot to on an X-ray film.

transfer buffer
50 mM Tris
50 mM boric acid

TBS-T
20 mM Tris pH 7.5
150 mM NaCl
0.2 % (v/v) Tween 20

self made ECL solution
2.5 mM luminol
0.4 mM p-coumaric acid
100 mM Tris pH 8.5
0.0175 % H_2O_2 (added immediately before use)

3.3.8 Stripping of blot membranes

For re-probing of membranes former immunocomplexes were removed by incubation of the membrane in stripping buffer for 30 min at 50 °C. Afterwards the membrane was washed with TBS-T before incubation with the blocking reagent and antibodies.

stripping buffer
62.5 mM Tris pH 6.5
2 % (w/v) SDS
100 mM 2-mercaptoethanol

3.4 Molecular biological methods

3.4.1 Bacterial methods

3.4.1.1 Cultivation and long term storage of bacteria

Bacteria were cultivated in liquid LB medium at 37 °C under permanent agitation of 250 rpm or plated on solid agar plates which were incubated at 37 °C. For selection of transformed bacteria, media or agar plates were supplemented with appropriate antibodies (100 µg/ml ampicillin or 30 µg/ml kanamycin). For long-term storage, glycerol was added to the bacterial suspension to a final concentration of 12.5 % (v/v) and the culture was frozen at -80 °C.

LB medium
1 % (w/v) tryptone
0.5 % (w/v) yeast extract
0.5 % (w/v) NaCl
[1.2 % (w/v) agar for solid medium]
pH 7.0

3.4.1.2 Preparation of $CaCl_2$-competent *E. coli* DH5α

To prepare heat shock competent *E. coli* DH5α an overnight culture was diluted 1:50 in 50 ml LB medium and cells were grown at 37 °C at 250 rpm until the cell suspension reached an OD_{600nm} = 0.3 - 0.4. Then, the bacteria were spun down (10 min, 4 °C, 2 500 rpm, Heraeus Megafuge 1.OR) and the resultant pellet was resuspended in 40 ml ice cold 100 mM $CaCl_2$ solution. Following 30 min incubation on ice, cells were again pelleted and resuspended in 2 ml $CaCl_2$ supplemented with 20 % (v/v) glycerol. 50 µl aliquots of this cell suspension were frozen in liquid nitrogen and stored at -80 °C until use.

3.4.1.3 Transformation of $CaCl_2$ competent *E. coli* DH5α

50 µl $CaCl_2$ competent *E. coli* were slowly thawed on ice. 1 µg DNA or 1 µl ligation mixture were added and the cells were incubated for 30 min on ice. Afterwards the bacteria were exposed to a heat shock (1 min 42 °C) and regenerated on ice for 5 min. 1 ml antibiotic-free LB medium was added and the cells were incubated at 37 °C for 1 h under gentle agitation. For selection transformed bacteria were plated on LB agar plates containing the appropriate antibiotic and incubated overnight at 37 °C.

3.4.2 Methods of DNA preparation

3.4.2.1 Isolation and determination of plasmid DNA

For small scale isolation of plasmid DNA of a 2 ml overnight bacterial culture the Gene Elute Plasmid Miniprep Kit was used according to the manufacturer's instructions. For the isolation of larger amounts of DNA from a 200 ml overnight culture the JetStar Maxi Kit was used.

DNA concentration was determined by measuring the OD_{260nm} using the Eppendorf BioPhotometer. An OD_{260nm} of 1.0 accords to 50 µg/ml DNA.

3.4.2.2 Agarose gel electrophoresis

1 % (w/v) agarose were dissolved in 1 x TAE buffer by boiling and supplemented with 0.5 µg/ml ethidium bromide for DNA detection. The DNA samples were mixed with 6 x sample buffer and loaded together with an appropriate molecular weight marker onto the gel. Electrophoresis was carried out at 80 - 150 V and separated fragments were visualised by exposure to UV light (λ = 320 nm) on a transilluminator.

1 x TAE
40 mM Tris pH 8.0
40 mM glacial acetic acid
1 mM EDTA

3.4.2.3 Elution of DNA from agarose gels

The DNA was separated on an agarose gel and visualised using ethidium bromide (3.4.2.2). The appropriate band was cut out of the gel and the DNA was isolated using the QIAquick Gel Extraction Kit according to the manufacturer's protocol.

3.4.3 Enzymatic DNA methods

3.4.3.1 Restriction digests

For analytical restriction digests the DNA was incubated with specific enzymes in an appropriate buffer for 1 - 2 h at 37 °C. The used enzyme amount was calculated on the basis of λ-DNA reference restriction. The reaction buffer was chosen according to manufacturer's recommendation. Following incubation, restriction enzymes were heat-inactivated for 20 min at 80 °C and the restriction pattern was examined by agarose gel electrophoresis (3.4.2.2).

3.4.3.2 Ligation of DNA fragments

For ligations 1 µl T4 ligase was used per 30 µl 1 x T4 buffer. About 2 µg of total DNA were used and the molar ratio of the vector and the insert was chosen to be 1:3. The mixture was incubated overnight at RT. The DNA was stored at 4 °C until being transformed into *E. coli* (3.4.1.3).

3.4.3.3 PCR

For the amplification of DNA fragments a polymerase chain reaction (PCR) according to Saiki et al., 1988 was performed. 50 ng plasmid DNA was mixed with 3 µM primer (fwd and rev), 160 µM dNTPs (each) and 2.5 U PfuTurbo DNA polymerase in 50 µl 1 x Pfu DNA polymerase reaction buffer. The DNA was amplified in a thermocycler using the following PCR conditions: 95 °C for 2 min, followed by 30 cycles 95 °C / 30 s, 55 °C / 30 s and 72 °C / 30 s. After 7 min at 72 °C the PCR product was stored at 4 °C before being purified with the QIAquick Gel Extraction Kit using the QIAquick PCR Purification Kit protocol.

3.4.3.4 Colony PCR

The colony PCR was used to screen for successful ligations. For each reaction a mixture consisting of 1 µl GOTaq polymerase, 0.4 µM primers (fwd and rev) and 0.6 mM dNTPs in a total volume of 50 µl in 1 x PCR buffer was prepared. A small amount of an *E. coli* colony from an agar plate was transferred into the mixture with a yellow pipet tip and mixed. As controls the according plasmid with and without insert were included. 1 µl of this PCR mixture was transferred into 100 µl antibiotic containing LB to cultivate the bacterial clone at 37 °C under gentle agitation.

To amplify the DNA fragment the following PCR conditions were used: 95 °C for 5 min, followed by 35 cycles 95 °C / 60 s, 54 °C / 90 s and 72 °C / 60 s. After 5 min at 72 °C the PCR was stored at RT until being analysed on an agarose gel (3.4.2.2). Positive clones were selected and 1.9 ml LB medium containing the appropriate antibiotic was added to the bacteria culture for further growth.

3.4.3.5 Sequencing of DNA

DNA was sequenced using the sequency facility of the University Hospital Münster. For that purpose, the purified DNA was amplified via PCR using the BigDye Terminator Cycle Sequencing Kit.

300 ng plasmid DNA was incubated with 1 µl BigDye and 0.5 µM primer in 1 x BigDye buffer in a total volume of 10 µl in a thermocycler. The following PCR conditions were used: 96 °C for 5 min, followed by 25 cycles at 96 °C / 10 sec and 55 °C / 4 min. The reaction volume was adjusted to 20 µl and the DNA was stored at 4 °C until being sequenced.

3.4.3.6 Real-time PCR

The quantitative real-time PCR analysis was used to determine the mRNA level of annexin A1 and annexin A2 in PR8-infected A549, HeLa or HepG2 cells. The cells were infected in a 6 cm cell culture dish (3.5.1) and the mRNA was isolated at the indicated time points using the RNeasy Mini Kit. The mRNA was quantified using the Eppendorf BioPhotometer and 1 µg was transcribed into cDNA with the help of the High-Capacity cDNA Reverse Transcription Kit according to the manufacturer's protocol.

The cDNA preparations were then subjected to real-time PCR using an ABI Prism 7900 HT system. The reactions contained Platinum SYBR Green qPCR SuperMix UDG with ROX reference dye and appropriate primers (550 nM or 1 x QuantiTect Primer Assay). About 0.2 ng cDNA per 50 µl reaction mix were used.

The following PCR conditions were used: 50 °C for 2 min, then 95 °C for 2 min, followed by 40 cycles at 95 °C / 15 sec and 60 °C / 60 sec. All real-time PCR reactions were carried out in duplicate. The expression level of the gene of interest was normalised to GAPDH controls using the $2^{-\Delta\Delta C(T)}$-method (Livak and Schmittgen, 2001).

3.4.4 Cloning of mCherry labelled annexin A2 constructs

The GFP-tag of anxA2-GFP wt and mutants was substituted with mCherry to obtain red labelled annexin A2 constructs that could be used for Laurdan microscopy (3.2.7).

mCherry was amplified from pRSET-B mCherry using mCherry primers harbouring *Bam*H I and *Not* I cutting sites (3.4.3.3). The purified PCR product as well as the plasmid anxA2-GFP were digested with *Bam*H I and *Not* I for 2 h at 37 °C (3.4.3.1). After heat inactivation of the enzymes the DNAs were separated on an agarose gel. The desired vector backbone as well as the mCherry insert were isolated from the gel (3.4.2.3) and ligated (3.4.3.2). The ligation mixture was transformed into *E. coli* which were selected with kanamycin (3.4.1.3). For identification of successful ligations a colony PCR was performed using mCherry primers (3.4.3.4). Positive clones were amplified in a small scale and sequenced with pEGFP-N.3'.2-primer (3.4.3.5). The correct expression of mCherry tagged annexin A2 was verified by transfecting the construct into A549 cells (3.2.4.1) and analysing the red fluorescence by confocal microscopy. The mCherry insert of one positive clone was cut out with *Bam*H I and *Not* I and ligated with the purified vector backbone of either anxA2 YE-GFP, YF-GFP, KA-GFP, PM-GFP, PMCM-GFP or GFP that was cut with the same enzymes. Recombinant plasmids were identified by transformation of competent *E. coli* and selection with kanamycin, followed by colony PCR. The correct insertion of mCherry was verified by sequencing using pEGFP-N.3'.2-primer. Positive clones were amplified in large scale.

3.5 Virological methods

All experiments involving influenza A viruses were performed at the Institute of Medical Virology, University of Münster.

3.5.1 Viral infection of cells

Cells were washed with PBS before being incubated with an appropriate dilution of virus in infection PBS. The incubation was performed for 30 min at 37 °C and 5 % CO_2. Afterwards the virus was removed and the cells were washed before further cultivation in infection medium. To determine the amount of infectious virus particles in the supernatants of the infected cells a plaque assay was performed (3.5.2) and the infections were carried out in duplicate. Where indicated cell lysates of the infected cells were made (3.3.1) or the cells were prepared for real-time PCR analysis (3.4.3.6).

<u>infection PBS</u>
Dulbecco's PBS
1 mM $MgCl_2$
0.9 mM $CaCl_2$
100 units/ml penicillin
0.1 mg/ml streptomycin
0.2 % (w/v) BA

<u>infection medium</u>
DMEM or MEM
1 mM $MgCl_2$
0.9 mM $CaCl_2$
100 units/ml penicillin
0.1 mg/ml streptomycin
0.2 % (w/v) BA
[0.000 06 (v/v) % trypsin SOLO for PR8]

3.5.2 Plaque assay

To determine the amount of infectious virus particles in the supernatant of infected cells or to determine the virus titre of propagated viruses standard plaque assay on MDCK according to Gaush and Smith, 1968 was performed.

One 6-well plate of MDCK-IMV grown to confluency was used for each virus solution. The cells were infected with 500 µl of a logarithmic dilution of the virus as described above (3.5.1). After the infection the virus was removed and the cells were covered with 2 ml agar medium. This agar medium consisted of a fresh mixture of 15 ml 46 °C warm 3 % agar and 35 ml 37 °C warm 2 x MEM. After hardening of the agar medium the 6-well plates were incubated upside down in a CO_2 incubator until analysis of the plaques (2 d for FPV, 3 d for PR8). The plaques were visualised by staining the agar with a dilution of neutral red in PBS for 1 h at 37 °C. The plaques were counted and the amount of plaque forming units (PFU) per ml was calculated.

2 x MEM
14.3 % (v/v) 10 x MEM
143 units/ ml penicillin
0.143 mg/ml streptomycin
0.268 % $NaHCO_3$ (from 7.5 % (w/v) stock)
0.014 % (w/v) DEAE-dextran
0.3 % (w/v) BA
[0.000 086 % (v/v) Trypsin SOLO
1.43 mM $MgCl_2$
1.29 mM $CaCl_2$ for PR8]

3.5.3 Influenza virus propagation

3.5.3.1 Propagation of FPV in MDCK

FPV was propagated on MDCK-IMV by infecting the cells as described above (3.5.1). An MOI of 0.001 was used for this infection. When the cytopathic effect was visible (after 24 h to 48 h) the supernatant was harvested and clarified by low-speed centrifugation (10 min at 2 000 rpm; Eppendorf C5810R). The virus titre could be determined by plaque assay (3.5.2) or the virus was purified as described below (3.5.4).

3.5.3.2 Propagation of PR8 in embryonated chicken eggs

The human influenza virus PR8 efficiently propagates in chicken eggs. 11 - 14 days old chicken embryos were used. Inocculation of the eggs and harvesting of the virus were performed as sterile as possible. To achieve this, eggs and all materials used were disinfected with 70 % ethanol.
A small hole was drilled at the bottom side of an egg to inject the virus ($1*10^{-4}$ - $1*10^{-5}$ PFU / 100 µl infection PBS) with a sterile syringe into the allantoic fluid. The hole was closed with glue (Ponal) and the eggs were incubated for 50 h at 37 °C and 70 % humidity.
After the chicken embryos were killed by incubating the eggs at -20 °C for 2 h or at 4 °C overnight the virus was harvested by gently opening and removing the shell at the bottom of the egg with the help of a spoon and tweezers. The virus containing fluid of the allantois was removed. The amount of infectious virus particles was determined by plaque assay (3.5.2) and the virus was stored at -80 °C.

3.5.4 Influenza virus purification

1.5 ml of FPV propagated on MDCK-IMV cells for 24 h (3.5.3.1) was spun for 2 min at 14 000 rpm at 4 °C (Eppendorf 5417R) to remove cellular debris. The supernatant was then layered on top of a sterile 400 µl sucrose cushion (20 % (w/v) sucrose in water) in a 2 ml test tube. After centrifugation for 90 min at 14 000 rpm at 4 °C the supernatant was discarded except the last 20 µl which contain the purified virus particles.

4 Results

4.1 Role of annexin A2 in IAV infection

4.1.1 Annexin A2 dependency of IAV replication

4.1.1.1 IAV replication in XM expressing cells

Finding novel cellular proteins that are of importance for the infection of IAV could help in defining new strategies to fight the causative agent of the flu. To investigate whether annexin A2 is involved in the life cycle of IAV the replication of this virus in different cell lines with different annexin A2 protein levels was examined.

First, an MDCK cell line was used that can be induced to express a dominant negative annexin A2/p11 chimeric protein. This so-called XM protein precipitates endogenous annexin A2 and p11 and thus interferes with its function (Harder and Gerke, 1993). The mode of action of this chimeric protein is explained in detail in Figure 4-1.

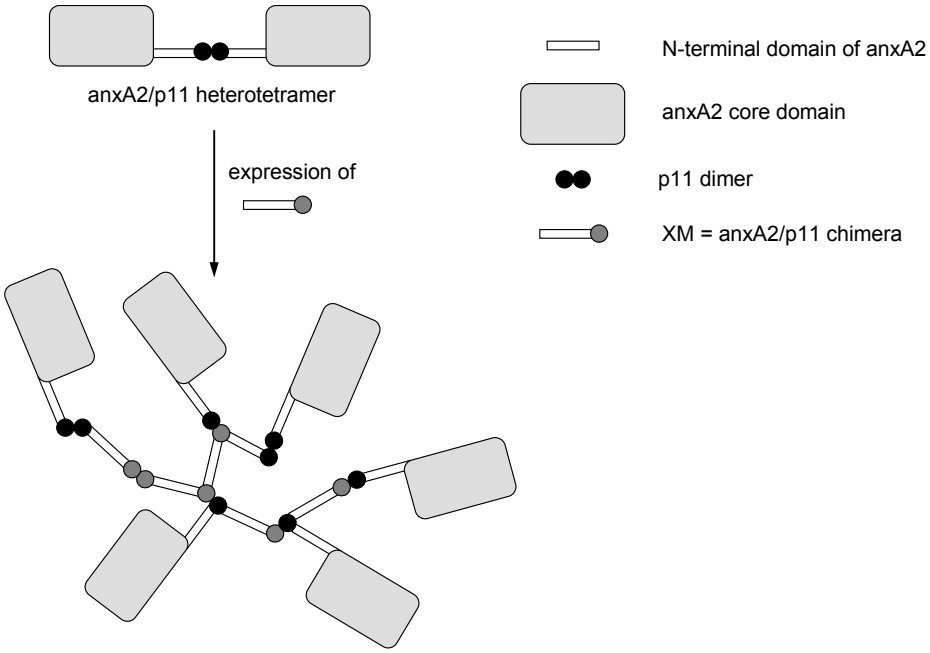

Figure 4-1: Schematic presentation of multimeric annexin A2/p11 aggregates induced by the anxA2/p11 chimera
A chimera comprising the N-terminal region of annexin A2, i.e. the entire p11-binding domain, fused to a complete p11 protein is still able to dimerise and bind annexin A2 and also binds additional p11 dimers via its N-terminus. Expression of such a trivalent chimera in cells containing the annexin A2/p11 complex therefore leads to the formation of large aggregates containing endogenous annexin A2 and p11 in addition to the chimeric protein. From Harder and Gerke, 1993.

The MDCK cell line used for these experiments stably expresses the XM protein under the control of a tetracycline (tet)-dependent promoter. For the induction of the chimeric protein the cells were incubated for four days without the addition of tet. The expression can be checked by immunofluorescence analysis. As shown in Figure 4-2 A the expression of the XM protein can be seen by the induction of aggregates of annexin A2 and p11. This leads to a depletion of cytosolic annexin A2. Membrane bound annexin A2 is influenced to a reduced extent by the expression of the

anxA2/p11 chimera. Another possibility to verify the XM expression is western blot analysis (Figure 4-2 B). The XM protein can be visualised with an anti-p11 antibody. The protein is about 2 kDa larger than endogenous p11.

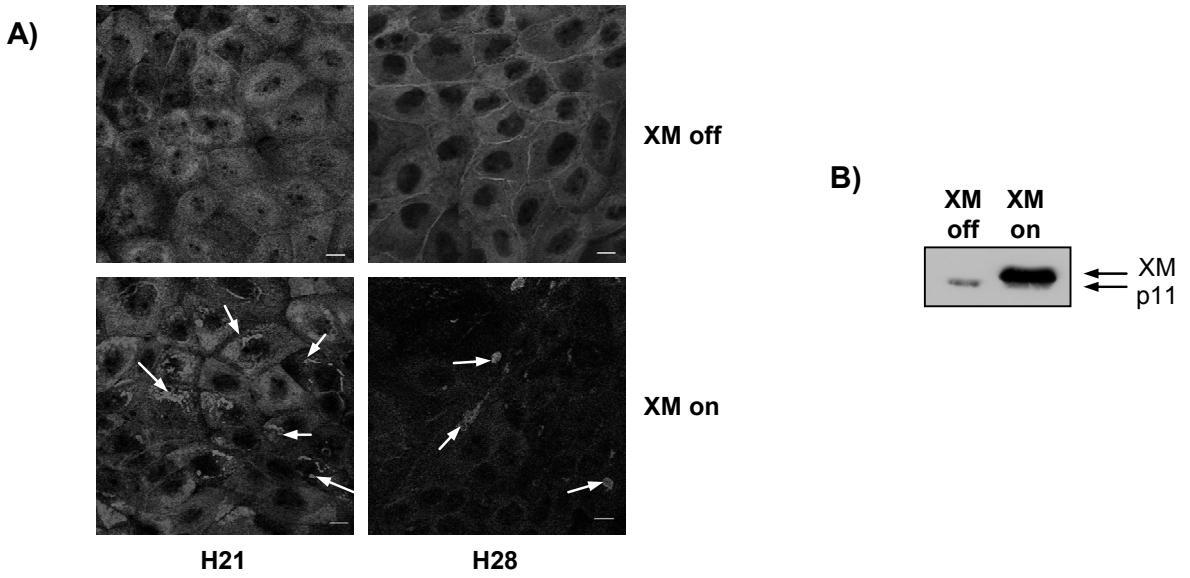

Figure 4-2: Immunofluorescence and western blot analysis of XM expression in MDCK
MDCK-XM cells were either cultivated as control in the presence of tet (XM off) or were induced to express the chimeric protein (XM on) by the removal of tet for four days. A) The expression of XM was verified by immunofluorescence analysis. Cells were fixed and permeabilised and annexin A2 was visualised with the antibody H28 and p11 with H21. As secondary antibody GαMs Cy2 was used. Precipitates of annexin A2 and p11 can be detected after the expression of XM (arrows; scale bars: 10 µm). B) The induction of the XM protein can be visualised in a western blot of cell extracts. An αp11 antibody (H21) reveals a band running slightly slower than p11 in XM expressing cells in addition to the endogenous p11 protein.

In initial experiments performed before this thesis the human influenza strain influenza A/Puerto-Rico/8/34 (PR8) appeared to replicate with about 50 % reduced efficiency in XM expressing cells in comparison to control cells (unpublished observation by Torben Hausrat). This influence of the XM protein could only be seen after a replication period of 8 h but not after 24 h any more and also not when the experiment was repeated. No alteration of the replication of the avian influenza virus A/Bratislava/79 (FPV) upon XM expression could be detected. For this reason and because it was thought to better reflect a relevant situation for humans PR8 was used for the infection experiments.

The expression of the XM protein was induced in MDCK-XM and four days afterwards the cells were infected with PR8. Prior to infection the cells were examined with a phase contrast microscope to verify that the cell number was not altered by the induction of the XM protein. The number of infectious virus particles in the supernatant of the cells was determined via plaque assay after the indicated time periods of infection. Different infection times were chosen varying from 8 h (about one replication cycle) to 24 h (about three replication cycles). Cell lysates were made of the infected cells to verify the expression of the XM protein via western blot analysis (one example can be seen in Figure 4-2 B). As control MDCK-XM cells that were not induced to express the chimeric protein were infected using the same conditions.

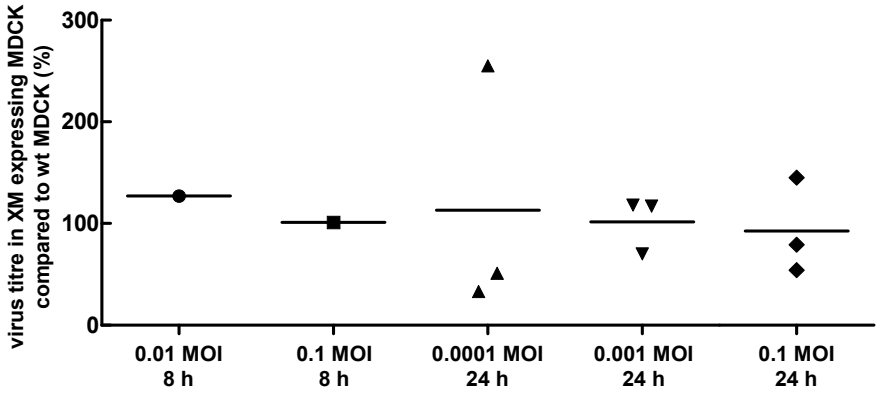

Figure 4-3: The expression of the XM protein does not have an obvious influence on the replication efficiency of PR8
MDCK-XM cells were induced to express the XM protein for four days. The cells were infected with PR8 for 30 min with different MOIs followed by different replication times. In parallel MDCK-XM cells not expressing the XM protein were infected as a control using the same conditions. The number of infectious virus particles in the supernatant of infected XM expressing cells and control cells not expressing the chimeric protein was determined via plaque assay. The virus titre in the supernatant of infected XM expressing MDCKs is presented as % of the supernatant of wt MDCK-XM infected under the same conditions. Three independent experiments were performed each using different MOIs and replication times which were partly overlapping and are indicated at the x-axis. The means are indicated by horizontal lines. The results of the individual experiments are presented in the appendix.

In MDCK cells expressing the XM protein endogenous annexin A2 and p11 form aggregates and cannot function any more in this state. This depletion of annexin A2 does not result in a detectable tendency to an altered replication efficiency of the human IAV PR8 (Figure 4-3). The observed differences were in the range of variances of viral infection assays and were not significant. Thus, the influenza replication in XM expressing cells seems to be as effective as in wt MDCKs not expressing this protein.

4.1.1.2 IAV replication in annexin A2 siRNA transfected cells

As a further approach to investigate a potential role of annexin A2 in influenza infection HeLa were depleted for endogenous annexin A2 by means of siRNA and infected with the human IAV strain PR8. HeLa cells are a human epithelial cell line derived from a cervical carcinoma that are easy to transfect and established. siRNA mediated down-regulation of annexin A2 in these cells leads to a decrease of the protein level to about 30 - 50 %. The reduction of the annexin A2 protein level was verified for each experiment via western blot analysis (Figure 4-4).

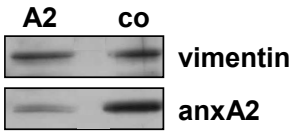

Figure 4-4: Annexin A2 depletion by siRNA in HeLa cells
HeLa were transfected with annexin A2 siRNA (A2) or non-targeting control siRNA (co). Two days after transfection total cellular lysates were subjected to SDS-PAGE and immunoblotted for annexin A2 (HH7) or vimentin as a loading control. Densitometric analysis revealed a reduction of the cellular annexin A2 level to 30 to 50 %.

However, IAV replication is described to be defective in HeLa cells. These cells have been reported to show defects in the maturation and membrane insertion of HA, in the M1 production and in the budding process (Gujuluva et al., 1994; Lohmeyer et al., 1979; Portincasa et al., 1990). Nevertheless, the HeLa cells used here were permissive to the IAV strain PR8. The achieved viral titres were in the

range of 10^5 - 10^6 PFU/ml and therewith hardly differ from those obtained in e.g. MDCK cells. IAV has been shown before to efficiently replicate in HeLa cells (Yang et al., 2009). Discrepancies to the above mentioned observations could possibly arise from the heterogeneities in specific cell clones in the various laboratories. Because HeLa cells are a well established model cell line and could be readily infected with IAV they were used for infection experiments, even though their use for influenza virus infection has been criticised.

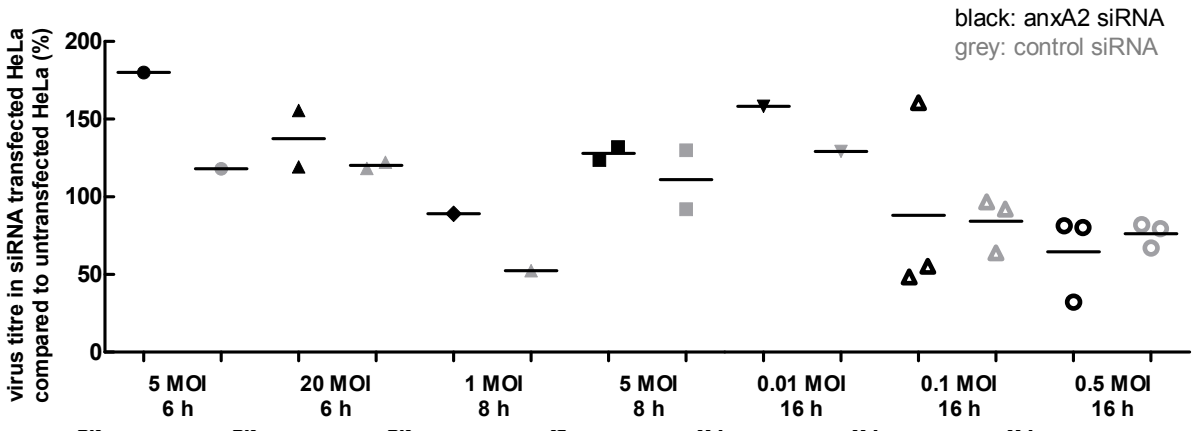

Figure 4-5: siRNA mediated down-regulation of cellular annexin A2 does not lead to a detectable difference in the replication efficiency of PR8 in HeLa cells
HeLa were transfected with annexin A2 siRNA or non-targeting control siRNA. Two days after transfection those cells as well as untransfected HeLa were infected with PR8. After different infection times the number of infectious virus particles in the supernatant of the cells was determined with a plaque assay. The virus titre in the supernatant of infected siRNA transfected cells is presented as % of the supernatant of untransfected cells infected under the same conditions (annexin A2 siRNA in black, control siRNA in grey). Five independent experiments were performed each using different MOIs and replication times which were partly overlapping and are indicated at the x-axis. The means are indicated by horizontal lines. The results of the individual experiments are presented in the appendix.

For the infection of siRNA transfected HeLa cells different experimental conditions were used as explained in the caption of Figure 4-5. Prior to infection the cells were examined with a phase contrast microscope to verify that the cell number was not altered by siRNA transfection. Infectious virus titres in the supernatant of infected siRNA transfected HeLa cells sometimes differ from those of untransfected cells but the differences were in the range of variances of plaque assays and were not significant. No tendency to an either reduced or an enhanced replication upon annexin A2 depletion could be detected. Hence, the transfection of annexin A2 siRNA as well as control siRNA in HeLa does not have a detectable influence on the replication efficiency of PR8 as can be concluded from the results of the plaque assay.

An analogous experiment was performed using the lung epithelial cell line A549 which is a well suitable model cell line for influenza infections since the lung is the location of the primary infection of this virus. Transfection of these cells with annexin A2 siRNA leads to an about 60 to 70 % reduction of the protein level which was verified for each experiment via western blot analysis (Figure 4-6).

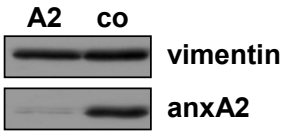

Figure 4-6: Annexin A2 depletion by siRNA in A549 cells
A549 were transfected with annexin A2 siRNA (A2) or non-targeting control siRNA (co). Two days after transfection total cellular lysates were subjected to SDS-PAGE and immunoblotted for annexin A2 (HH7) or vimentin as a loading control. Densitometric analysis revealed a reduction of the cellular annexin A2 level to about 30 to 40 %.

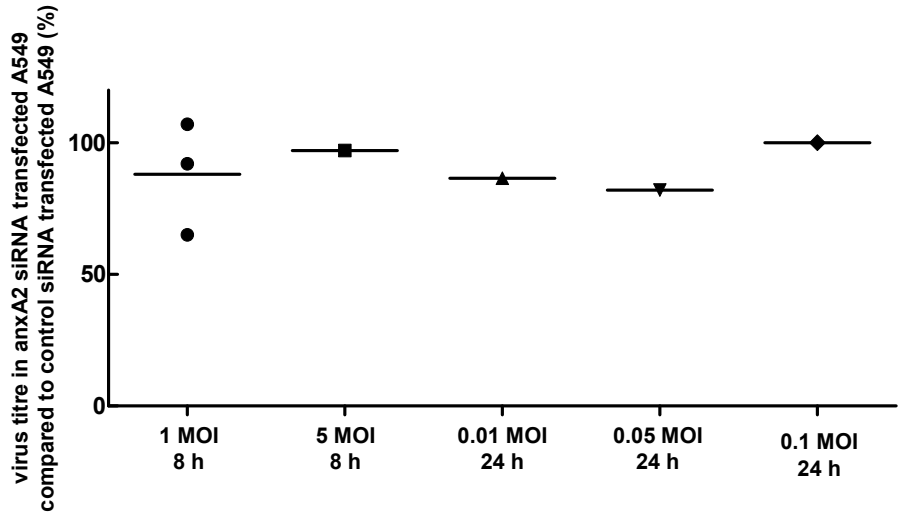

Figure 4-7: siRNA mediated down-regulation of cellular annexin A2 does not lead to a detectable difference in the replication efficiency of PR8 in A549
A549 were transfected with annexin A2 or non-targeting control siRNA. Two days after transfection those cells were infected with PR8. After different viral replication times the number of infectious virus particles in the supernatant of the cells was determined via plaque assay. The virus titres in the supernatants of infected annexin A2 siRNA transfected cells is presented as % of the supernatants of control siRNA transfected cells infected using the same conditions. Three independent experiments were performed each using different MOIs and replication times which were partly overlapping and are indicated at the x-axis. The means are indicated by horizontal lines. The results of the individual experiments are presented in the appendix.

A549 cells transfected with annexin A2 or control siRNA were infected with the human IAV strain PR8. The number of infectious virus particles in the supernatant of annexin A2 siRNA transfected A549 cells compared to control siRNA transfected A549 cells was determined via plaque assay but no tendency to an altered virus replication could be detected (
Figure **4-7**).

Untransfected cells were not included in the data analysis because virus titres in the supernatant of these cells were much higher than in the supernatant of siRNA transfected cells. This remarkably elevated virus propagation was probably due to an enhanced viability of untransfected cells since the transfection procedure with Lipofectamine 2000 stressed the A549 cells to a visible extent.

4.1.1.3 IAV replication in CMECs from an annexin A2 knockout mouse

In the above mentioned approaches to investigate the influence of annexin A2 on IAV propagation only an incomplete down-regulation of the annexin A2 protein level could be achieved. Cytosolic annexin A2 levels are reduced sufficiently by transient siRNA transfection or XM expression. However, membrane bound annexin A2 remains rather unaffected (Zobiack et al., 2003). Thus, a role of membrane associated annexin A2 in IAV replication cannot be ruled out. Since the achieved reductions of the annexin A2 protein level are only partly and not absolute it might furthermore be

possible that a certain threshold level of the protein is still present in the siRNA transfected cells that is sufficient for efficient IAV replication.

Therefore, as another possibility to investigate a potential role of annexin A2 in IAV infection a cell line from the annexin A2 knockout mouse from the group of Katherine A. Hajjar was used in another line of experiments. Cardiac microvascular endothelial cells (CMECs) isolated from a wt mouse or an anxA2$^{-/-}$ mouse were available for this analysis (Ling et al., 2004).

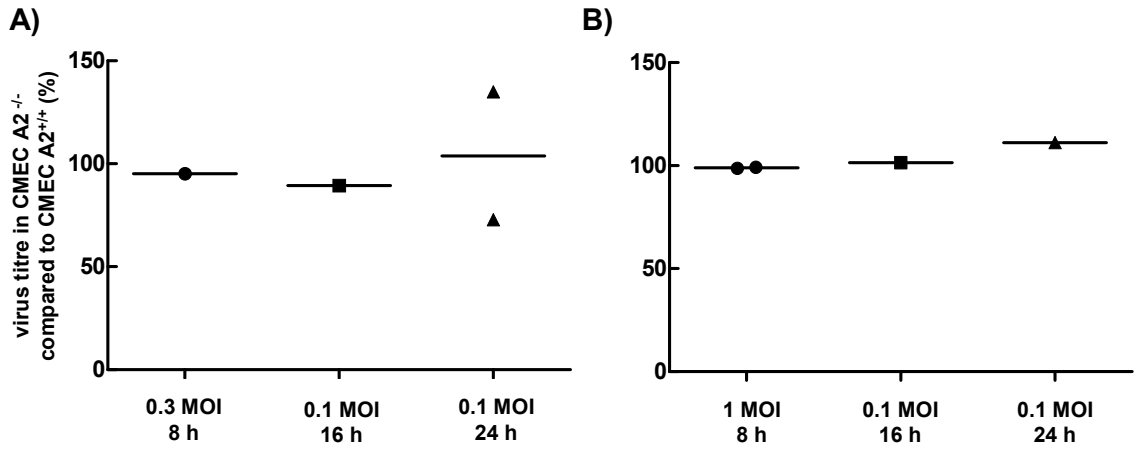

Figure 4-8: IAV replication in CMECs of an anxA2$^{-/-}$ mouse seems to be as effective as in CMECs of an anxA2$^{+/+}$ mouse
CMECs of the anxA2$^{-/-}$ mouse as well as CMECs of an anxA2$^{+/+}$ mouse were infected either with A) the human IAV PR8 or B) the avian IAV FPV. At different time points p.i. the supernatant was harvested and the amount of infectious virus particles was determined via plaque assay. The virus titre in the supernatant of infected CMECs of the anxA2$^{-/-}$ mouse is presented as % of the titre in the supernatant of CMECs of the anxA2$^{+/+}$ mouse that were infected using the same experimental conditions. Three independent experiments were performed each using different MOIs and replication times which were partly overlapping and are indicated at the x-axis. The means are indicated by horizontal lines. The results of the individual experiments are presented in the appendix.

The cells were infected for different time points with different MOIs (Figure 4-8). For these experiments not only the human IAV strain PR8 but also the avian influenza virus A/Bratislava/79 (FPV) was used to also analyse a different IAV strain for its dependency on annexin A2. The viral titres that could be achieved in this epithelial cell line ranged between 10^4 - 10^5 PFU/ml for PR8 and 10^5 - 10^7 PFU/ml for FPV. Hence, this cell line could be readily infected by IAV. However, the number of infectious virus particles in the supernatant of infected CMECs of the anxA2$^{-/-}$ mouse does not show a detectable tendency to differ from that in the supernatant of CMECs of an anxA2$^{+/+}$ mouse.

4.1.2 Real-time PCR analysis of annexin A1 and annexin A2 after IAV infection

Viral infections usually result in alterations in the host cell proteome which determine the fate of the infected cells and the progress of pathogenesis. Also the IAV is known to influence the transcription of a range of proteins.

To determine whether IAV infection has an influence on the mRNA level of annexin A2 quantitative real-time PCR analysis of PR8 infected cells was performed. Not only was the regulation of annexin A2 mRNA determined but also the regulation of annexin A1 mRNA. Annexin A1 is another well characterised member of the annexin protein family. It has anti-inflammatory activities (Perretti and Gavins, 2003). Furthermore, annexin A1 is a major substrate of the EGF receptor tyrosine kinase and has been implicated in the endocytic transport of this receptor. The phosphorylation by the EGF

receptor kinase can probably be linked to an anti-proliferative activity on annexin A1. For a review on annexin A1, see Lim and Pervaiz, 2007. Because IAV interacts with the cellular innate immune signalling (Ehrhardt et al., 2009) and cellular proliferation is also of importance for influenza virus propagation annexin A1 might be of importance for influenza replication.

The cell lines HeLa and A549 were used for this real-time PCR analysis. Those cell lines were used for IAV infection experiments before. Furthermore, PR8 infected HepG2 cells were analysed. This cell line expresses no or very little endogenous annexin A2 and p11 protein but it still possess the mRNA coding for p11 (Puisieux et al., 1996). The statements in the literature concerning the annexin A2 mRNA are contradictory. Puisieux and Ozturk were not able to detect annexin A2 mRNA in HepG2 (Puisieux et al., 1996). In contrast, Mayer and colleagues did identify annexin A2 mRNA in this cell line by real-time PCR analysis (Mayer et al., 2008). However, how this mRNA is regulated is not clear. The HepG2 clone used in this thesis also possesses annexin A2 mRNA but the protein could not be detected by western blot analysis (data not shown).

Table 4-1: Quantitative real-time PCR analysis does not reveal a difference in annexin A1 or annexin A2 mRNA level after IAV infection

A549, HeLa or HepG2 were infected with 5 MOI PR8 for 2.5 h, 5.5 h, 8 h or 16 h. The mRNA of the cells was isolated and the levels of annexin A1, annexin A2, M1 and GAPDH mRNAs were determined via real-time PCR analysis. Presented in the table are the calculated “n-fold induction” of different time points of three independent experiments. (n.d.: not determined)

mRNA	cell line	infection time	experiment 1	experiment 2	experiment 3
annexin A2	A549	2.5 h	1.1	-1.0	1.0
		5.5 h	n.d.	-1.2	-2.5
		8 h	-1.4	1.5	-1.1
		16 h	n.d.	-4.1	-1.1
	HeLa	2.5 h	n.d.	-1.1	1.1
		5.5 h	n.d.	1.4	2.6
		8 h	n.d.	-1.3	-1.2
		16 h	n.d.	2.3	-1.3
	HepG2	2.5 h	n.d.	-1.9	1.1
		5.5 h	n.d.		1.0
		8 h	n.d.	-3.2	-1.3
		16 h	n.d.		-1.2
annexin A1	A549	2.5 h	1.1	-1.1	1.1
		5.5 h	n.d.	2.4	-5.3
		8 h	-1.1	2.0	1.0
		16 h	n.d.	-33.7	1.0
	HeLa	2.5 h	n.d.	-1.3	1.2
		5.5 h	n.d.	-1.4	6.8
		8 h	n.d.	-1.3	1.1
		16 h	n.d.	18.2	-1.2

M1 is a viral structural protein highly expressed in IAV infected cells. M1 mRNA was detected to verify that the infection of the cells and the transcription of viral genes occurred. A remarkable up-regulation of M1 mRNA could be detected after 2.5 h and 5.5 h (data not shown).
In the HepG2 cell line not every time point could be analysed because the corresponding C(T) values of GAPDH could not be determined. Furthermore, the level of annexin A1 mRNA in this cell line was below the detection limit of the real-time PCR. Therefore, HepG2 could not be analysed for the expression of this protein. An alteration of the annexin A1 or annexin A2 mRNA after PR8 infection could not be measured in any of the cell lines used under the experimental conditions chosen here.

4.1.3 Hemagglutinin localisation in annexin A2 depleted cells

Annexin A2 is involved in the apical transport of raft associated proteins in polarised cells (Jacob et al., 2004). Influenza HA is a raft associated protein and this association is of importance for an efficient viral replication (Takeda et al., 2003). Therefore, the question arose whether annexin A2 is involved in the transport of influenza HA. A549 cells that were depleted for annexin A2 by means of siRNA were used for these experiments. These cells were transfected with a plasmid encoding the HA protein of influenza A/FPV/Rostock/34 (H7-HA) (Marjuki et al., 2006). The surface localisation of H7-HA was first analysed by immunofluorescence (
Figure 4-9).

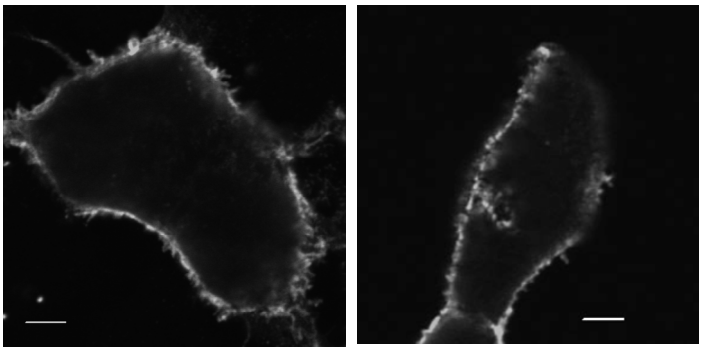

control siRNA **anxA2 siRNA**

Figure 4-9: Annexin A2 depletion of A549 does not alter the surface localisation of influenza HA as determined by confocal immunofluorescence analysis
A549 seeded on coverslips were transfected with annexin A2 or control siRNA. 48 h after siRNA transfection the cells were transfected with a plasmid encoding H7-HA. The next day surface localisation of hemagglutinin was determined after fixation of the cells and incubation with a polyclonal αH7-HA antibody and Cy2 labelled GαMs antibody. Cells were not permeabilised to ensure that only surface HA is visualised. Representative pictures of four independent experiments are depicted here. (scale bars: 5 µm)

The plasmid encoded HA of FPV/Rostock localises to the surface of A549 cells as determined by confocal immunofluorescence microscopy. This localisation is not altered upon depletion of cytosolic annexin A2 by siRNA.

The surface expression of HA was quantified via flow cytometric analysis. A549 cells transiently expressing H7-HA were labelled with specific antibodies and analysed by FACS measurements. Cells that were transfected with annexin A2 or control siRNA prior to plasmid transfection were included in these experiments to be able to assess the role of annexin A2 in the surface transport of influenza HA in A549.

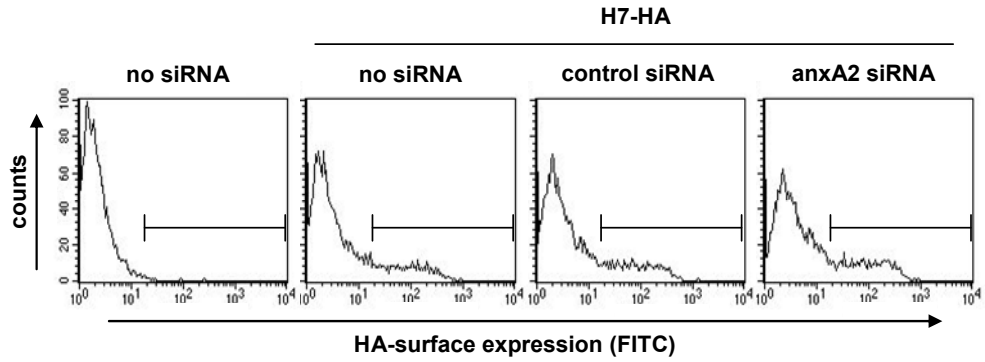

Figure 4-10: Flow cytometric analysis of HA surface expression in A549 does not reveal a dependency of HA transport on cytosolic annexin A2
A549 were depleted for annexin A2 by transfection with annexin A2 siRNA. 48 h later the cells were transfected with a plasmid encoding H7-HA. 72 h after siRNA transfection the surface localisation of HA was determined via flow cytometry using the monoclonal αH7-HA antibody and a FITC labelled GαRb antibody. As controls untransfected cells as well as cells transfected with H7-HA but not depleted for annexin A2 (either no siRNA or control siRNA) were stained and analysed. Gates were set to quantify the fluorescence. Here representative histograms of the HA fluorescence of three independent experiments are depicted.

Surface expression of HA could be detected by a shift of the fluorescence in the flow cytometer. About 15 to 25 % of the total fluorescence was shifted to the right when H7-HA was expressed. This amount was not altered significantly when cells were transfected with control or annexin A2 siRNA.
These data as well as the immunofluorescence data indicate that the A549 cells used for these experiments do not require cytosolic annexin A2 for the transport of influenza HA to the cell surface.

4.1.4 Annexin A2 and FPV localisation in infected cells

To further determine a possible involvement of annexin A2 in IAV infection the localisation of this protein as well as the localisation of the virus in FPV infected A549 cells was analysed via confocal immunofluorescence microscopy. The avian influenza FPV was used for this study because an antibody was available to visualise this virus. This was not the case for PR8. Different time points were chosen for this analysis varying from 0 h to determine the background staining of the antibody to 8 h at the end of the viral replication cycle (Figure 4-11).

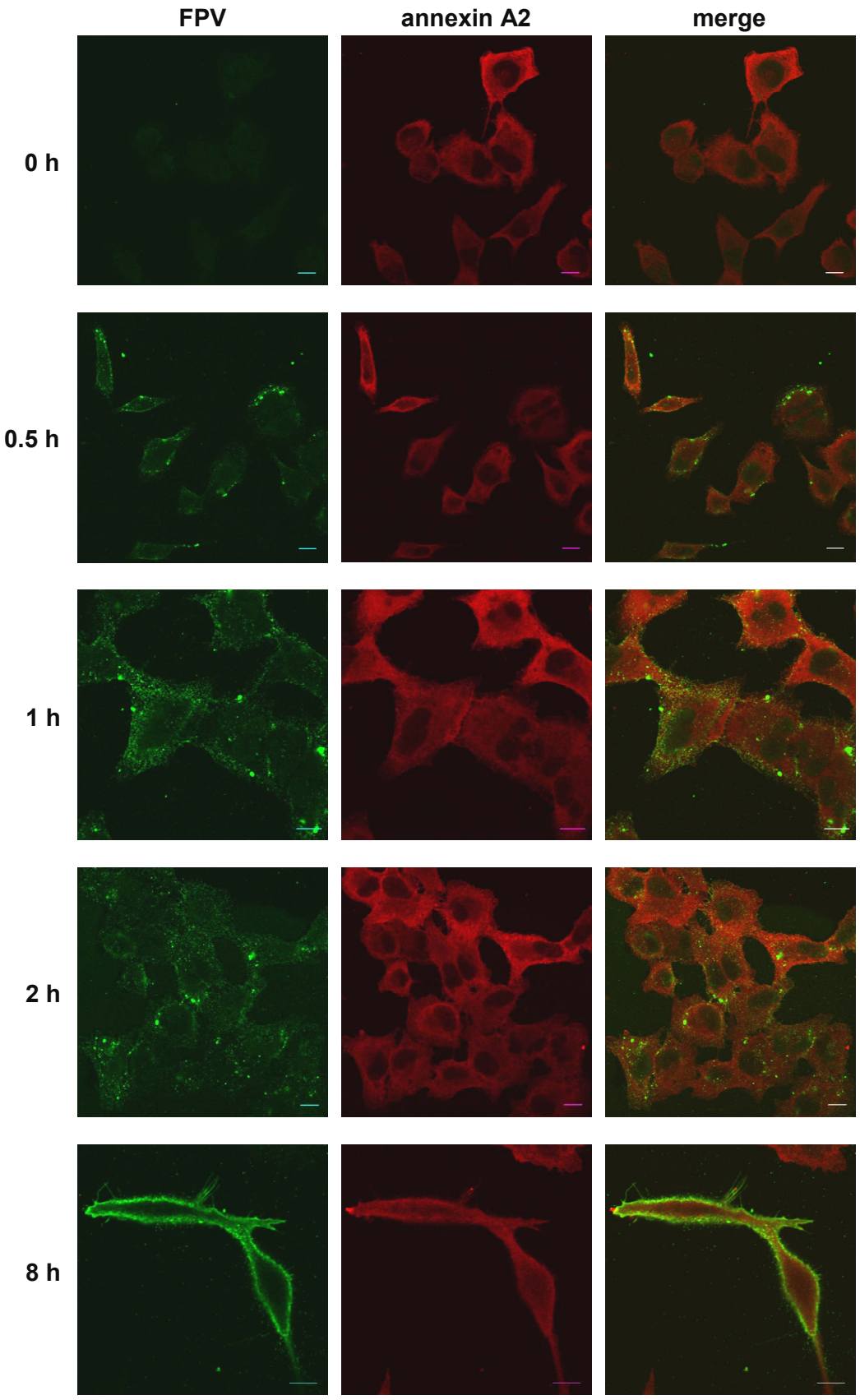

Figure 4-11: Annexin A2 and IAV do not colocalise in A549 cells
A549 seeded on coverslips were infected with 30 MOI FPV for 0 h, 30 min, 1 h, 2 h or 8 h, fixed, permeabilised and stained with αH7-HA in combination with GαRb Alexa488 as a secondary antibody. Annexin A2 was visualised using HH7 and GαMs TxRed. Representative pictures of three independent experiments are depicted here. (scale bars: 10 µm)

In IAV infected cells annexin A2 shows a typical cytoplasmatic distribution. It is excluded from the nucleus and sometimes localised to the cellular membrane. At early infection points a patchy distribution of the virus on or near the cellular surface could be detected. After 30 min infection the anti-FPV antibody decorates structures localised near the cellular membrane. After 1 h and 2 h these punctual structures are distributed more throughout the cytosol. Following 8 h infection viral protein could mostly be detected close to the cellular membrane, indicating that new virus particles assemble at these sites and the replication cycle is almost completed.
At none of these infection time points a redistribution of annexin A2 or a colocalisation of this protein with FPV-positive structures was detectable.

4.1.5 Annexin A2 incorporation in IAV particles

Enveloped virions released from infected cells carry numerous proteins from the host cell. Some of the identified host cell proteins may play an important role in viral replication (Cantin et al., 2005). Also annexin A2 and other annexins have been shown to be incorporated into viral particles of e.g. HIV-1, herpes simplex virus 1, vesicular stomatitis virus and HCMV (Harrist et al., 2009; Moerdyk-Schauwecker et al., 2009; Padula et al., 2009; Wright et al., 1995).
To investigate whether annexin A2 was incorporated into influenza virions purified virus particles were analysed via western blot for annexin A2 (Figure 4-12). For this study the avian virus FPV was used because it can easily be propagated on MDCKs and much higher virus concentrations can be achieved with this strain in comparison to the human strain PR8.

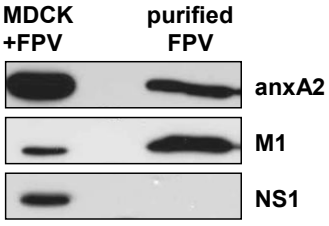

Figure 4-12: Annexin A2 is incorporated into influenza A virions
FPV was propagated on MDCK cells and purified by centrifugation through a 20 % sucrose cushion. The pelleted virus particles were resuspended in sample buffer, separated on an SDS-PAG and analysed via western blotting. M1 and NS1 were detected with the help of specific antibodies. Annexin A2 was visualised using HH7. The left lane shows cell lysates of MDCKs infected with FPV, the right lane shows lysates of the purified virions. Presented here is the only experiment that did not show a contamination with NS1.

Western blot analysis revealed the presence of annexin A2 in purified FPV particles in addition to the viral matrix protein M1. In contrast, the non-structural protein NS1 was not detected in the virions. This influenza protein is synthesised in the host cell during the course of infection but it is not a structural protein of the virus particle. The absence of NS1 in the FPV preparation indicates that the virus lysate contains no or only very little contamination with cellular debris.

4.2 Involvement of annexin A2 in apoptotic processes

Influenza viruses induce apoptosis in infected cells. On the one hand this is a host mechanism to limit virus spread but on the other hand IAV has taken advantage of some of the apoptotic processes to efficiently replicate. E.g. it has been demonstrated that the activation of caspase-3 is important for efficient IAV replication (Wurzer et al., 2003).

In the experiments performed here IAV infected cells showed morphological changes reflecting those of apoptosis: the cell body rounds up and looses the contact to the substratum. It was noted that annexin A2 depleted cells showed more drastic morphological changes upon IAV infection than control siRNA transfected cells. To verify whether this visual observation is indeed due to increased apoptosis the cleavage of PARP (poly(ADP-ribose) polymerase) was detected. PARP is a direct substrate of the effector caspase-3. The cleavage of PARP as detected by western blot analysis is therefore an indicator for the onset of apoptosis.

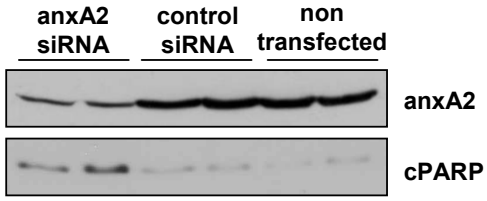

Figure 4-13: PARP cleavage after IAV infection is increased in annexin A2 depleted cells
HeLa cells transfected with the indicated siRNAs were infected with 5 MOI PR8 for 8 h and cell lysates were made. The lysates of the infected cells were separated on an SDS-PAG, transferred onto a PVDF membrane and cleaved PARP was detected by means of a specific antibody. Annexin A2 depletion was confirmed by detection of the protein level with the antibody HH7. The experiment was performed in duplicate because the amount of infectious virus particles in the supernatants of the cells was analysed by plaque assay (see Figure 4-5). A representative blot of three independent experiments, each employing several infection conditions, is depicted here.

HeLa cells that were depleted for annexin A2 by means of siRNA were infected with PR8. The virus titres in the supernatants of the cells were determined by plaque assay as described above (see Figure 4-5). Lysates of the cells were analysed by western blot for the cleavage of PARP and for annexin A2 depletion. Cells that were depleted for annexin A2 show a remarkable increase in the cleavage of PARP (
Figure 4-13). This phenomenon could also be seen with other virus titres and infection times and also in A549 cells (data not shown). This indicates that the visual observation that annexin A2 depleted IAV infected cells show more drastic apoptotic like morphological changes than control cells indeed reflects a different onset of apoptosis.

When infecting CMECs with influenza the cells from the annexin A2 knockout mouse showed increased morphological changes when compared to wt CMECs. This visual observation was similar to that of PR8 infected HeLa cells. Therefore, also cell lysates of virus infected CMECs were made and analysed for PARP cleavage (Figure 4-14). CMECs of the anxA2$^{-/-}$ mouse show an increase of the PARP cleavage after IAV infection when compared to wt CMECs. This effect could only be seen after prolonged infection times though.

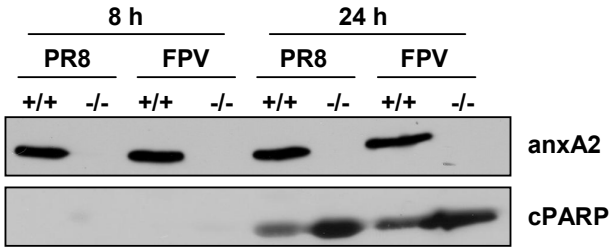

Figure 4-14: PARP cleavage is enhanced in IAV infected CMECs of the anxA2$^{-/-}$ mouse than in CMECs of a wt mouse
CMECs were infected with IAV as described in the caption of Figure 4-8. The lysates of the infected cells were used to detect the PARP cleavage by western blot analysis. Furthermore, annexin A2 was detected with the help of the specific antibody from BD Transduction Lab to demonstrate the cellular level of this protein. The viral titres used in this experiment were for PR8 0.3 MOI for 8 h and 0.1 MOI for 24 h and for FPV 1 MOI for 8 h and 0.1 MOI for 24 h. A representative blot of three different experiments is shown here.

The mechanisms being involved in influenza-induced apoptosis are very complex and only partly understood. To better understand the involvement of annexin A2 in apoptotic processes the influence of annexin A2 depletion on the effects of other apoptotic stimuli was investigated.

Staurosporine is commonly used as an initiator of apoptosis (Bertrand et al., 1994). The exact mechanism of action of this broad-specificity kinase inhibitor remains poorly understood. It has been shown in melanoma cells that staurosporine activates Bax and the mitochondrial caspase-dependent apoptotic pathway but it also induces apoptosis by caspase-independent pathways (Zhang et al., 2004).

In addition, TNFα was used as an activator of the receptor mediated apoptotic pathway. TNF-induced cytotoxicity is potentiated by inhibitors of protein synthesis like cycloheximide (CHX) (Polunovsky et al., 1994).

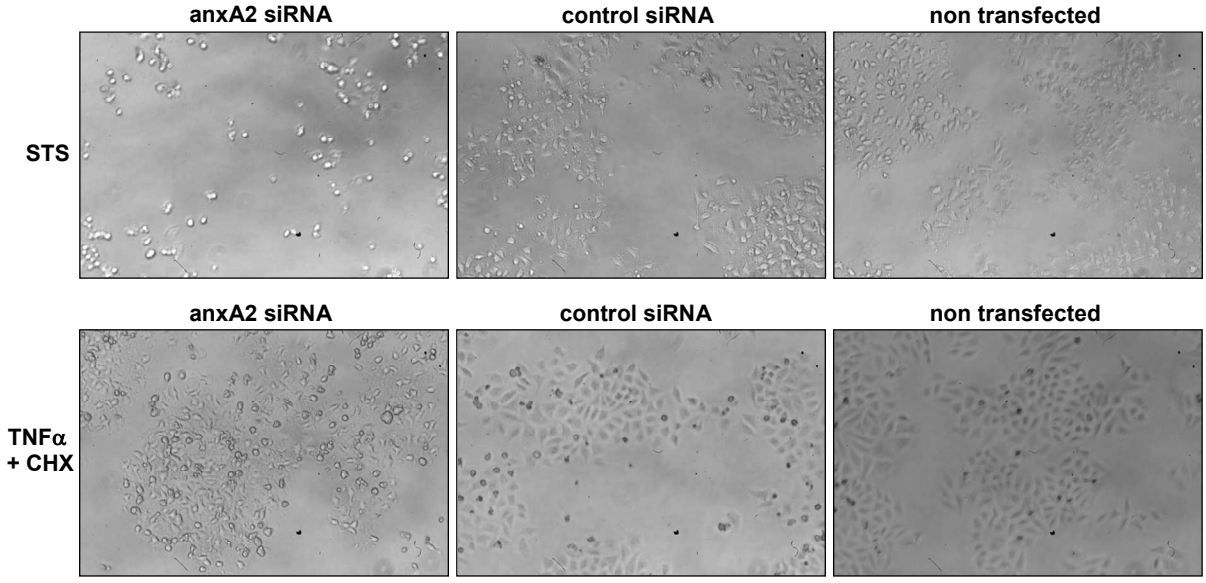

Figure 4-15: Annexin A2 depletion increases apoptosis induction by staurosporine and TNFα which can be seen through a phase contrast microscope
Two days after transfecting HeLa cells with the indicated siRNAs the cells were stimulated either with 0.1 µM staurosporine (STS) or with 0.1 ng/ml TNFα + 10 µg/ml CHX for 5 h. Pictures were taken using an Axiovert 40 C brightfield microscope with a 10 x objective using an EOS 350D camera. This effect could be seen in four independent experiments using different incubation times.

HeLa cells were incubated with either staurosporine or TNFα in combination with CHX. Already after a short time the apoptosis induction was visible. Annexin A2 depleted cells showed more drastic morphological changes than control cells. They appeared more rounded up and detached. This observation was similar to the morphological changes of annexin A2 depleted cells upon IAV infection. Pictures of cells treated for 5 h with staurosporine or TNFα + CHX are depicted here to demonstrate this visual observation (Figure 4-15).

Cell lysates were made at different time points after apoptosis induction to check for the cleavage of PARP as an indicator for the onset of apoptosis (Figure 4-16). The PARP cleavage was more drastic in annexin A2 depleted cells. This effect was independent of the apoptotic stimuli. Even without the induction of apoptosis an enhanced PARP cleavage could be seen in some cases. This PARP cleavage is probably due to the stress induced by the transfection procedure.

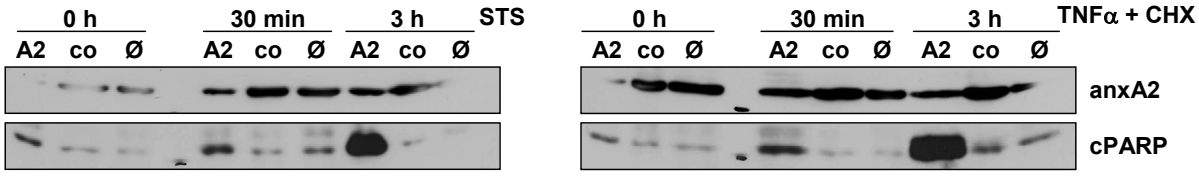

Figure 4-16: Annexin A2 depletion enhances staurosporine and TNFα induced PARP cleavage
HeLa cells were transfected with the indicated siRNAs (A2: annexin A2, co: control) or not transfected (Ø) and were stimulated with 0.1 µM STS or 0.1 ng/ml TNFα + 10 µg/ml CHX. After 0 h, 30 min or 3 h cell lysates were made and analysed by means of western blot. Cleaved PARP was detected with a specific antibody and annexin A2 depletion was verified with the HH7 antibody. A representative blot of four independent experiments is shown here.

The decrease of cellular annexin A2 leads to an increased sensitivity of cells to apoptotic stimuli not only in HeLa cells but also in A549 cells (data not shown). Overall the signal of the cleaved PARP in a western blot is about three times more intense in annexin A2 depleted cells in comparison to control cells as could be determined by densitometric measurements.

The cleavage of PARP is a measure of the activity of the effector caspase-3. Caspase-3 on the other hand can be activated by the upstream initiator caspases-8 and -9. To investigate to which extent the activation of these caspases is also influenced by annexin A2 depletion, HeLa cells were transfected with annexin A2 siRNA or control siRNA and stimulated with staurosporine or TNFα + CHX for different time durations. Cell lysates were made and analysed for the cleaved products of these caspases via western blot (Figure 4-17). Not only the PARP cleavage was enhanced in annexin A2 depleted cells but also the cleavage of the analysed caspase-8 and caspase-9.

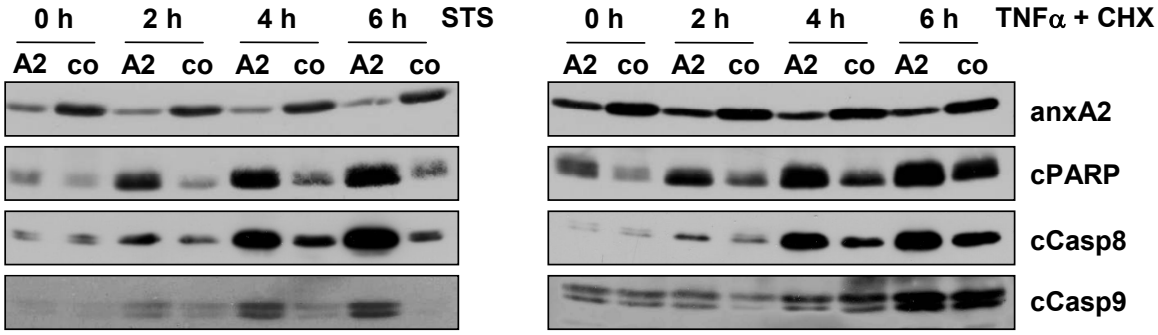

Figure 4-17: Annexin A2 depletion enhances staurosporine- and TNFα-induced caspase-8 and caspase-9 cleavage
HeLa cells transfected with the indicated siRNAs (A2: annexin A2, co: control) were stimulated with 0.1 µM STS or 0.1 ng/ml TNFα + 10 µg/ml CHX. After 0 h, 2 h, 4 h or 6 h cell lysates were made and analysed by means of western blot. The cleavage of PARP as well as the cleavage of caspase-8 and caspase-9 was detected with specific antibodies and annexin A2 depletion was verified with the antibody from BD Transduction Lab. A representative blot of three independent experiments is depicted here.

4.3 Association of annexin A2 with membrane microdomains

Membrane rafts have been identified to be the sites of influenza virus budding. Those microdomains provide a mean for cellular membranes to locally concentrate effectors to form platforms that function in multiple cellular processes. In the case of influenza virus budding they function by locally concentrating the influenza glycoproteins HA and NA which leads to the further recruitment of other viral components (Suomalainen, 2002). Annexin A2 is one of the few known structural proteins on the cytoplasmic site of membrane rafts and is involved in the aggregation and stabilisation of these microdomains. This feature of annexin A2 could affect influenza infectivity (see above) and also influence a whole range of other pathogens that employ membrane rafts or raft components to enter their host (Rosenberger et al., 2000). To further illuminate the function of annexin A2 as a raft protein it was investigated which features of annexin A2 are important for the association of this protein with these membrane microdomains.

4.3.1 Cell fractionation by DRM flotation gradient

Resistance to extraction by detergents, most prominently Triton X-100, at 4 °C is widely used as a criterion for rafts and raft-association of cellular proteins and lipids (Brown and London, 1998). Isolation of detergent resistant membranes (DRMs) can be followed by equilibrium density gradient centrifugation. The DRMs float because of their detergent resistant association with lipids. Separating DRMs from detergent soluble material using gradient centrifugation is usually preferable to pelleting. Pelleting of DRMs from detergent extracts might lead to contaminations with other sedimentable material, e.g. cytoskeletal components (Celis, 2005).

To analyse the association of endogenous and ectopically expressed annexin A2 with DRMs MDCK-anxA2-GFP were extracted with Triton X-100 on ice and submitted to a flotation gradient centrifugation. This cell line stably expresses GFP labelled annexin A2 in addition to the endogenous protein.

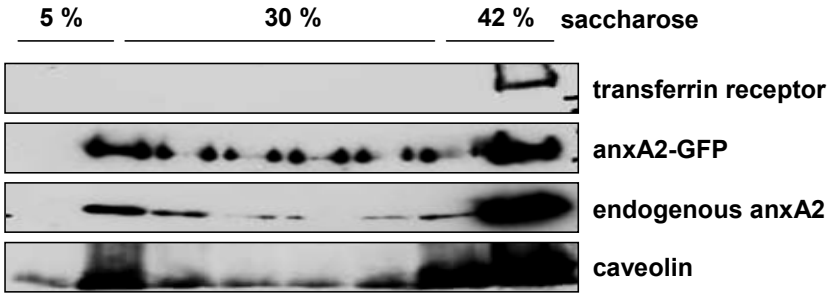

Figure 4-18: Detergent incubation and subsequent saccharose density gradient centrifugation results in the flotation of endogenous and ectopically expressed annexin A2 to low density fractions
MDCKs stably expressing GFP-tagged annexin A2 (MDCK-anxA2-GFP) were extracted with 1 % Triton X-100 on ice and a saccharose gradient centrifugation was performed. Fractions were collected from the top and the proteins were concentrated by TCA precipitation. The proteins were separated on an SDS-PAG and transferred onto a PVDF membrane. Caveolin as a marker for detergent resistant membranes and transferrin receptor as a marker for detergent soluble fractions were visualised with the help of specific antibodies. For the detection of endogenous annexin A2 and ectopic annexin A2-GFP the αannexin A2 antibody from BD transduction laboratories and the αGFP antibody were used, respectively. This blot depicts the only successful gradient centrifugation performed in this thesis.

The endogenous annexin A2 of MDCK-anxA2-GFP as well as the ectopically expressed annexin A2-GFP float to low density fractions in a saccharose gradient as does the raft marker caveolin. The non-raft marker transferrin receptor can only be detected in high density fractions.

However, fairly often flotation density gradients did not show the expected results. The DRM marker caveolin did not float in these cases. And in some cases the non-raft marker transferrin receptor could be detected to a remarkable extent in low density fractions. This is probably due to the fact that this method shows an inherent variability in terms of results (Lingwood and Simons, 2007). For this reason and because a high number of cells is needed for a gradient centrifugation the focus was shifted to simple detergent extraction followed by pelleting - without performing a flotation gradient. With this assay not only wt annexin A2 was analysed but also the phosphorylated protein and several variants of this protein harbouring mutations at different sites.

4.3.2 Influence of Tyr23 phosphorylation and PI(4,5)P_2-binding on the association of annexin A2 with membrane microdomains

One of the posttranslational modifications of annexin A2 is the phosphorylation on Tyr23. This residue is e.g. phosphorylated by the src kinase of Rous sarcoma virus. This indicates a role of this phosphorylation in cellular transformation that recently was verified (de Graauw et al., 2008; Rescher et al., 2008). The influence of this phosphorylation of annexin A2 on the association of this protein with DRMs was investigated in the following.

It was shown that in a BHK cell line stably expressing the insulin receptor (IR) annexin A2 is phosphorylated after the stimulation of these cells with insulin (Rescher et al., 2008). This phosphorylation can also be achieved by incubating the cells with the insulinomimetic agent hydrogen peroxide (H_2O_2) in combination with the phosphatase inhibitor orthovanadate (Na_3VO_4) (Heffetz et al., 1992). BHK-IR cells were stimulated with insulin or H_2O_2 + Na_3VO_4 and extracted with 1 % Triton X-100 on ice. The Triton soluble and insoluble fractions were analysed by western blot analysis (Figure 4-19).

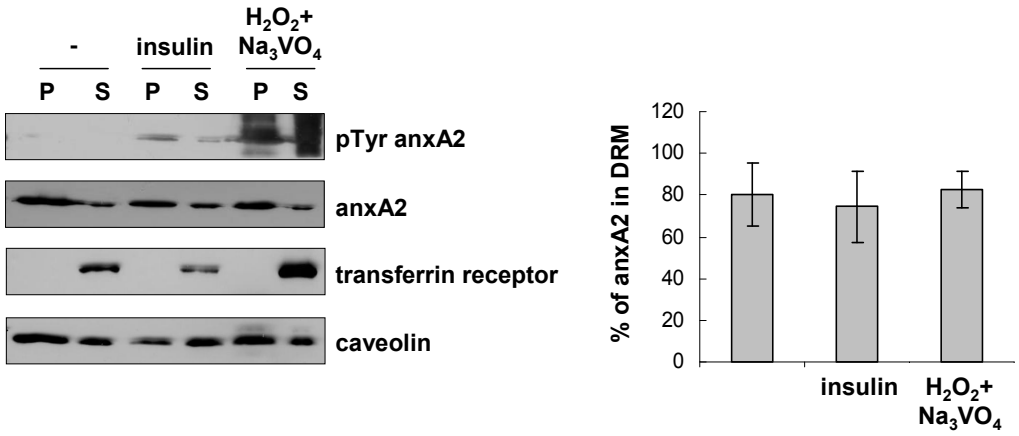

Figure 4-19: Phosphorylation of annexin A2 does not alter its association with DRMs in BHK-IR
BHK-IR were serum starved overnight and stimulated with either 5 µg/ml insulin or 17 µM H_2O_2 + 100 µM Na_3VO_4 for 30 min. The cells were extracted with 1 % Triton X-100 on ice in the presence of 50 nM Ca^{2+} and the Triton soluble fraction (S = supernatant) and the Triton insoluble fraction (P = pellet) were separated via a centrifugation step. The proteins were separated on an SDS-PAG and transferred to a PVDF membrane. Caveolin was detected as a DRM marker and transferrin receptor as a Triton soluble marker. Phosphorylated tyrosine (pTyr) of annexin A2 was detected with the help of the 4G10 platinum antibody and the αannexin A2 antibody from BD Transduction Labs was used to detect total annexin A2. Error bars represent SD from n = 3.

A preferential localisation of caveolin in the Triton insoluble pellet could be detected. Furthermore, the transferrin receptor is localised in Triton soluble fractions. These two markers indicate that the extraction of BHK-IR with cold detergent was successful in terms of separating different membrane domains. The endogenous annexin A2 in these cells shows a preferential localisation in the Triton insoluble pellet (about 80 % of the total protein). Annexin A2 is phosphorylated after the stimulation of BHK-IR with insulin or with H_2O_2 in combination with Na_3VO_4 as can be detected with the help of an anti-phosphotyrosine antibody. This phosphorylation does not alter the association of the endogenous annexin A2 with DRMs in these cells.

Another approach to investigate the influence of annexin A2 Tyr23 phosphorylation on the DRM association of this protein was the analysis of ectopically expressed annexin A2 variants harbouring mutations at this residue. The substitution of the tyrosine with the negatively charged residue Glu mimics the phosphorylation on the amino acid 23 (YE) (de Graauw et al., 2008; Rescher et al., 2008). On the other hand the substitution with the neutral residue Phe (YF) renders this site unable to be phosphorylated. In parallel an annexin A2 variant harbouring the amino acid substitution K281A in the PI(4,5)P_2-binding site was analysed (KA). This substitution has been described to interfere with the binding of annexin A2 to PI(4,5)P_2 *in vitro* (Gokhale et al., 2005). The localisations of the mutations in the annexin A2 sequence are depicted in Figure 4-20.

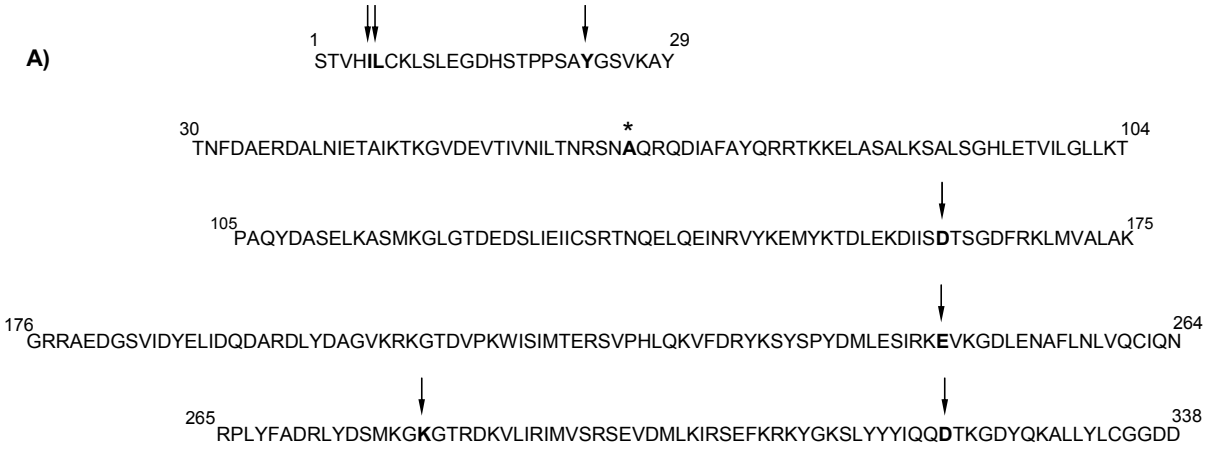

B)

anxA2 mutant	aa substitution	function	reference
YE	Y23E	phospho-mimicking	Rescher et al., 2008
YF	Y23F	phospho-deficient	
KA	K281A	PI(4,5)P_2-binding deficient	Gokhale et al., 2005
PM	I6E, L7E	p11-binding deficient	Thiel et al., 1992
CM	D161A, E246A, D321A	Ca^{2+}-binding deficient	Jost et al., 1992
PMCM	I6E, L7E + D161A, E246A, D321A	p11- and Ca^{2+}-binding deficient	Jost et al., 1997

Figure 4-20: Positions of amino acid replacements in the sequence of human annexin A2
A) The annexin A2 sequence is given in five blocks, representing the N-terminus (upper row) and the four annexin repeats. Positions of aa exchanges are indicated by arrows. All annexin A2 mutants used in this thesis contain the A65E substitution (asterisk) which reconstitutes the epitope for the monoclonal antibody H28. B) The different annexin A2 mutants used in this thesis including the according references are depicted table form.

MDCK II cells are a good model system for epithelial cells since they are able to polarise *in vitro*. Annexin A2 was studied in this cell line before and it appears to be concentrated underneath the apical membrane (Gerke and Weber, 1984). Furthermore, Annexin A2 is the major component of the Triton X-100 insoluble low-density fraction prepared from MDCK (Harder and Gerke, 1994). The clone MDCK-Tet used in this thesis is readily able to polarise on filters and form cysts and therewith reflects some of the major characteristics of this cell line.

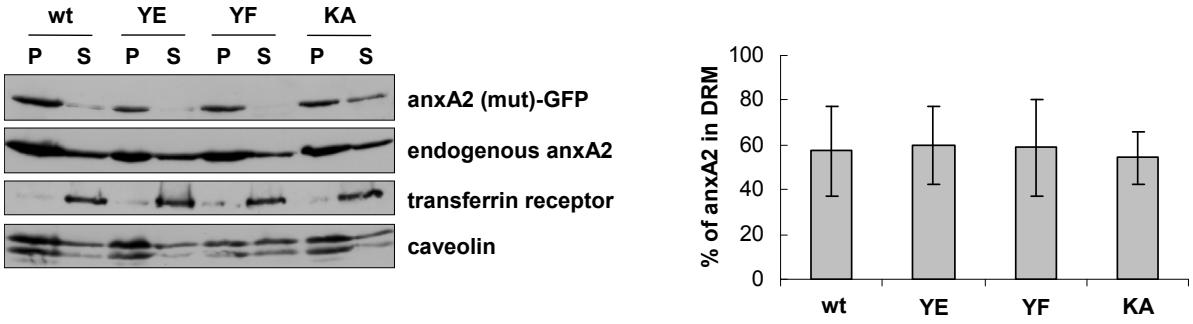

Figure 4-21: DRM association of ectopically expressed annexin A2 is not altered by mutations on Tyr23 or in the PI(4,5)P_2-binding domain
MDCK-Tet cells were transfected with plasmids coding for the indicated GFP labelled annexin A2 variants. 24 h or 48 h after transfection the cells were extracted with 1 % Triton X-100 on ice in the presence of 50 µM Ca^{2+} and the Triton soluble fraction (S = supernatant) and the Triton insoluble fraction (P = pellet) were separated via a centrifugation step. The proteins were separated on an SDS-PAG and transferred to a PVDF membrane. Caveolin was detected as a Triton insoluble marker and transferrin receptor as a Triton soluble marker with the help of specific antibodies. For the detection of endogenous annexin A2 and ectopic annexin A2-GFP variants the αannexin A2 antibody from BD transduction laboratories and the αGFP antibody were used, respectively. Error bars represent SD from $n \geq 5$.

MDCK-Tet cells transiently expressing annexin A2 wt, YE, YF or KA-GFP were extracted with Triton X-100 on ice and the DRM association of these variants was analysed (Figure 4-21). About 60 % of the endogenous annexin A2 in these cells resides in DRM fractions. The same is the case for ectopically expressed GFP-tagged annexin A2 wt. Mutations of the Tyr23 phosphorylation site or the PI(4,5)P_2-binding site do not alter this distribution.

There are also other means to assess the raft association of a protein than detergent extraction. One has recently been described by the group of Kai Simons. They showed that rafts of cellular membranes are able to coalesce into micrometer-size raft-based phases that can be visualised by microscopy. These slower diffusing membrane phases are enriched in cholesterol and raft transmembrane proteins like GPI-anchored proteins (Lingwood et al., 2008). To induce these large membrane phases cells are incubated overnight with a hypotonic buffer. This cell swelling procedure generates membrane preparations called plasma membrane spheres (PMSs) which are separated from the underlying cytoskeleton and endo- or exocytotic processes. PMSs appear as a spherical membrane outgrowth, 20 - 30 µm in diameter, which are still attached to the remaining cell body. By clustering the raft ganglioside GM1 with cholera toxin B (CtxB) at 37 °C raft-based phases, called GM1 phases, can be induced in these spheres. For this phase induction a high concentration of GM1 is critical. Therefore, A431 are a well suitable cell line for this analysis.
To establish the system of selective GM1 phases in A431 cells, these cells were induced to form phase separated PMSs and the localisation of one raft marker and one non-raft marker was analysed. As a raft marker the pleckstrin homology domain (PHD) of phospholipase C (PLC)-δ1 was used. The PHD selectively binds PI(4,5)P_2 which is enriched in cholesterol rich membrane microdomains (Pike and Casey, 1996; Varnai and Balla, 1998). As a non-raft marker the transferrin receptor was used which is excluded from raft microdomains (Janes et al., 1999).

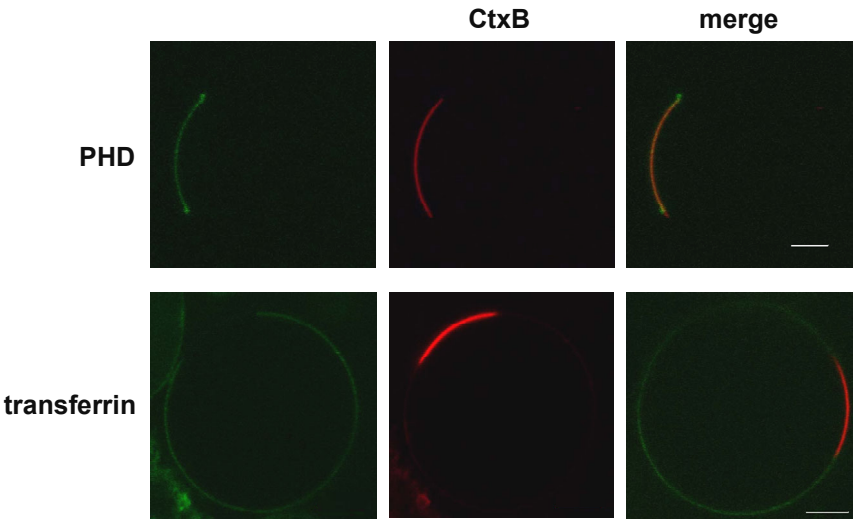

Figure 4-22: The GM1 phases of PMSs of A431 cells include PI(4,5)P_2 and exclude the transferrin receptor
A431 were transfected with a plasmid encoding a YFP labelled PHD or left untransfected. Spheres were induced by the addition of PMS buffer. Clustering of GM1 by CtxB Alexa Fluor 549 leads to the induction of GM1 phases to which PHD is recruited as a marker for PI(4,5)P_2. The untransfected cells were incubated for 1 h with FITC labelled transferrin to visualise the transferrin receptor which is excluded from the CtxB-positive membrane phases. Shown are representatives of 5 (for PHD) or 10 (for transferrin) pictures. (scale bars: 5 µm)

A431 cells were transfected with a plasmid coding for a YFP labelled PHD or left untransfected. The cells were induced to form phase separated PMSs. The transfected PHD localises to the GM1 phase indicating that PI(4,5)P_2 as a raft associated phospholipid is recruited to these raft based membrane phases in this system. The phase separated PMSs of untransfected cells were incubated with FITC labelled transferrin to visualise the transferrin receptor. The membrane-bound transferrin was not recruited to the coalesced GM1 phase, indicating that this lateral reorganisation of membrane structure was selective in composition (Figure 4-22).

To investigate the association of annexin A2 with these GM1 phases A431 were transfected with GFP-tagged annexin A2. Also the GFP labelled annexin A2 variants harbouring mutations on Tyr23 (YE and YF) or in the PI(4,5)P_2-binding site (KA) were analysed (Figure 4-23). Microscopical analysis of the phase separated spheres revealed that ectopically expressed annexin A2 localises to the GM1 phase in PMSs. This association is not influenced by mutations on Tyr23 or in the PI(4,5)P_2-binding site.

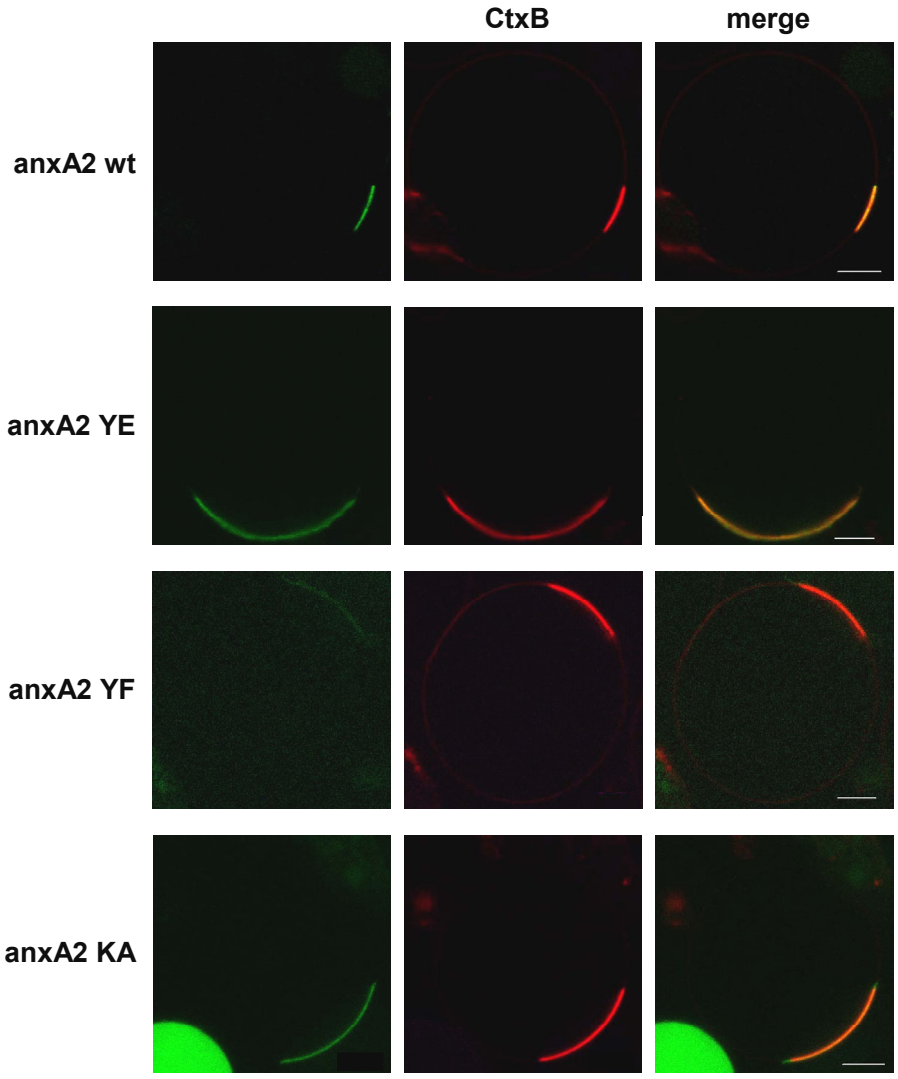

Figure 4-23: Annexin A2 wt, YE, YF and KA localise to GM1 phases in PMSs of A431 cells
A431 were transfected with plasmids coding for the indicated GFP labelled annexin A2 variants. The next day cells were incubated with PMS buffer overnight and afterwards induced to phase separate by the addition of labelled CtxB. All investigated proteins localise to the CtxB positive membrane phases. Shown are representatives of 7 (for wt and YE), 4 (for YF) or 5 (for KA) pictures. (scale bars: 5 µm)

4.3.3 Influence of p11- and Ca^{2+}- binding on the association of annexin A2 with membrane microdomains

Annexin A2 harbours three high affinity Ca^{2+}-binding sites. These type II binding sites were inactivated by substituting Asp161, Glu246 and Asp321 by the nonpolar amino acid Ala (Jost et al., 1992). This so-called CM mutant shows a greatly reduced affinity for the divalent cation and much higher Ca^{2+} concentrations are needed for half-maximal phosphatidylserine binding *in vitro* (Jost et al., 1994).

The N-terminal 14 amino acids of annexin A2 have been shown to be responsible for p11 binding. Exchanges of the neutral amino acids Ile6 and Leu7 with the negatively charged residue Glu render this protein unable to bind p11. This monomeric annexin A2 mutant was termed PM (Thiel et al., 1992).

To assess the role of Ca^{2+}- and p11-binding for the association of annexin A2 with membrane microdomains the CM and the PM mutant were analysed. Also a double mutant PMCM, harbouring inactive p11- and Ca^{2+}-binding sites (Jost et al., 1997), was available for these experiments. The localisations of the mutations in the annexin A2 sequence are depicted in Figure 4-20.

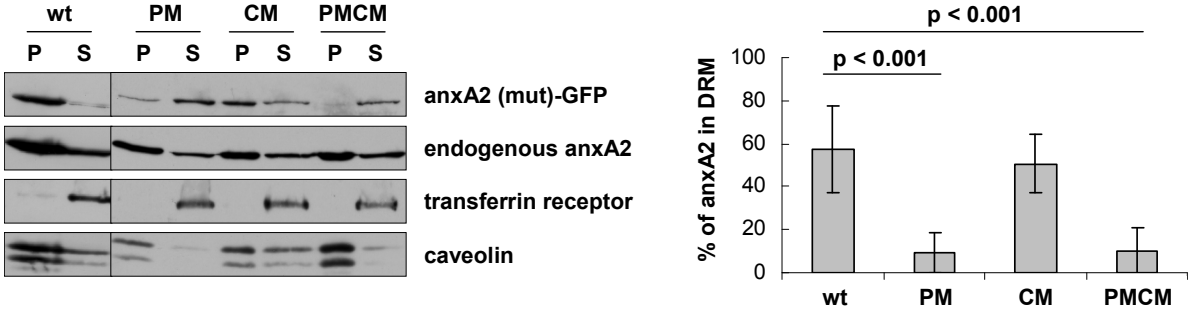

Figure 4-24: An intact p11-binding site of annexin A2 is essential for the DRM association of this protein
MDCK-Tet were transfected with plasmids coding for the indicated GFP labelled annexin A2 variants. 24 h or 48 h after transfection the DRM association of these proteins was analysed by detergent extraction and subsequent western blot analysis as described in Figure 4-21. Error bars represent SD from $n \geq 5$. The statistical significances were evaluated by unpaired *t*-tests.

The annexin A2 variants were transiently expressed in MDCK cells which were extracted on ice with Triton X-100 (Figure 4-24). The association of annexin A2 with DRMs is significantly decreased when the p11-binding site is inactivated. Mutations in the high affinity Ca^{2+}-binding sites alone do not appear to influence the association with the Triton insoluble fraction.

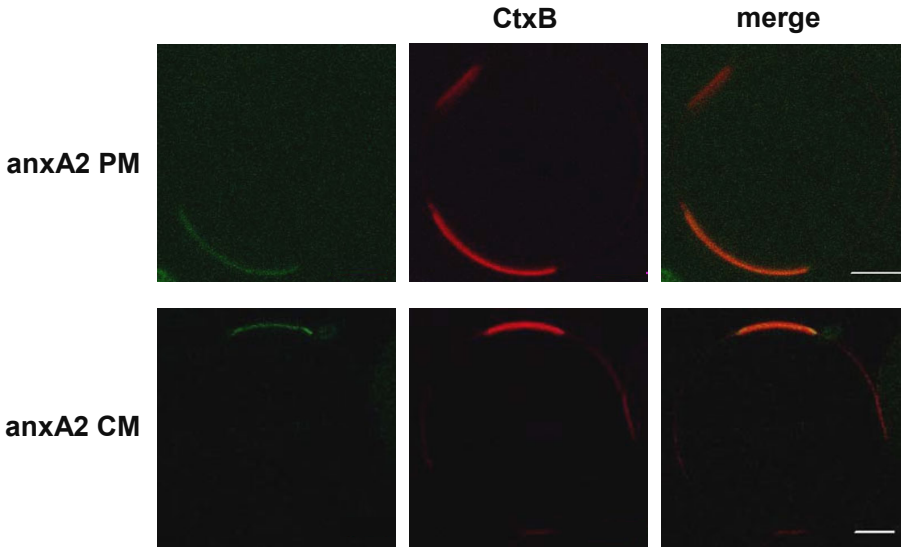

Figure 4-25: Annexin A2 PM and CM localise to GM1 phases in PMSs of A431 cells
A431 were transfected with plasmids coding for the indicated GFP labelled annexin A2 variants. The next day cells were incubated with PMS buffer overnight and afterwards induced to phase separate by the addition of labelled CtxB. All investigated proteins localise to the CtxB positive membrane phases. Shown are representatives of 10 (for PM) or 3 (for CM) pictures. (scale bars: 5 µm)

The localisations of the annexin A2 CM-GFP and PM-GFP variants in phase separated PMSs were also investigated (Figure 4-25). Both of the proteins associated with the GM1 phase.

All analysed annexin A2 mutants behave as the wt protein in the experiments using phase separated PMSs and are recruited to GM1 phases. This is in contrast to the DRM association analysis. In these assays p11-binding deficient mutants (PM and PMCM) show a significantly reduced affinity to DRMs in contrast to all other annexin A2 variants tested.

Annexins are Ca^{2+}-dependent proteins. Presumably the Ca^{2+} concentration in PMSs is rather high (Keller et al., 2009). Since cells die upon induction of spheres the membrane integrity is lost and the Ca^{2+} concentration inside the cell can be the same as in the surrounding buffer, i.e. 1.5 mM $CaCl_2$ in this case.

Hence, the elevated Ca^{2+} concentration could influence annexin A2 characteristics and contribute to an altered behaviour of the PM mutant. The Ca^{2+} concentration in the buffers used for detergent extraction can be tightly controlled - in contrast to the Ca^{2+} levels inside the PMSs. Therefore, annexin A2 PM-GFP expressing MDCKs were detergent extracted in the presence of different Ca^{2+} concentrations (Figure 4-26).

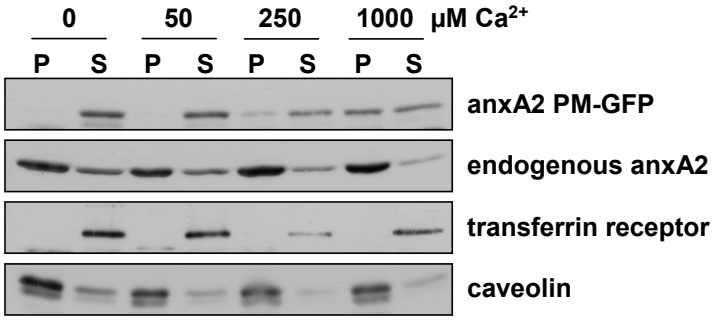

Figure 4-26: DRM association of endogenous annexin A2 and of p11-binding deficient annexin A2 is influenced by different Ca^{2+} concentrations
MDCK-Tet were transfected with a plasmid coding for annexin A2 PM-GFP. 48 h after transfection the DRM association of this protein was analysed by detergent extraction and subsequent western blot analysis as described in Figure 4-21. Different Ca^{2+} concentrations were added to the extraction buffers as indicated. Depicted here is one of two performed experiments.

The association of endogenous annexin A2 of MDCK cells with DRMs is influenced by the addition of Ca^{2+} to the extraction buffers. Elevated Ca^{2+} concentrations result in an enhanced shift of annexin A2 to detergent insoluble fractions. The same holds true for an ectopically expressed p11-binding deficient mutant of annexin A2. In contrast to endogenous annexin A2 hardly any annexin A2 PM can be detected in the Triton insoluble pellet without the addition of Ca^{2+} to the buffers. With increasing Ca^{2+} concentrations this protein is shifted to the Triton insoluble fraction. However, the fraction of annexin A2 PM that localises to the DRMs at 1 mM Ca^{2+} is by far less than that of the endogenous annexin A2.

4.3.4 Laurdan 2-photon microscopy of annexin A2 expressing cells

One approach to analyse membrane rafts in cells is Laurdan microscopy. This method is based on the model of cellular rafts as ordered membrane phases which float in a disordered environment of non-raft membranes (Brown and London, 2000). Membrane order can be assessed by the degree of packing order, as loosely packed membranes are more polar due to increased penetration of water molecules into the lipid bilayer. Laurdan is a lipophilic dye that aligns itself parallel to the hydrophobic tails of membrane phospholipids (Figure 4-27 A). It is a polarity-sensitive probe with two excited states

and its fluorescence exhibits a 50 nm blue shift in emission with increasing membrane condensation thereby allowing the visualisation of membrane fluidity (Gaus et al., 2003). The principle of this spectral shift is demonstrated in Figure 4-27 B.

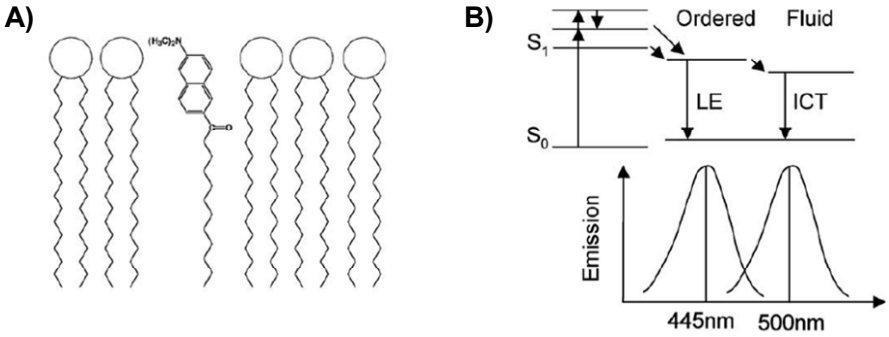

Figure 4-27: Principles of Laurdan
A) Structure of Laurdan and its orientation in a phospholipid layer. B) The Jablonski diagram of Laurdan shows the spectral shift of Laurdan emission in different membrane phases. Depending on the surrounding membrane order emission of Laurdan can occur from two possible excited states: the locally excited state (LE) in less polar environments and the internal charge transfer state (ICT) in more polar environments. An increment in membrane polarity results in an increased dipole moment of the molecule and therefore a shift of its emission to longer wavelengths. A schematic representation of the corresponding emission maxima peaks of Laurdan in ordered and fluid phases is also shown. From Gaus et al., 2006.

To visualise membrane structure, two intensity (I) images of Laurdan between 400 - 460 nm and 470 - 530 nm are recorded simultaneously, with channel 1 (400 - 460 nm) recording Laurdan in more condensed membranes and channel 2 (470 - 530 nm) recording Laurdan in more fluid membranes. From the ratio of the emission intensities the so-called Generalised Polarisation (GP) can be calculated. The GP value is defined as

$$GP = \frac{I_{(400-460)} - I_{(470-530)}}{I_{(400-460)} + I_{(470-530)}}.$$

The GP value as a relative measure for membrane order can theoretically assume values from +1 (most condensed) to -1 (most fluid). This emission shift of Laurdan in different membrane phases can be calculated for each pixel and together with colocalisation studies, the preferential localisation of a specific protein in ordered (condensed) / disordered (fluid) domains of the plasma membrane can be determined.

The fluorescence of Laurdan was excited with a 2-photon laser. Low energy photons reaching a fluorophore at the same time can induce a single photon emission with higher energy in a process called multi-photon excitation. The excited Laurdan emits a single photon as if it were excited by a single higher energy photon.
Since the simultaneous absorption of two photons only takes place in the centre of a pulsed laser, only the focal plane of interest is excited. This and the fact that photons of a longer wavelength are scattered to a reduced extent leads to the fact that a deeper penetration depth can be achieved allowing the visualisation of tissue sections. Furthermore, the usage of a longer wavelength of less energy leads to a reduced phototoxicity for live cell imaging. Another important advantage of the usage of 2-photon microscopy for the excitement of Laurdan is the fact that the photo-bleaching of the fluorophore itself is decreased significantly.

As a measure for the association of annexin A2 with ordered domains the membrane order at sites of the localisation of this protein was investigated. Not only annexin A2 wt but also the phosphorylation mutants YE and YF, the PI(4,5)P_2-binding deficient mutant KA as well as the p11-binding deficient mutants PM and PMCM were analysed. mCherry labelled constructs were used since GFP would interfere with the Laurdan emission.

The tissue culture for microscopy was conducted in the laboratory of Thomas Grewal (Faculty of Pharmacy, University of Sydney, Sydney, Australia) and the microscopy was performed in the laboratory of Katharina Gaus (Cellular Membrane Biology Lab, Centre for Vascular Research, University of New South Wales, Sydney, Australia). MDCK cells were used for this analysis to work with the same cell line that was used for detergent extraction experiments. However, not exactly the same cell clone was used.

MDCK-TG cells were transiently transfected with mCherry labelled annexin A2 variants or mCherry as a control and labelled with Laurdan as described in Material and Methods. Fixed cells were used for Laurdan microscopy. Examples of confocal images of the mCherry fluorescence of the used proteins are presented in Figure 4-28.

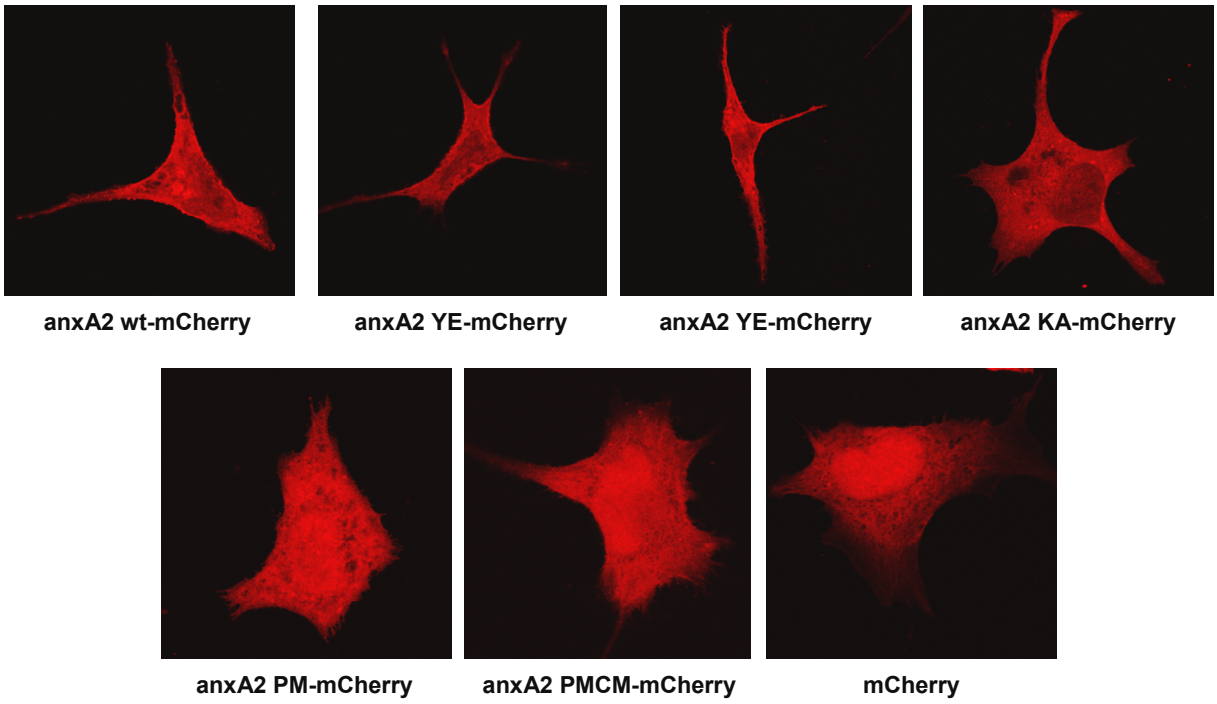

Figure 4-28: Localisation of different annexin A2 mutants in MDCK
MDCK-TG cells grown on coverslips were transiently transfected with plasmids encoding mCherry labelled variants of annexin A2 (wt, YE, YF, KA, PM or PMCM) or an mCherry encoding control vector. 24 h after transfection the cells were fixed, mounted in Mowiol and analysed by confocal microscopy.

Conventional single-photon confocal images were obtained in parallel to 2-photon Laurdan intensity images to determine the membrane order in regions of protein localisation. An example for this image analysis is depicted in Figure 4-29.

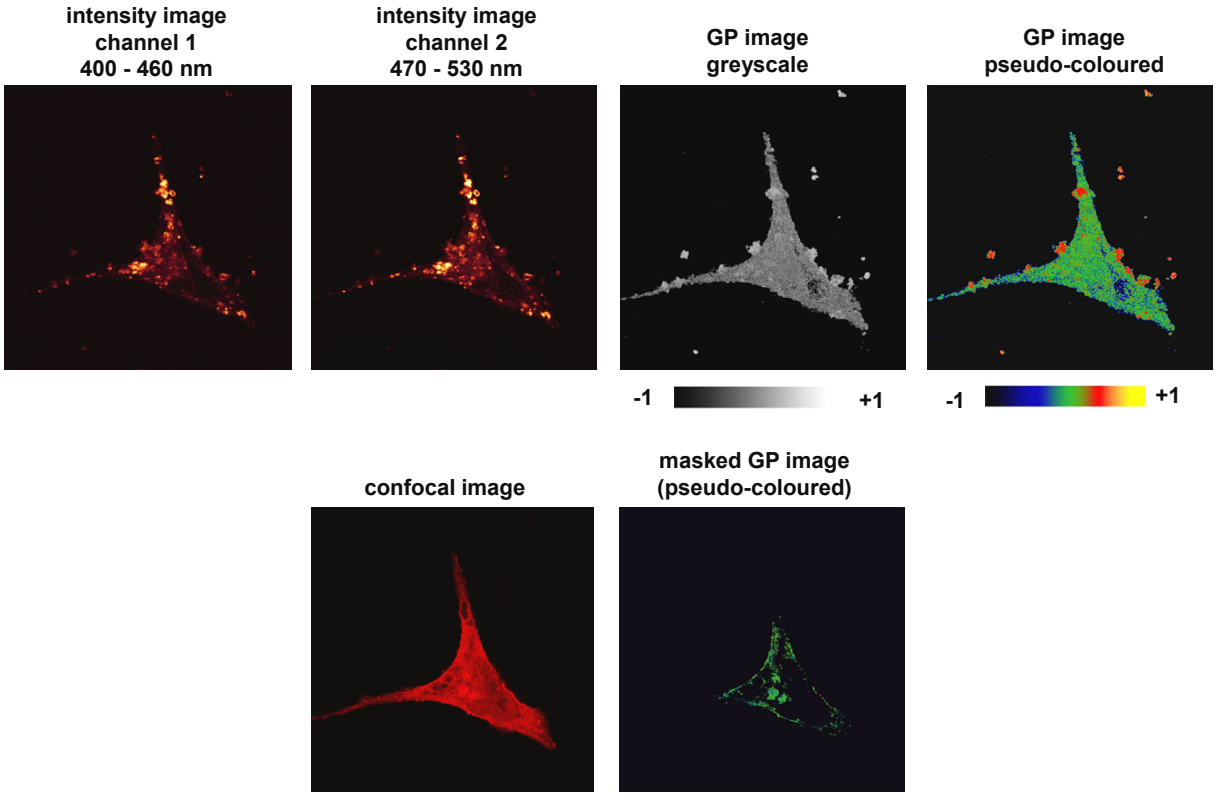

Figure 4-29: Membrane order at sites of annexin A2 localisation
MDCK-TG transiently expressing mCherry labelled annexin A2 wt were labelled with Laurdan and fixed as described in Material and Methods. Intensity images of channel 1 (400 - 460 nm), channel 2 (470 - 530 nm) and the corresponding GP image are shown in the upper panel. The GP image is presented in greyscale and also in pseudo-colours as indicated by the scale illustrating GP values varying from -1 to +1. The confocal image shows the fluorescence of mCherry labelled annexin A2. This image was used to determine regions of high fluorescence - hence protein localisation - to create a mask in Adobe Photoshop. This mask was layered on top of the corresponding GP image to determine the GP value in the regions of protein localisation.

Using the pseudo-coloured GP image, the order of membrane structure becomes visible. Membrane rafts represent liquid-ordered domains which are condensed and appear yellow in a pseudo-coloured GP image because of their high GP value, whereas non-raft domains are liquid disordered and fluid and appear green because of their low GP value. In this case of a resting MDCK cell no distinct regions of increased membrane condensation can be seen (Figure 4-29). The confocal image of annexin A2 was used to determine the GP values in the regions where the protein is localised by creating a mask. Since in the overall GP image no regions of increased membrane condensation can be detected the regions with high protein localisation do not show an elevated GP value.

The GP values of regions of protein localisation were determined for all the proteins depicted in Figure 4-28. The results are shown in Figure 4-30.

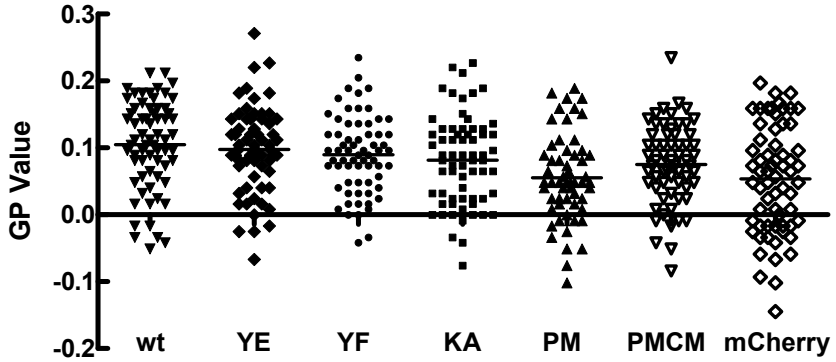

Figure 4-30: GP values at regions of high expression of mCherry labelled annexin A2 variants in MDCKs do not differ
MDCK-TG ectopically expressing mCherry labelled annexin A2 wt, annexin A2 mutants (YE, YF, KA, PM, PMCM) or an mCherry control were labelled with Laurdan, fixed and imaged as described in Material and Methods. GP images and confocal images at identical focal planes were used to determine the GP value at sites of protein localisation as described in Figure 4-29. About 30 cells were analysed per experiment and two independent experiments were performed that are both demonstrated in this diagram. The means are indicated by horizontal lines.

The pseudo-coloured GP image in Figure 4-29 showed no regions with increased membrane condensation. The same was true for the masked GP image. When mCherry labelled annexin A2 variants were used to mask the GP images no domains of increased or decreased membrane order could be detected either as seen in Figure 4-30.

5 Discussion

5.1 Annexin A2 in IAV infection

The pathogenic virus influenza A causes pandemic and epidemic outbreaks on a periodical basis that still claim many lives. The so-called Spanish flu caused by an H1N1 virus was responsible for the deaths of even at least 40 million people in 1918/1919 (Horimoto and Kawaoka, 2005). Like other viruses IAV is an obligate intracellular pathogen. Its replication dependents on a variety of intracellular processes. For IAV these processes involve actin dynamics, a range of transport processes and the organisation of membrane rafts. Those rafts define the assembly and budding site of influenza. Raft-lipid domains are selectively incorporated into the influenza virus envelope (Scheiffele et al., 1999) and the envelope glycoproteins HA and NA preferentially cluster in membrane rafts of polarised and non-polarised cells (Scheiffele et al., 1997). Cholesterol depletion of either the host cell or the virus with methyl-β-cyclodextrin interferes with influenza replication (Barman and Nayak, 2007; Sun and Whittaker, 2003).

Defining the cellular proteins and mechanisms involved in influenza A replication might help in finding agents to fight this pathogen. Annexin A2 is a possible candidate that could be important for IAV infection. Annexin A2 is a multifunctional protein involved in several biological processes. One of its key features is the regulated binding to negatively charged phospholipids. This binding property accounts for its involvement in membrane organisation and trafficking. It is located on endosomal compartments and it promotes membrane fusion during Ca^{2+}-regulated exocytosis (for reviews, see Gerke and Moss, 1997 or Gerke et al., 2005). Annexin A2 has been described to bind the cytoplasmic site of $PI(4,5)P_2$-enriched membrane microdomains, thereby stabilising these domains and linking them to the cortical actin cytoskeleton (Rescher and Gerke, 2004). The actin aggregating effect of annexin A2 is implicated to be of importance for the actin rearrangements induced by enteropathogenic and enterohemorrhagic *E. coli* (Miyahara et al., 2009; Zobiack et al., 2002). Other pathogens also depend on this host cell protein for efficient replication. E.g. annexin A2 has been described to act as a receptor of HCMV (Wright et al., 1994) or respiratory syncytial virus (Malhotra et al., 2003).

Therewith, annexin A2 is involved in numerous processes that are of importance for the IAV replication cycle, namely membrane domain organisation, transport processes and actin dynamics. This implies a potential role of annexin A2 in IAV replication. Therefore, a closer look was taken at a possible involvement of annexin A2 in this process. However, from the experimental data obtained in this thesis an active involvement of annexin A2 in influenza A replication cannot be concluded.

First, the number of infectious virus particles in the supernatant of infected annexin A2 manipulated cells was determined. No difference in the virus replication could be detected. The virus titres deviated in the range of variations that are normal for viral infection experiments. No tendency to either an enhanced or a reduced viral replication could be detected, independent of the replication time or the virus titre used.

In the first experiments cells were depleted for annexin A2 by means of siRNA or manipulated by the expression of a mutant annexin A2 protein causing the aggregation of annexin A2 and its ligand p11. These methods deplete cytosolic annexin A2 but they hardly affect the membrane bound form (Zobiack et al., 2003) since this population is somewhat shielded and has a longer half life (Zokas and Glenney, 1987). The virus infection experiments were also performed with cells devoid of annexin A2, i.e. CMECs from the annexin A2 knockout mouse, and compared to the replication in cells of a wt mouse, but no significant difference in influenza A replication could be detected.
The fact that no tendency to an altered virus replication could be detected in cells with different annexin A2 levels is astonishing taking into account that the cells showed different morphological changes reflecting a different onset of apoptosis. Annexin A2 depleted cells were more apoptotic as could be determined not only by visual observations but also by the detection of PARP cleavage by western blot analysis (discussed below). Influenza viruses induce apoptosis in infected cells. On the one hand this is a host mechanism to limit virus spread but on the other hand IAV has taken advantage of some of the apoptotic processes to efficiently replicate. E.g. activation of caspase-3 is essential for the nuclear export of viral RNP complexes (Wurzer et al., 2003).
The influenza virus might possibly take advantage of early apoptotic events of, such as caspase-3 activity, while the full execution of the apoptotisis leads to a diminished cell number. A reduction of the cell number results in the fact that the remaining virus meets a decreased number of cells to replicate, which may result in reduced end titres (Wurzer et al., 2003). Therefore, an either reduced or an enhanced virus replication would be expected in annexin A2 depleted cells since they are more apoptotic. This is neither the case for early nor for late time points p.i.. The reason for this discrepancy remains to be determined.

It has to be taken into account that the cells used for these influenza infection experiments were not polarised. In polarised cells annexin A2 appears concentrated underneath the apical membrane (Gerke and Weber, 1984). This apical side of polarised cells also defines the site of influenza virus entry and exit. The behaviour of influenza virus in polarised cells might differ from that in non-polarised cells. E.g. it has been reported that a dynamic actin cytoskeleton is indispensable for influenza virus entry into polarised epithelial cells, but not for non-polarised cells (Sun and Whittaker, 2007). However, a depletion of annexin A2 prevents normal development of the apical surface (Martin-Belmonte et al., 2007) and cells that already established an apical-basolateral polarity are almost impossible to transfect.

This objection also holds true for the experiments that were performed to analyse the surface localisation of influenza HA. Annexin A2 has been described to be essential for the apical transport of the raft associated protein sucrose isomaltase in polarised MDCKs (Jacob et al., 2004). Nevertheless, to our knowledge no such analysis was performed in non-polarised cells. Membrane trafficking in polarised cells differs from non-polarised cells (Tuma et al., 2002). In polarised cells as well as in non-polarised cells influenza HA is readily transported to the plasma membranes to regions that are resistant to the extraction with non-ionic detergents (Skibbens et al., 1989). However, the proteins being involved in these transport processes might differ profoundly. Therefore, an involvement of

annexin A2 in the apical transport of influenza HA cannot be excluded. At least, this protein does not have an impact on the surface HA transport in non-polarised A549 cells.

Quantitative real-time PCR analysis was performed on PR8 infected cells and the mRNA level of annexin A2 and annexin A1 were determined. The latter was included since it is involved in host immune response and cellular proliferation (Lim and Pervaiz, 2007). However, IAV does not seem to alter the mRNA levels of these two annexins. No difference can be seen in the mRNA levels of PR8 infected HeLa, A549 or HepG2 cells when they were compared to uninfected cells.

Double immunofluorescence labelling was carried out to investigate a possible colocalisation of annexin A2 with influenza particles in infected cells. For this analysis A549 were infected with avian influenza FPV. 30 min p.i. the antibody decorates dot like structures close to the cellular surface which probably resemble endosomes. These structures are more distributed throughout the cytosol 1 h or 2 h p.i., indicating that the virus containing endosomes approach the nucleus where the viral RNA is released. At late time points the fluorescence increases due to newly synthesised influenza proteins. This protein concentrates at the plasma membrane from where finally new virus particles can bud. Thus, with the antibody used for this immunofluorescence staining some of the major hallmarks of influenza virus replication could be visualised. At none of these time points a colocalisation with either cytosolic or membrane bound annexin A2 could be seen. However, with the fixation technique used here the endosomal localisation of annexin A2 could not be visualised.

Even though no colocalisation of FPV with annexin A2 in influenza infected cells could be seen, an incorporation of this host cell protein into purified virions could be detected. The NS1 protein was not detectable in the purified virus fraction indicating that the detected annexin A2 does not result from contaminations by cellular remnants. Annexin A2 has been described to be incorporated into a whole range of enveloped virus particles, like HIV-1 (Harrist et al., 2009), herpes simplex virus 1 (Loret et al., 2008; Padula et al., 2009), vesicular stomatitis virus (Moerdyk-Schauwecker et al., 2009), vaccinia virus (Chung et al., 2006), alcelaphine herpesvirus-1 (Dry et al., 2008; Zhu et al., 2005), Kaposi's sarcoma-associated herpesvirus (Zhu et al., 2005) and HCMV (Wright et al., 1995). The fact that annexin A2 incorporation into virus particles is so common indicates that annexin A2 could play a general role in the infection process of enveloped viruses.
The group of Béatrice Riteau also found annexin A2 to be associated with influenza A virions. They hypothesised that this protein is actively involved in promoting IAV infection by being involved in the proteolytic activation of influenza HA (LeBouder et al., 2008). Annexin A2 and p11 were identified in purified virus particles by western blot analysis and the presence of annexin A2 was confirmed by immunogold labelling and subsequent electron microscopy. LeBouder and coworkers describe that the ability of annexin A2 to activate plasminogen could be of importance for IAV infection. Plasmin might serve as a trypsin-like protease that cleaves influenza HA. The activation of this protein by cleavage is essential for influenza virus infection. Therefore, annexin A2 mediated activation of plasminogen might support the replication of influenza viruses which may contribute to their pathogenicity (LeBouder et al., 2008).

Recently, a mass spectrometry approach of influenza virus particles was performed by the group of Peter Palese. 36 host-encoded proteins including annexin A2 were detected (Shaw et al., 2008). Annexin A2 could also be identified by western blot analysis of purified virions. The annexin A2 protein amount of subtilisin protease treated virions does not seem to be decreased when compared to untreated virions. This reveals that annexin A2 is - at least partly - localised inside the virion. But it has to be taken into account that the purification buffers contained 1 mM EDTA. Chelation of Ca^{2+} ions results in the removal of surface bound annexin A2 (Falcone et al., 2001) so it would not be detected any more in this analysis. Therefore, these data do are not sufficient confirm that annexin A2 is localised on the surface of influenza virus particles where it might possibly be involved in plasminogen activation (LeBouder et al., 2008).
Hence, the observation in this thesis that annexin A2 is incorporated into influenza A virus particles is in accordance with recently published data. However, an involvement of annexin A2 in the plasminogen conversion (LeBouder et al., 2008) could not be validated. Cells died upon application of plasminogen. HepG2, A549 and MDCK were used for these experiments (data not shown). The onset of cell death was probably due to uncontrolled plasminogen activation on the cell surface. This presumably results in the proteolysis of fibronectin and lamin, which is followed by cell detachment and apoptosis (Rossignol et al., 2004). The group of Béatrice Riteau also used MDCK cells. Nevertheless, discrepancies could arise from the well-known heterogeneities in specific cell clones in the various laboratories.
In the work performed here the purification of influenza virions was rather problematic. Only one of many virus preparations did not show detectable amounts of influenza NS1 which was used to detect contaminations by cellular debris. NS1 is only produced in infected cells but not incorporated into the virus particle. Since the purification of the virions quite often was not successful and the incorporation of annexin A2 has been demonstrated in the meantime by two different working groups the purification and further characterisation of purified virus particles was not pursued any further. However, it would be interesting to detect if the annexin A2 in the influenza virus particles harbours posttranslational modifications or is indeed localised on the surface of the virion.

Shaw and colleagues not only identified annexin A2 in influenza A particles but also annexin A1, annexin A4, annexin A5, annexin A11 and S100A11, which is a binding partner of annexin A1 and annexin A2 (Shaw et al., 2008). However, the incorporation of the S100 protein p11, as a major binding partner of annexin A2, was not described in this study. This is in contrast to the observations by LeBouder and co-workers who detected p11 in purified influenza A particles by western blot analysis (LeBouder et al., 2008).
A role of annexin A5 in influenza virus infection has been discussed before. In general IAV binds sialic acid containing receptors on the cell surface (for a review, see Dimmock, 1982). Otto and co-workers found a sialic acid-free cellular protein that binds IAV. They identified this protein to be annexin A5. A role of this protein in influenza A entry was hypothesised (Huang et al., 1996; Otto et al., 1994).

5.2 Annexin A2 in apoptotic processes

Annexin A2 appears to be a key regulator of cellular proliferation (Chiang et al., 1999). An involvement of annexin A2 in cellular transformation has been hypothesised ever since the initial identification of this protein as a major substrate of the tyrosine kinase pp60v-src (Radke et al., 1980). By now it could be shown that the tyrosine phosphorylation at position Tyr23 in the N-terminal domain is involved in the reorganisation of the membrane-associated actin cytoskeleton during cellular transformation (de Graauw et al., 2008; Rescher et al., 2008). Furthermore, Yamada and colleagues demonstrated that the annexin A2/p11 complex is involved in the formation of the E-cadherin-based adherent junctions in MDCK cells, which itself is important for cell migration (Yamada et al., 2005).
It could be shown that annexin A2 is overexpressed in acute myeloid leukaemia (Menell et al., 1999), brain tumours (Roseman et al., 1994), breast cancer (Sharma et al., 2006), pancreatic cancer (Esposito et al., 2006) and gastric cancer (Emoto et al., 2001). Since annexin A2 is a receptor for tissue plasminogen activator and thereby is involved in the activation of plasminogen (Hajjar and Krishnan, 1999), extracellular annexin A2 might activate the fibrinolytic system associated with cancer metastasis. The annexin A2 knockout mouse shows microvascular fibrin accumulation, stressing the fact that annexin A2 is important for fibrinolysis. Moreover, the directed migration of endothelial cells from the annexin A2 knockout mouse through fibrin and collagen lattices was reduced *in vitro* (Ling et al., 2004). This is in accordance with a possible positive correlation of annexin A2 with cancer metastasis.
Furthermore, annexin A2 down-regulation by siRNA can inhibit the proliferation and the invasive potential of Jurkat cells remarkably (Bao et al., 2009b) and in multiple myeloma cell lines the depletion of this protein resulted in a decreased proliferation and invasive potential and an increased apoptosis of the cells (Bao et al., 2009a). An up-regulation of annexin A2 in cancer cells might therefore protect them from apoptosis.

An increased sensitivity towards apoptosis-inducing agents upon annexin A2 depletion was also observed during the course of this thesis using different cell lines. The apoptotic stimuli used here included the IAV strains PR8 and FPV, staurosporine and TNFα. But also transfection stress was sometimes sufficient to induce apoptosis. The differences in apoptosis progression were visualised by the detection of cleaved PARP which is a direct substrate of the major executive caspase-3. Also the activation of upstream initiator caspases-8 and -9 was determined in staurosporine and TNFα treated HeLa cells.
TNFα is an initiator of the receptor mediated extrinsic apoptotic pathway. Since it has been described that the extrinsic pathway converges with the intrinsic pathway through the activation of Bid by caspase-8 (Li et al., 1998) it is not astonishing that also caspase-9 is found to be activated after the stimulation of cells with TNFα.
Staurosporine was used as an activator of the mitochondrial caspase-dependent apoptotic pathway including caspase-9 (Scarlett et al., 2000). In the experiments performed here staurosporine treatment of HeLa cells also resulted in an increase in the cleavage of caspase-8. It has been demonstrated before that caspase-8 can be activated in the absence of death receptor signalling (Wesselborg et al.,

1999). In a macrophage cell line the treatment with staurosporine induced an increase in TNFα levels which led to the activation of caspase-8 by an autocrine effect of TNFα (Nakamura-Lopez et al., 2009). Furthermore, caspase-8 has also been described to be activated in the context of staurosporine induced-apoptosis in cells derived from human cervical cancer and it is hypothesised that the initiator caspases are cell specific (Nicolier et al., 2009). Therefore, it is not astonishing that in the experiments performed here, using the cervical cancer cell line HeLa, the treatment of cells with staurosporine also resulted in the activation of the extrinsic apoptotic pathway involving caspase-9.
Independent of the apoptotic stimulus used for these experiments (i.e. staurosporine or TNFα) the initiator caspases-8 and -9 were activated. This activation seems to be quite simultaneous, stressing the fact that the extrinsic and intrinsic apoptosis-inducing pathways cannot be fully separated. The fact that both, caspase-8 and -9, are activated to a larger extent in annexin A2 depleted cells indicates that the influence of annexin A2 on the onset of apoptosis cannot be directly linked to either of the two caspases.

Annexin A2 has been described in the context of apoptosis before. As mentioned above down-regulation of this protein results in an increased apoptosis rate of multiple myeloma cells (Bao et al., 2009a). In renal cell carcinoma cells annexin A2 depletion leads to a decrease in proliferation resulting in apoptosis (Tanaka et al., 2004) and it was reported that the depletion of annexin A2 renders cells more susceptible to UVC-induced cell death (Tong et al., 2008). Furthermore, it was shown that annexin A2 may be involved in cellular apoptosis induced by p53, one of the best studied tumour suppressor genes. Annexin A2 is down-regulated in human lung carcinoma cells expressing p53, especially in cells with high metastatic potential which are more sensitive for p53-induced apoptosis (Huang et al., 2005; Huang et al., 2008). However, there is also evidence that annexin A2 is overexpressed in response to the overexpression of the p53 gene in human glioblastoma cells (Saffari et al., 2009). Discrepancies between these observations could be based on the different cell systems used.
A regulation of the p53 gene in influenza infected cells has also been described. p53 protein levels as well as p53 dependent gene transcription are up-regulated upon influenza virus infection in mouse embryo fibroblasts and human lung cells including A549 (Turpin et al., 2005) as well as in MDCK and Vero cells (Shen et al., 2009). Surprisingly, viral replication was elevated in cells with inhibited p53 activity, which might be a result of a decreased interferon response (Turpin et al., 2005).
p53 accumulation in TNFα treated apoptotic sensitive cells was reported for human cervical cancer cells (Donato and Perez, 1998) and human breast cancer cells (Jeoung et al., 1995). And also after staurosporine treatment the p53 protein level was described to be up-regulated in mouse neuroblastoma / rat glioma hybrid cells (Zhang et al., 2003). By contrast, a down-regulation was observed in a mouse sarcoma cell line (Zong et al., 1999) pointing to a cell type specific involvement of p53 in staurosporine mediated apoptotic responses.
The p53 status of influenza A infected cells or of cells treated with staurosporine or TNFα was not determined. Therefore, no conclusion can be drawn concerning a possible correlation of p53 and annexin A2 in the apoptotic processes described in this thesis.

The protein level of annexin A2 in PR8 infected cells in comparison to non infected cells was unaltered as could be seen by western blot analysis. Furthermore, real-time PCR analysis of PR8 infected HeLa, A549 or HepG2 did not reveal a regulation of the corresponding mRNAs in response to virus infection. The protein level of annexin A2 was not altered in staurosporine or TNFα treated cells either. And also no cleavage of this protein was detectable. This is in contrast to the observations of Wang and co-workers. They detected that after apoptosis induction annexin A2 is time-dependently cleaved (Wang et al., 2009). They analysed serum withdrawal-induced cell cycle inhibition and anticancer drug-induced apoptosis in different cell lines. Hence, the apoptotic stimuli differ from those used in this thesis which could possibly result in the different observations.

Annexin A2 harbours a nuclear export signal suggesting a function of this protein in the nuclear compartment (Eberhard et al., 2001). It has been identified as part of the primer recognition complex that interacts with DNA polymerase α and it enhances the activity of this complex *in vitro* (Jindal et al., 1991). It has been shown that annexin A2 is involved in DNA replication in Xenopus egg extracts, demonstrating that annexin A2 is indeed involved in DNA replication and plays a role in the cell cycle of higher eukaryotes (Vishwanatha and Kumble, 1993). Treatment of HeLa cells with antisense oligonucleotides to annexin A2 reduces DNA synthesis and retards progression through the cell cycle (Chiang et al., 1999; Kumble et al., 1992). No influence on cellular proliferation upon siRNA transfection was visible in the experiments performed here. Nevertheless, it is possible that impairment in cell cycle progression might eventually lead to the observed enhanced sensitivity towards apoptosis induction in annexin A2 depleted cells.
The activity of annexin A2 as an mRNA binding protein might also be of importance for its involvement in apoptotic processes. One mRNA that is bound by this protein is that of c-Myc (Mickleburgh et al., 2005). The proto-oncogene c-Myc codes for a transcription factor that is involved in various cellular processes, like cell growth, proliferation, inhibition of terminal differentiation and apoptosis. This protein is activated in a variety of human tumours (Pelengaris et al., 2002). Transfection of LNCaP cells with annexin A2 resulted in up-regulation of c-Myc protein (Filipenko et al., 2004). Hence, a deregulation of c-Myc could possibly be responsible for the increased sensitivity towards apoptotic stimuli in annexin A2 depleted cells.

5.3 Annexin A2 association with membrane microdomains

5.3.1 DRM association of annexin A2 mutants

The lateral organisation of membranes plays a crucial role in many cellular events. This organisation arises from preferential packing of sphingolipids and cholesterol into membrane microdomains, so-called lipid rafts (Simons and Ikonen, 1997). These microdomains serve as platforms for multiple cellular processes by the recruitment and concentration of molecules. They are involved in membrane sorting and signal transduction and they also play an important role in the replication of several pathogens. E.g. mammalian viruses like influenza, human immunodeficiency virus (HIV), measles and ebola bud from membrane rafts (Manes et al., 2003; Simons and Ikonen, 1997; Simons and Toomre, 2000). The resistance of proteins to detergent extraction in the cold is widely used as a criterion for the association of these proteins with membrane rafts in living cells (Brown and London, 1998).

Annexin A2 has been described to be associated with membrane rafts and is involved in the stabilisation and aggregation of these domains. It binds to negatively charged phospholipids in the membrane in a Ca^{2+}-regulated manner and by lateral segregation is specifically recruited to $PI(4,5)P_2$ containing membrane rafts (Rescher and Gerke, 2004). Furthermore, annexin A2 binds to cholesterol enriched microdomains in a Ca^{2+}-independent way (Harder et al., 1997). The capability of annexin A2 to self aggregate on membranes could promote the aggregation of raft microdomains (Menke et al., 2004).

In the experiments performed here phosphorylated annexin A2 and different annexin A2 mutants were employed to investigate which features of annexin A2 are important for the association of this molecule with membrane microdomains which could also be relevant for pathogen infections. Therefore, the resistance to detergent extraction on ice was analysed.

First, the impact of the phosphorylation on Tyr23 was analysed. Recently, a link was drawn to directly relate Tyr23 phosphorylation to cellular transformation. Expression of the phospho-mimicking annexin A2 mutant Y23E itself was sufficient to induce actin rearrangement and cell scattering in MDCK cells (de Graauw et al., 2008). Furthermore, this phosphorylation of annexin A2 leads to the reorganisation of membrane-associated actin cytoskeleton resulting in a loss of cell substratum contact in BHK cells overexpressing the insulin receptor (Rescher et al., 2008). This actin remodelling probably results from an up-regulation of the Rho/ROCK pathway. Rho is a small GTPase and is a key regulator of the cytoskeletal remodelling required for cell spreading, motility and cell-shape changes (for a review, see Ridley, 2001). ROCK is a serine/threonine kinase acting as an effector of Rho (Riento and Ridley, 2003). The direct interaction of annexin A2 with another Rho protein, namely Cdc42, and its implication for cellular functions has been demonstrated before (Martin-Belmonte et al., 2007).

The phosphorylation of annexin A2 might also alter its ability to act as a membrane-cytoskeleton linker or membrane domain organiser (Rescher et al., 2008). There is evidence that tyrosine phosphorylation of annexin A2 inhibits the ability of this protein to bind to and bundle F-actin (Hubaishy et al., 1995).

To specifically analyse the association of Tyr23 phosphorylated annexin A2 with DRMs BHK-IR were stimulated with either insulin or H_2O_2 in combination with Na_3VO_4. These stimuli lead to a

phosphorylation of annexin A2 on Tyr23 (Heffetz et al., 1992; Rescher et al., 2008). Furthermore, ectopically expressed phosphorylation mutants were analysed in MDCK. The annexin A2 YE mutant mimics the phosphorylation of amino acid 23 and annexin A2 YF cannot be phosphorylated on this residue any more. Using these two different approaches no influence of the Tyr23 phosphorylation on the resistance to detergent extraction in the cold could be detected.
Powell and Glenney analysed the binding of annexin A2 to phosphatidylserine liposomes and observed a reduced affinity upon phosphorylation on Tyr23 (Powell and Glenney, 1987). However, cellular membranes are more complex than liposomes and a whole range of molecules can contribute to the association of proteins with membranes and in this case with membrane microdomains that are resistant to detergent extraction in the cold. Therefore, Tyr23 phosphorylation of annexin A2 seems not to be of regulating importance for the association of this protein with cellular membrane rafts. However, it has to be taken into account that the analysed annexin A2 derivatives are still able to bind p11. Therefore, a localisation to DRMs might be mediated by forming mixed heterotetramers with endogenous annexin A2 and p11.

One key feature of annexin A2 that is thought to contribute to raft organisation is the ability to bind $PI(4,5)P_2$ (Gokhale et al., 2005). $PI(4,5)P_2$-binding proteins can be divided into two groups. The first group contains a structurally defined module responsible for the binding to this phospholipid, e.g. a pleckstrin homology domain. The second group does not harbour such a distinct domain but is characterised by clusters of basic residues of relatively undefined structure that are capable of mediating $PI(4,5)P_2$ binding (McLaughlin et al., 2002). Such cationic residues have also been identified in annexin A2 and the mutation of either Lys279 or Lys281 to Asp resulted in a remarkably decreased affinity for plasma membrane mimetic vesicles of the respective bacterially expressed monomeric proteins. Furthermore, annexin A2 mutants harbouring these mutations are not able to cluster $PI(4,5)P_2$ on giant unilamellar vesicles any more (Gokhale et al., 2005). The annexin A2 derivative KA harbouring a substitution at Lys281 was analysed for its association with cellular membrane microdomains.
DRM analysis revealed that the ectopically expressed KA mutant showed the same resistance to detergent extraction as ectopically expressed wt annexin A2 in MDCKs. Hence, the basic Lys281 that is supposed to be essential for $PI(4,5)P_2$-binding and -clustering *in vitro* does not have a major impact on the resistance of annexin A2 to detergent extraction in the cold. Different subsets of membrane rafts exist. Some of these possess a reduced level of $PI(4,5)P_2$. Binding to these domains can be mediated by other interactions of annexin A2 and possibly result the DRM association seen in these experiments. Furthermore, and as mentioned above, in living cells interaction mechanisms might be much more complex. Cellular membranes are not only composed of lipids but also of a variety of proteins and also the cellular cytoskeleton underneath the plasma membrane contributes to membrane architecture. Therefore, interactions might not be limited to a single amino acid. Maybe a double or triple mutant harbouring more mutations in the $PI(4,5)P_2$ binding site might show a reduced binding to DRMs in this system. Possible candidates for these mutations would be Lys279 and Arg284 that present two further conserved cationic residues in the putative $PI(4,5)P_2$-binding region of annexin A2. The substitution of Lys279 with Ala has already been demonstrated to interfere with the capability of annexin A2 to bind to and cluster $PI(4,5)P_2$ *in vitro* (Gokhale et al., 2005). However, also

in the case of the annexin A2 KA mutant it has to be taken into account that this protein could still be recruited to DRMs by mixed heterotetramers in which a p11 dimer links the derivative to endogenous intact annexin A2.

Ca^{2+}-binding is one of the most prominent characteristics of annexins. Annexin A2 harbours three high affinity type II Ca^{2+}-binding sites and two type III Ca^{2+}-binding sites. Inactivation of the type II sites results in the so-called CM mutant that shows a remarkably reduced affinity for the divalent cation and requires much higher Ca^{2+} concentrations for half-maximal phosphatidylserine binding (Jost et al., 1994). In the experiments performed in this thesis about 60 % of ectopically expressed annexin A2 CM and also about 60 % of annexin A2 wt associate with DRMs. Therefore, this mutation does not interfere with detergent resistance in the cold.
The group of David M. Waisman report that heterotetrameric annexin A2 CM Ca^{2+}-independently binds to phospholipids and F-actin. They propose that the inactivation of Ca^{2+}-binding sites by site-directed mutagenesis results in a conformational change that promotes binding to anionic phospholipid and F-actin (Filipenko et al., 2000). This could be a possible explanation for an association of the CM mutant with DRMs.
However, it is also known that annexin A2 can Ca^{2+}-independently bind to membranes (Jost et al., 1997), especially of those harbouring high amounts of cholesterol (Harder et al., 1997; Zeuschner et al., 2001). Therefore, the observed association of annexin A2 with DRMs might result from Ca^{2+}-independent membrane binding sites that have not been characterised yet. Furthermore, also the CM mutant could be localised to DRMs by forming mixed heterotetramers with p11 and endogenous annexin A2.

Many annexin A2 functions can be attributed to its heterotetrameric form with p11 (Gerke, 1989). Monomeric annexin A2 is reported to need higher Ca^{2+} concentrations for binding to phospholipids and membranes (Evans and Nelsestuen, 1994). DRM association analysis revealed that also the resistance to detergent extraction is altered. Only about 10 % of monomeric annexin A2 mutants incapable of binding p11 localised to detergent resistant fractions, in contrast to 60 % of the wt protein. Therefore, p11-binding is essential for the association of annexin A2 with DRMs.
The experiments were performed using 50 µM Ca^{2+} in the extraction buffers. Since it has been described that monomeric annexin A2 needs an increased amount of Ca^{2+} to bind phospholipids also the association with DRMs at higher Ca^{2+} concentrations was analysed. Indeed, the p11-binding deficient mutant of annexin A2 was shifted to the Triton insoluble fraction at higher Ca^{2+} concentrations (up to 1 mM). This indicates that not only the general phospholipid binding of the annexin A2 monomer requires a high amount of Ca^{2+} but also its association with membrane microdomains that are resistant to detergent extraction in the cold. This is in accordance with results obtained by Eberhard and co-workers. They worked with an N-terminally GFP-tagged annexin A2 construct which was unable to form heterotetrameric complexes with endogenous p11 and annexin A2. In their experiments endogenous annexin A2 associated with the Triton insoluble fraction at 100 µM Ca^{2+}, whereas the monomeric GFP-tagged annexin A2 was not detected in this fraction below 1 mM Ca^{2+} (Eberhard et al., 2001).

The ability to form heterotetramers might also be of critical importance for the association of the other annexin A2 derivatives tested here, as already mentioned above. They still possess an active p11-binding site and this might enable them to be recruited to membrane microdomains by forming mixed heterotetrameric complexes with endogenous annexin A2 and p11. It would be interesting to analyse these proteins in a cell system devoid of endogenous annexin A2. It is striking that only the proteins harbouring mutations in the p11-bindings sites (i.e. PM and PMCM) lost the ability to bind to detergent resistant membranes at somewhat physiological Ca^{2+} concentrations. Therefore, it is tempting to speculate that the p11-binding is of critical importance for the association of annexin A2 with membrane rafts in living cells.

However, DRMs are products of an artificial aggregation process and cannot be considered physiological membrane rafts. Resistance to extraction by detergents, most prominently Triton X-100, at 4 °C is widely used as a defining criterion for rafts and raft-association of cellular proteins and lipids (Brown and London, 1998). While the analysis of association to DRMs has been a valuable entry point for the raft research area, the concept of equating DRMs with raft membrane microdomains of cells has been criticised (Munro, 2003). From studies in model membranes (Heerklotz, 2002) and isolated cellular membranes (Gaus et al., 2005) it turned out that the detergent treatment itself can induce the formation of membrane domains which do not exist in the membranes prior to detergent extraction. Hence, detergent-resistant membranes should not be assumed to resemble biological rafts in size, structure or composition. Therefore, there is need for other experimental approaches to analyse these membrane microdomains.

5.3.2 Localisation of annexin A2 in the GM1 phase of PMSs

Model membrane systems, including giant unilamellar vesicles, allow optical discrimination of coexisting lipid phase types. But the cellular plasma membrane is very dynamic, has a complex protein and lipid composition and is connected to the underlying cytoskeleton. This complexity might prevent fluid phase segregation into optically resolvable microdomains that is seen in artificial membrane vesicles.

However, two recent studies demonstrated that microscopic phase separation can occur in cellular membranes under certain conditions. Baumgart and co-workers used chemical membrane blebbing to generate giant plasma membrane vesicles (GPMVs) that separate into micrometer-scale fluid phase domains upon cooling. These domains represent l_o-like and l_d-like phases as identified by fluorescent probes (Baumgart et al., 2007). In another approach Lingwood and colleagues used a hypotonic cell swelling procedure to generate membrane preparations called plasma membrane spheres (PMSs). By addition of CtxB phase separation was induced by clustering of the raft ganglioside GM1 at 37 °C. The emerging GM1 phase is enriched in cholesterol and transmembrane and lipid-anchored raft proteins (Lingwood et al., 2008). Both of these membrane outgrowths are devoid of actin cytoskeletal influence and endo- and exocytotic processes. Presumably, this uncoupling from the underlying cytoskeleton allows the coalescence of large-scale raft-based phases (Baumgart et al., 2007).

The association of annexin A2 and annexin A2 derivatives with the GM1 phase of PMSs was analysed. All annexin A2 variants tested localised to the CtxB positive membrane phase, indicating that the mutations applied here do not alter the binding to the large-scale raft-based phases of PMSs.

Thus, there is a discrepancy between the association of the p11-binding deficient annexin A2 mutant to the GM1 phase of PMSs and the observed reduced binding of this mutant to DRMs. In this context it is important to remember that detergent extraction only produces an artificial coalescence of proteins and lipids into a fraction that is enriched in raft proteins and raft lipids. Triton X-100 is quite a strong detergent and is thought to disrupt weak associations of proteins to rafts. For an association with the GM1 phase in PMSs probably only a weak or transient association with this raft-based membrane phase is sufficient for the protein to be clustered into a more stable platform upon glycolipid or protein oligomerisation (personal communication with Daniel Lingwood, Dresden, Germany). Therefore, it might be possible that monomeric annexin A2 displays a weak association with cholesterol rich microdomains that might be destroyed by detergent extraction in the cold. However, it has to be noted that the system of the phase separation in PMSs is not characterised very well either and extrapolating these membrane phases to living cell membranes should be considered with caution.

One other explanation for the association of the monomeric annexin A2 to the GM1 phase of PMSs could be an elevated Ca^{2+} concentration in the spheres. As mentioned above a rise in the Ca^{2+} level results in a recruitment of annexin A2 PM to DRMs. This might also hold true for the association of annexin A2 to GM1 phases in PMSs.
Keller and colleagues demonstrated that Ca^{2+} is an important component of the blebbing solution of GPMVs. The induction of the membrane outgrowths is accompanied by a raise of the Ca^{2+} level inside the cells. Only very few vesicles form in the absence of Ca^{2+} (Keller et al., 2009). It is hypothesised that the increase of intracellular Ca^{2+} leads to restructuration of the plasma membrane. The Ca^{2+} concentration in PMSs or the formation of PMSs in the absence of Ca^{2+} was not determined. However, Keller and co-workers propose that similar mechanisms apply for GPMVs and PMSs formation and that Ca^{2+} is of critical importance (Keller et al., 2009).
Therefore, the localisation of the monomeric annexin A2 PM variant in the GM1 phase could indeed result from high intracellular Ca^{2+} levels. This interaction could be similar to the DRM association of annexin A2 PM at unphysiologically high Ca^{2+} concentrations. Hence, PMSs are probably not suitable model systems to analyse Ca^{2+} dependent proteins like annexins. In this context, the analysis of a double annexin A2 mutant harbouring not only an inactive p11-binding site but also inactive Ca^{2+}-binding sites (i.e. the annexin A2 PMCM derivative) could be interesting.

5.3.3 Laurdan 2-photon analysis of cells expressing annexin A2 variants

Membrane rafts show a higher order packing than the surrounding membrane and therefore a reduced penetration by water molecules. Hence, the membrane condensation can be visualised using a polarity-sensitive probe like Laurdan. In order to understand how the condensed membrane phases relate to the classical definition of membrane rafts, usually two distinct regions of cellular membranes are distinguished. Gaus and colleagues discriminated between regions with a mean GP of 0.10 - 0.25 corresponding to liquid-disordered domains and domains with a mean GP of 0.35 - 0.55 corresponding to liquid ordered domains (Gaus et al., 2006). In combination with the use of fluorescently labelled proteins the overlay of the confocal image with the GP image can identify the localisation of proteins in liquid-disordered / liquid-ordered (low / high GP value) regions, respectively.

Laurdan studies labelling large unilamellar vesicles containing 3 mol % $PI(4,5)P_2$ revealed that annexin A2 is capable of inducing a spectral shift of Laurdan, indicating that annexin A2 is able to induce the formation of higher ordered membrane domains in model membranes. Annexin A2 variants harbouring mutations in the $PI(4,5)P_2$-binding site however do not evoke a spectral shift in these artificial model systems (Gokhale et al., 2005).

Here, it was analysed whether the expression of annexin A2 in living cells results in the formation of detectable domains of higher order or if the protein specifically localises to ordered membrane domains. Furthermore, various annexin A2 derivatives were analysed to investigate if different mutations affect this localisation.
mCherry tagged annexin A2 wt and different annexin A2 mutants were expressed in MDCK and the cells were labelled with Laurdan to investigate the membrane order at sites of protein localisation. Confocal images of the different proteins revealed a rather typical localisation. Annexin A2 wt as well as the phosphorylation mutants YE and YF, the $PI(4,5)P_2$-binding deficient KA mutant and the protein with mutated high affinity Ca^{2+}-binding sites are diffusely distributed throughout the cytoplasm and excluded from the nucleus. It has been described that p11 binding to annexin A2 prevents a sequestration of the complex into the nucleus (Eberhard et al., 2001). Therefore, the p11-binding deficient mutants PM and PMCM are not restricted to the cytoplasm but can also be found in the nucleus. The staining pattern of these two derivatives is similar to that observed for mCherry that was used as a control.

In the GP image of one representative example no regions of increased membrane condensation could be detected in the cell except for a few “red patches” in the pseudo-coloured image. Those probably arise from precipitated Laurdan. Domains of increased condensation were absent in all cells examined. However, it has to be pointed out that the analysed cells show a rather low average GP value of about 0.1. A GP value of 0.1 would correspond to liquid-disordered domains. The GP values of Laurdan in cells are usually higher. This points the possibility that the experimental setup was not optimal. The Laurdan measurements were performed during a three month international laboratory exchange in Sydney, Australia, and unfortunately there was not enough time to optimise the experimental conditions.

The absence of membrane domains that possess an increased membrane order could also be due to the fact that the cells were quiescent. To overcome this problem cells could be stimulated to form larger domains of higher membrane order that can be resolved with a conventional microscope. Raft size can be modulated by oligomerisation of raft components. E.g. the pentameric B-subunit of cholera toxin is often used to cluster raft domains. Also antibody-crosslinking of GPI-anchored proteins like placental alkaline phosphatise (PLAP) can form optically resolvable membrane microdomains (Harder et al., 1998). More high GP domains are revealed in fibroblasts when membrane proteins are cross-linked (Gaus et al., 2003). And the incubation of T lymphocytes with anti-CD3-coated beads leads to domains of higher order at sites of T cell receptor activation (Gaus et al., 2005).

The amount of annexin A2 localised to the membrane in the cells analysed here is rather small. Most of the protein is cytosolic. It is reported that annexin A2 preferentially localises to the plasma membrane at sites of cell-cell contact (Nigg et al., 1983). Singular cells were investigated here to be able to take a look at distinct cell membranes of discrete cells. Therefore, the localisation of annexin A2 at cell-cell contacts cannot be seen in this assay. Furthermore, the model cells used here were relatively flat. This makes it difficult to image the plasma membrane. At the same time, Laurdan internalises very fast and the amount of intracellular staining is fairly high in contrast to the membrane staining. Life cell imaging could improve the results (personal communication with Carles Rentero, Barcelona, Spain).

No measurable differences were detectable for the degree of membrane order in regions of the localisation of different annexin A2 derivatives or an mCherry control. This can probably be explained by the fact that regions of increased membrane condensation are missing. From the observation that annexin A2 expressing cells are devoid of membrane domains with increased order it could be concluded that the expression of this raft associated protein alone is not sufficient to induce the formation of Laurdan detectable microdomains in living cells under the experimental conditions chosen here. However, this conclusion should be considered with caution since the experimental setup might not have been optimal as mentioned above.

6 References

Abrami, L., Fivaz, M., Glauser, P.E., Parton, R.G., and van der Goot, F.G. (1998). A pore-forming toxin interacts with a GPI-anchored protein and causes vacuolation of the endoplasmic reticulum. J. Cell Biol. *140,* 525-540.

Adams, J.M., and Cory, S. (2002). Apoptosomes: engines for caspase activation. Curr. Opin. Cell Biol. *14,* 715-720.

Babiychuk, E.B., and Draeger, A. (2000). Annexins in cell membrane dynamics. Ca(2+)-regulated association of lipid microdomains. J. Cell Biol. *150,* 1113-1124.

Bao, H., Jiang, M., Zhu, M., Sheng, F., Ruan, J., and Ruan, C. (2009a). Overexpression of Annexin II affects the proliferation, apoptosis, invasion and production of proangiogenic factors in multiple myeloma. Int. J. Hematol. *90,* 177-185.

Bao, H.Y., Jiang, M., Ma, Z.N., Sheng, F., Zhu, M.Q., Chen, L., Xie, L.Q., Dong, N.Z., and Ruan, C.G. (2009b). Effects of Annexin II gene silencing by siRNA on proliferation and invasive potential of Jurkat lymphoma cells. Zhonghua Xue Ye Xue Za Zhi *30,* 303-306.

Baorto, D.M., Gao, Z., Malaviya, R., Dustin, M.L., van der Merwe, A., Lublin, D.M., and Abraham, S.N. (1997). Survival of FimH-expressing enterobacteria in macrophages relies on glycolipid traffic. Nature *389,* 636-639.

Barman, S., and Nayak, D.P. (2007). Lipid raft disruption by cholesterol depletion enhances influenza A virus budding from MDCK cells. J. Virol. *81,* 12169-12178.

Bastian, B.C. (1997). Annexins in cancer and autoimmune diseases. Cell Mol. Life Sci. *53,* 554-556.

Baumgart, T., Hammond, A.T., Sengupta, P., Hess, S.T., Holowka, D.A., Baird, B.A., and Webb, W.W. (2007). Large-scale fluid/fluid phase separation of proteins and lipids in giant plasma membrane vesicles. Proc. Natl. Acad. Sci. U. S. A. *104,* 3165-3170.

Beaton, A.R., Rodriguez, J., Reddy, Y.K., and Roy, P. (2002). The membrane trafficking protein calpactin forms a complex with bluetongue virus protein NS3 and mediates virus release. Proc. Natl. Acad. Sci. U. S. A. *99,* 13154-13159.

Becker, T., Weber, K., and Johnsson, N. (1990). Protein-protein recognition via short amphiphilic helices; a mutational analysis of the binding site of annexin II for p11. EMBO J. *9,* 4207-4213.

Bertrand, R., Solary, E., O'Connor, P., Kohn, K.W., and Pommier, Y. (1994). Induction of a common pathway of apoptosis by staurosporine. Exp. Cell Res. *211,* 314-321.

Bradford, M.M. (1976). A rapid and sensitive method for the quantitation of microgram quantities of protein utilizing the principle of protein-dye binding. Anal. Biochem. *72,* 248-254.

Brambilla, R., Zippel, R., Sturani, E., Morello, L., Peres, A., and Alberghina, L. (1991). Characterization of the tyrosine phosphorylation of calpactin I (annexin II) induced by platelet-derived growth factor. Biochem. J. *278 (Pt 2),* 447-452.

Brown, D.A., and London, E. (2000). Structure and function of sphingolipid- and cholesterol-rich membrane rafts. J. Biol. Chem. *275,* 17221-17224.

Brown, D.A., and London, E. (1998). Functions of lipid rafts in biological membranes. Annu. Rev. Cell Dev. Biol. *14,* 111-136.

Brown, D.A., and Rose, J.K. (1992). Sorting of GPI-anchored proteins to glycolipid-enriched membrane subdomains during transport to the apical cell surface. Cell *68,* 533-544.

Brownstein, C., Falcone, D.J., Jacovina, A., and Hajjar, K.A. (2001). A mediator of cell surface-specific plasmin generation. Ann. N. Y. Acad. Sci. *947,* 143-55; discussion 155-6.

Brydon, E.W., Smith, H., and Sweet, C. (2003). Influenza A virus-induced apoptosis in bronchiolar epithelial (NCI-H292) cells limits pro-inflammatory cytokine release. J. Gen. Virol. *84,* 2389-2400.

Budihardjo, I., Oliver, H., Lutter, M., Luo, X., and Wang, X. (1999). Biochemical pathways of caspase activation during apoptosis. Annu. Rev. Cell Dev. Biol. *15,* 269-290.

Cantin, R., Methot, S., and Tremblay, M.J. (2005). Plunder and stowaways: incorporation of cellular proteins by enveloped viruses. J. Virol. *79,* 6577-6587.

Celis, J.E. (2005). Cell biology : a laboratory handbook. Elsevier Academic Press.

Chen, W., Calvo, P.A., Malide, D., Gibbs, J., Schubert, U., Bacik, I., Basta, S., O'Neill, R., Schickli, J., Palese, P*., et al.* (2001). A novel influenza A virus mitochondrial protein that induces cell death. Nat. Med. *7,* 1306-1312.

Cheung, T.K., and Poon, L.L. (2007). Biology of influenza a virus. Ann. N. Y. Acad. Sci. *1102,* 1-25.

Chiang, Y., Rizzino, A., Sibenaller, Z.A., Wold, M.S., and Vishwanatha, J.K. (1999). Specific down-regulation of annexin II expression in human cells interferes with cell proliferation. Mol. Cell. Biochem. *199,* 139-147.

Chipuk, J.E., Kuwana, T., Bouchier-Hayes, L., Droin, N.M., Newmeyer, D.D., Schuler, M., and Green, D.R. (2004). Direct activation of Bax by p53 mediates mitochondrial membrane permeabilization and apoptosis. Science *303,* 1010-1014.

Chung, C.S., Chen, C.H., Ho, M.Y., Huang, C.Y., Liao, C.L., and Chang, W. (2006). Vaccinia virus proteome: identification of proteins in vaccinia virus intracellular mature virion particles. J. Virol. *80,* 2127-2140.

Chung, C.Y., Murphy-Ullrich, J.E., and Erickson, H.P. (1996). Mitogenesis, cell migration, and loss of focal adhesions induced by tenascin-C interacting with its cell surface receptor, annexin II. Mol. Biol. Cell *7,* 883-892.

Collins, M. (1995). Potential roles of apoptosis in viral pathogenesis. Am. J. Respir. Crit. Care Med. *152,* S20-4.

Creutz, C.E. (1992). The annexins and exocytosis. Science *258,* 924-931.

Daugas, E., Susin, S.A., Zamzami, N., Ferri, K.F., Irinopoulou, T., Larochette, N., Prevost, M.C., Leber, B., Andrews, D., Penninger, J., and Kroemer, G. (2000). Mitochondrio-nuclear translocation of AIF in apoptosis and necrosis. FASEB J. *14,* 729-739.

de Graauw, M., Tijdens, I., Smeets, M.B., Hensbergen, P.J., Deelder, A.M., and van de Water, B. (2008). Annexin A2 phosphorylation mediates cell scattering and branching morphogenesis via cofilin Activation. Mol. Cell. Biol. *28,* 1029-1040.

Dimmock, N.J. (1982). Review article initial stages in infection with animal viruses. J. Gen. Virol. *59,* 1-22.

Donato, N.J., and Perez, M. (1998). Tumor necrosis factor-induced apoptosis stimulates p53 accumulation and p21WAF1 proteolysis in ME-180 cells. J. Biol. Chem. *273,* 5067-5072.

Donato, R. (2001). S100: a multigenic family of calcium-modulated proteins of the EF-hand type with intracellular and extracellular functional roles. Int. J. Biochem. Cell Biol. *33,* 637-668.

Donato, R. (1999). Functional roles of S100 proteins, calcium-binding proteins of the EF-hand type. Biochim. Biophys. Acta *1450,* 191-231.

Drust, D.S., and Creutz, C.E. (1988). Aggregation of chromaffin granules by calpactin at micromolar levels of calcium. Nature *331,* 88-91.

Dry, I., Haig, D.M., Inglis, N.F., Imrie, L., Stewart, J.P., and Russell, G.C. (2008). Proteomic analysis of pathogenic and attenuated alcelaphine herpesvirus 1. J. Virol. *82,* 5390-5397.

Dubois, T., Oudinet, J.P., Mira, J.P., and Russo-Marie, F. (1996). Annexins and protein kinases C. Biochim. Biophys. Acta *1313,* 290-294.

Earnshaw, W.C. (1995). Nuclear changes in apoptosis. Curr. Opin. Cell Biol. *7,* 337-343.

Eberhard, D.A., Karns, L.R., VandenBerg, S.R., and Creutz, C.E. (2001). Control of the nuclear-cytoplasmic partitioning of annexin II by a nuclear export signal and by p11 binding. J. Cell. Sci. *114,* 3155-3166.

Ehrhardt, C., Seyer, R., Hrincius, E.R., Eierhoff, T., Wolff, T., and Ludwig, S. (2009). Interplay between influenza A virus and the innate immune signaling. Microbes Infect.

Ehrhardt, C., Wolff, T., and Ludwig, S. (2007). Activation of phosphatidylinositol 3-kinase signaling by the nonstructural NS1 protein is not conserved among type A and B influenza viruses. J. Virol. *81,* 12097-12100.

Emoto, K., Sawada, H., Yamada, Y., Fujimoto, H., Takahama, Y., Ueno, M., Takayama, T., Uchida, H., Kamada, K., Naito, A., Hirao, S., and Nakajima, Y. (2001). Annexin II overexpression is correlated with poor prognosis in human gastric carcinoma. Anticancer Res. *21,* 1339-1345.

Erikson, E., and Erikson, R.L. (1980). Identification of a cellular protein substrate phosphorylated by the avian sarcoma virus-transforming gene product. Cell *21,* 829-836.

Esposito, I., Penzel, R., Chaib-Harrireche, M., Barcena, U., Bergmann, F., Riedl, S., Kayed, H., Giese, N., Kleeff, J., Friess, H., and Schirmacher, P. (2006). Tenascin C and annexin II expression in the process of pancreatic carcinogenesis. J. Pathol. *208,* 673-685.

Evans, T.C.,Jr, and Nelsestuen, G.L. (1994). Calcium and membrane-binding properties of monomeric and multimeric annexin II. Biochemistry *33,* 13231-13238.

Falcone, D.J., Borth, W., Khan, K.M., and Hajjar, K.A. (2001). Plasminogen-mediated matrix invasion and degradation by macrophages is dependent on surface expression of annexin II. Blood *97,* 777-784.

Fava, R.A., and Cohen, S. (1984). Isolation of a calcium-dependent 35-kilodalton substrate for the epidermal growth factor receptor/kinase from A-431 cells. J. Biol. Chem. *259,* 2636-2645.

Filipek, A., Gerke, V., Weber, K., and Kuznicki, J. (1991). Characterization of the cell-cycle-regulated protein calcyclin from Ehrlich ascites tumor cells. Identification of two binding proteins obtained by Ca2(+)-dependent affinity chromatography. Eur. J. Biochem. *195,* 795-800.

Filipenko, N.R., Kang, H.M., and Waisman, D.M. (2000). Characterization of the Ca2+-binding sites of annexin II tetramer. J. Biol. Chem. *275,* 38877-38884.

Filipenko, N.R., MacLeod, T.J., Yoon, C.S., and Waisman, D.M. (2004). Annexin A2 is a novel RNA-binding protein. J. Biol. Chem. *279,* 8723-8731.

Filipenko, N.R., and Waisman, D.M. (2001). The C terminus of annexin II mediates binding to F-actin. J. Biol. Chem. *276,* 5310-5315.

Futter, C.E., and White, I.J. (2007). Annexins and endocytosis. Traffic *8,* 951-958.

Gaus, K., Chklovskaia, E., Fazekas de St Groth, B., Jessup, W., and Harder, T. (2005). Condensation of the plasma membrane at the site of T lymphocyte activation. J. Cell Biol. *171,* 121-131.

Gaus, K., Gratton, E., Kable, E.P., Jones, A.S., Gelissen, I., Kritharides, L., and Jessup, W. (2003). Visualizing lipid structure and raft domains in living cells with two-photon microscopy. Proc. Natl. Acad. Sci. U. S. A. *100,* 15554-15559.

Gaus, K., Rodriguez, M., Ruberu, K.R., Gelissen, I., Sloane, T.M., Kritharides, L., and Jessup, W. (2005). Domain-specific lipid distribution in macrophage plasma membranes. J. Lipid Res. *46,* 1526-1538.

Gaus, K., Zech, T., and Harder, T. (2006). Visualizing membrane microdomains by Laurdan 2-photon microscopy. Mol. Membr. Biol. *23,* 41-48.

Gaush, C.R., and Smith, T.F. (1968). Replication and plaque assay of influenza virus in an established line of canine kidney cells. Appl. Microbiol. *16,* 588-594.

Gerke, V. (1989). Tyrosine protein kinase substrate p36: a member of the annexin family of Ca2+/phospholipid-binding proteins. Cell Motil. Cytoskeleton *14,* 449-454.

Gerke, V., Creutz, C.E., and Moss, S.E. (2005). Annexins: linking Ca2+ signalling to membrane dynamics. Nat. Rev. Mol. Cell Biol. *6,* 449-461.

Gerke, V., and Moss, S.E. (2002). Annexins: from structure to function. Physiol. Rev. *82,* 331-371.

Gerke, V., and Moss, S.E. (1997). Annexins and membrane dynamics. Biochim. Biophys. Acta *1357,* 129-154.

Gerke, V., and Weber, K. (1985). The regulatory chain in the p36-kd substrate complex of viral tyrosine-specific protein kinases is related in sequence to the S-100 protein of glial cells. EMBO J. *4,* 2917-2920.

Gerke, V., and Weber, K. (1984). Identity of p36K phosphorylated upon Rous sarcoma virus transformation with a protein purified from brush borders; calcium-dependent binding to non-erythroid spectrin and F-actin. EMBO J. *3,* 227-233.

Gewies, A. (2003). ApoReview: Introduction to Apoptosis. Retrieved November 13, 2009, from http://www.celldeath.de/encyclo/aporev/aporev.htm

Gokhale, N.A., Abraham, A., Digman, M.A., Gratton, E., and Cho, W. (2005). Phosphoinositide specificity of and mechanism of lipid domain formation by annexin A2-p11 heterotetramer. J. Biol. Chem. *280,* 42831-42840.

Gong, Z.J., De Meyer, S., van Pelt, J., Hertogs, K., Depla, E., Soumillion, A., Fevery, J., and Yap, S.H. (1999). Transfection of a rat hepatoma cell line with a construct expressing human liver annexin V confers susceptibility to hepatitis B virus infection. Hepatology *29,* 576-584.

Gonzalez-Reyes, S., Garcia-Manso, A., Del Barrio, G., Dalton, K.P., Gonzalez-Molleda, L., Arrojo-Fernandez, J., Nicieza, I., and Parra, F. (2009). Role of annexin A2 in cellular entry of rabbit vesivirus. J. Gen. Virol. *90,* 2724-2730.

Green, D.R., and Reed, J.C. (1998). Mitochondria and apoptosis. Science *281,* 1309-1312.

Gujuluva, C.N., Kundu, A., Murti, K.G., and Nayak, D.P. (1994). Abortive replication of influenza virus A/WSN/33 in HeLa229 cells: defective viral entry and budding processes. Virology *204,* 491-505.

Hajjar, K.A., Jacovina, A.T., and Chacko, J. (1994). An endothelial cell receptor for plasminogen/tissue plasminogen activator. I. Identity with annexin II. J. Biol. Chem. *269,* 21191-21197.

Hajjar, K.A., and Krishnan, S. (1999). Annexin II: a mediator of the plasmin/plasminogen activator system. Trends Cardiovasc. Med. *9,* 128-138.

Harder, T., and Gerke, V. (1994). The annexin II2p11(2) complex is the major protein component of the triton X-100-insoluble low-density fraction prepared from MDCK cells in the presence of Ca2+. Biochim. Biophys. Acta *1223,* 375-382.

Harder, T., and Gerke, V. (1993). The subcellular distribution of early endosomes is affected by the annexin II2p11(2) complex. J. Cell Biol. *123,* 1119-1132.

Harder, T., Kellner, R., Parton, R.G., and Gruenberg, J. (1997). Specific release of membrane-bound annexin II and cortical cytoskeletal elements by sequestration of membrane cholesterol. Mol. Biol. Cell *8,* 533-545.

Harder, T., Scheiffele, P., Verkade, P., and Simons, K. (1998). Lipid domain structure of the plasma membrane revealed by patching of membrane components. J. Cell Biol. *141,* 929-942.

Harrist, A.V., Ryzhova, E.V., Harvey, T., and Gonzalez-Scarano, F. (2009). Anx2 interacts with HIV-1 Gag at phosphatidylinositol (4,5) bisphosphate-containing lipid rafts and increases viral production in 293T cells. PLoS One *4,* e5020.

Hayes, M.J., Rescher, U., Gerke, V., and Moss, S.E. (2004). Annexin-actin interactions. Traffic *5,* 571-576.

He, K.L., Deora, A.B., Xiong, H., Ling, Q., Weksler, B.B., Niesvizky, R., and Hajjar, K.A. (2008). Endothelial cell annexin A2 regulates polyubiquitination and degradation of its binding partner S100A10/p11. J. Biol. Chem. *283,* 19192-19200.

Heerklotz, H. (2002). Triton promotes domain formation in lipid raft mixtures. Biophys. J. *83,* 2693-2701.

Heffetz, D., Rutter, W.J., and Zick, Y. (1992). The insulinomimetic agents H2O2 and vanadate stimulate tyrosine phosphorylation of potential target proteins for the insulin receptor kinase in intact cells. Biochem. J. *288 (Pt 2),* 631-635.

Hertogs, K., Leenders, W.P., Depla, E., De Bruin, W.C., Meheus, L., Raymackers, J., Moshage, H., and Yap, S.H. (1993). Endonexin II, present on human liver plasma membranes, is a specific binding protein of small hepatitis B virus (HBV) envelope protein. Virology *197,* 549-557.

Hinshaw, V.S., Olsen, C.W., Dybdahl-Sissoko, N., and Evans, D. (1994). Apoptosis: a mechanism of cell killing by influenza A and B viruses. J. Virol. *68,* 3667-3673.

Horimoto, T., and Kawaoka, Y. (2005). Influenza: lessons from past pandemics, warnings from current incidents. Nat. Rev. Microbiol. *3,* 591-600.

Huang, R.T., Lichtenberg, B., and Rick, O. (1996). Involvement of annexin V in the entry of influenza viruses and role of phospholipids in infection. FEBS Lett. *392,* 59-62.

Huang, Y., Jin, Y., Yan, C.H., Yu, Y., Bai, J., Chen, F., Zhao, Y.Z., and Fu, S.B. (2008). Involvement of Annexin A2 in p53 induced apoptosis in lung cancer. Mol. Cell. Biochem. *309,* 117-123.

Huang, Y., Yan, C.H., and Fu, S.B. (2005). The cloning and expression of apoptosis associated gene ANNEXIN A2 induced by p53 gene. Zhonghua Yi Xue Yi Chuan Xue Za Zhi *22,* 661-664.

Hubaishy, I., Jones, P.G., Bjorge, J., Bellagamba, C., Fitzpatrick, S., Fujita, D.J., and Waisman, D.M. (1995). Modulation of annexin II tetramer by tyrosine phosphorylation. Biochemistry *34,* 14527-14534.

Hwang, H.J., Moon, C.H., Kim, H.G., Kim, J.Y., Lee, J.M., Park, J.W., and Chung, D.K. (2007). Identification and functional analysis of salmon annexin 1 induced by a virus infection in a fish cell line. J. Virol. *81,* 13816-13824.

Ipsen, J.H., Karlstrom, G., Mouritsen, O.G., Wennerstrom, H., and Zuckermann, M.J. (1987). Phase equilibria in the phosphatidylcholine-cholesterol system. Biochim. Biophys. Acta *905,* 162-172.

Ivanova, S., Repnik, U., Bojic, L., Petelin, A., Turk, V., and Turk, B. (2008). Lysosomes in apoptosis. Methods Enzymol. *442,* 183-199.

Jacob, R., Heine, M., Eikemeyer, J., Frerker, N., Zimmer, K.P., Rescher, U., Gerke, V., and Naim, H.Y. (2004). Annexin II is required for apical transport in polarized epithelial cells. J. Biol. Chem. *279,* 3680-3684.

Janes, P.W., Ley, S.C., and Magee, A.I. (1999). Aggregation of lipid rafts accompanies signaling via the T cell antigen receptor. J. Cell Biol. *147,* 447-461.

Jeoung, D.I., Tang, B., and Sonenberg, M. (1995). Effects of tumor necrosis factor-alpha on antimitogenicity and cell cycle-related proteins in MCF-7 cells. J. Biol. Chem. *270,* 18367-18373.

Jindal, H.K., Chaney, W.G., Anderson, C.W., Davis, R.G., and Vishwanatha, J.K. (1991). The protein-tyrosine kinase substrate, calpactin I heavy chain (p36), is part of the primer recognition protein complex that interacts with DNA polymerase alpha. J. Biol. Chem. *266,* 5169-5176.

Johnsson, N., Gerke, V., and Weber, K. (1990). P36, member of the CA2+/lipid binding proteins (annexins, calpactins, lipocortins) and its complex with P11; molecular aspects. Prog. Clin. Biol. Res. *349,* 123-133.

Johnsson, N., Marriott, G., and Weber, K. (1988). P36, the Major Cytoplasmic Substrate of Src Tyrosine Protein Kinase, Binds to its P11 Regulatory Subunit Via a Short Amino-Terminal Amphiphatic Helix. EMBO J. *7,* 2435-2442.

Johnsson, N., Nguyen Van, P., Soling, H.D., and Weber, K. (1986). Functionally distinct serine phosphorylation sites of p36, the cellular substrate of retroviral protein kinase; differential inhibition of reassociation with p11. EMBO J. *5,* 3455-3460.

Jost, M., and Gerke, V. (1996). Mapping of a regulatory important site for protein kinase C phosphorylation in the N-terminal domain of annexin II. Biochim. Biophys. Acta *1313,* 283-289.

Jost, M., Thiel, C., Weber, K., and Gerke, V. (1992). Mapping of three unique Ca(2+)-binding sites in human annexin II. Eur. J. Biochem. *207,* 923-930.

Jost, M., Weber, K., and Gerke, V. (1994). Annexin II contains two types of Ca(2+)-binding sites. Biochem. J. *298 Pt 3,* 553-559.

Jost, M., Zeuschner, D., Seemann, J., Weber, K., and Gerke, V. (1997). Identification and characterization of a novel type of annexin-membrane interaction: Ca2+ is not required for the association of annexin II with early endosomes. J. Cell. Sci. *110 (Pt 2),* 221-228.

Karasik, A., Pepinsky, R.B., Shoelson, S.E., and Kahn, C.R. (1988). Lipocortins 1 and 2 as substrates for the insulin receptor kinase in rat liver. J. Biol. Chem. *263,* 11862-11867.

Keller, H., Lorizate, M., and Schwille, P. (2009). PI(4,5)P(2) Degradation Promotes the Formation of Cytoskeleton-Free Model Membrane Systems. Chemphyschem

Kerr, J.F., Wyllie, A.H., and Currie, A.R. (1972). Apoptosis: a basic biological phenomenon with wide-ranging implications in tissue kinetics. Br. J. Cancer *26,* 239-257.

Kirschnek, S., Adams, C., and Gulbins, E. (2005). Annexin II is a novel receptor for Pseudomonas aeruginosa. Biochem. Biophys. Res. Commun. *327,* 900-906.

Kumble, K.D., Iversen, P.L., and Vishwanatha, J.K. (1992). The role of primer recognition proteins in DNA replication: inhibition of cellular proliferation by antisense oligodeoxyribonucleotides. J. Cell. Sci. *101 (Pt 1),* 35-41.

Laemmli, U.K. (1970). Cleavage of structural proteins during the assembly of the head of bacteriophage T4. Nature *227,* 680-685.

Lakadamyali, M., Rust, M.J., and Zhuang, X. (2004). Endocytosis of influenza viruses. Microbes Infect. *6,* 929-936.

Le Cabec, V., and Maridonneau-Parini, I. (1994). Annexin 3 is associated with cytoplasmic granules in neutrophils and monocytes and translocates to the plasma membrane in activated cells. Biochem. J. *303 (Pt 2),* 481-487.

LeBouder, F., Morello, E., Rimmelzwaan, G.F., Bosse, F., Pechoux, C., Delmas, B., and Riteau, B. (2008). Annexin II incorporated into influenza virus particles supports virus replication by converting plasminogen into plasmin. J. Virol. *82,* 6820-6828.

Li, H., Zhu, H., Xu, C.J., and Yuan, J. (1998). Cleavage of BID by caspase 8 mediates the mitochondrial damage in the Fas pathway of apoptosis. Cell *94,* 491-501.

Lim, L.H., and Pervaiz, S. (2007). Annexin 1: the new face of an old molecule. FASEB J. *21,* 968-975.

Ling, Q., Jacovina, A.T., Deora, A., Febbraio, M., Simantov, R., Silverstein, R.L., Hempstead, B., Mark, W.H., and Hajjar, K.A. (2004). Annexin II regulates fibrin homeostasis and neoangiogenesis in vivo. J. Clin. Invest. *113,* 38-48.

Lingwood, D., Ries, J., Schwille, P., and Simons, K. (2008). Plasma membranes are poised for activation of raft phase coalescence at physiological temperature. Proc. Natl. Acad. Sci. U. S. A. *105,* 10005-10010.

Lingwood, D., and Simons, K. (2007). Detergent resistance as a tool in membrane research. Nat. Protoc. *2,* 2159-2165.

Livak, K.J., and Schmittgen, T.D. (2001). Analysis of relative gene expression data using real-time quantitative PCR and the 2(-Delta Delta C(T)) Method. Methods *25,* 402-408.

Locksley, R.M., Killeen, N., and Lenardo, M.J. (2001). The TNF and TNF receptor superfamilies: integrating mammalian biology. Cell *104,* 487-501.

Lohmeyer, J., Talens, L.T., and Klenk, H.D. (1979). Biosynthesis of the influenza virus envelope in abortive infection. J. Gen. Virol. *42,* 73-88.

Loret, S., Guay, G., and Lippe, R. (2008). Comprehensive characterization of extracellular herpes simplex virus type 1 virions. J. Virol. *82,* 8605-8618.

Ludwig, S., Planz, O., Pleschka, S., and Wolff, T. (2003). Influenza-virus-induced signaling cascades: targets for antiviral therapy? Trends Mol. Med. *9,* 46-52.

Ludwig, S., Pleschka, S., and Wolff, T. (1999). A fatal relationship--influenza virus interactions with the host cell. Viral Immunol. *12,* 175-196.

Ma, G., Greenwell-Wild, T., Lei, K., Jin, W., Swisher, J., Hardegen, N., Wild, C.T., and Wahl, S.M. (2004). Secretory leukocyte protease inhibitor binds to annexin II, a cofactor for macrophage HIV-1 infection. J. Exp. Med. *200,* 1337-1346.

Malhotra, R., Ward, M., Bright, H., Priest, R., Foster, M.R., Hurle, M., Blair, E., and Bird, M. (2003). Isolation and characterisation of potential respiratory syncytial virus receptor(s) on epithelial cells. Microbes Infect. *5,* 123-133.

Manes, S., del Real, G., and Martinez-A, C. (2003). Pathogens: raft hijackers. Nat. Rev. Immunol. *3,* 557-568.

Marjuki, H., Alam, M.I., Ehrhardt, C., Wagner, R., Planz, O., Klenk, H.D., Ludwig, S., and Pleschka, S. (2006). Membrane accumulation of influenza A virus hemagglutinin triggers nuclear export of the viral genome via protein kinase Calpha-mediated activation of ERK signaling. J. Biol. Chem. *281,* 16707-16715.

Martin, S.J., Reutelingsperger, C.P., McGahon, A.J., Rader, J.A., van Schie, R.C., LaFace, D.M., and Green, D.R. (1995). Early redistribution of plasma membrane phosphatidylserine is a general feature of apoptosis regardless of the initiating stimulus: inhibition by overexpression of Bcl-2 and Abl. J. Exp. Med. *182,* 1545-1556.

Martin-Belmonte, F., Gassama, A., Datta, A., Yu, W., Rescher, U., Gerke, V., and Mostov, K. (2007). PTEN-mediated apical segregation of phosphoinositides controls epithelial morphogenesis through Cdc42. Cell *128,* 383-397.

Mayer, G., Poirier, S., and Seidah, N.G. (2008). Annexin A2 is a C-terminal PCSK9-binding protein that regulates endogenous low density lipoprotein receptor levels. J. Biol. Chem. *283,* 31791-31801.

McLaughlin, S., Wang, J., Gambhir, A., and Murray, D. (2002). PIP2 and proteins: interactions, organization, and information flow. Annu. Rev. Biophys. Biomol. Struct. *31*, 151-175.

Menell, J.S., Cesarman, G.M., Jacovina, A.T., McLaughlin, M.A., Lev, E.A., and Hajjar, K.A. (1999). Annexin II and bleeding in acute promyelocytic leukemia. N. Engl. J. Med. *340,* 994-1004.

Menke, M., Ross, M., Gerke, V., and Steinem, C. (2004). The molecular arrangement of membrane-bound annexin A2-S100A10 tetramer as revealed by scanning force microscopy. Chembiochem *5,* 1003-1006.

Merrifield, C.J., Rescher, U., Almers, W., Proust, J., Gerke, V., Sechi, A.S., and Moss, S.E. (2001). Annexin 2 has an essential role in actin-based macropinocytic rocketing. Curr. Biol. *11,* 1136-1141.

Mickleburgh, I., Burtle, B., Hollas, H., Campbell, G., Chrzanowska-Lightowlers, Z., Vedeler, A., and Hesketh, J. (2005). Annexin A2 binds to the localization signal in the 3' untranslated region of c-myc mRNA. FEBS J. *272,* 413-421.

Miyahara, A., Nakanishi, N., Ooka, T., Hayashi, T., Sugimoto, N., and Tobe, T. (2009). Enterohemorrhagic Escherichia coli effector EspL2 induces actin microfilament aggregation through annexin 2 activation. Cell. Microbiol. *11,* 337-350.

Moerdyk-Schauwecker, M., Hwang, S.I., and Grdzelishvili, V.Z. (2009). Analysis of virion associated host proteins in vesicular stomatitis virus using a proteomics approach. Virol. J. *6,* 166.

Morgan, R.O., Martin-Almedina, S., Iglesias, J.M., Gonzalez-Florez, M.I., and Fernandez, M.P. (2004). Evolutionary perspective on annexin calcium-binding domains. Biochim. Biophys. Acta *1742,* 133-140.

Moss, S.E., and Morgan, R.O. (2004). The annexins. Genome Biol. *5,* 219.

Mund, T., Gewies, A., Schoenfeld, N., Bauer, M.K., and Grimm, S. (2003). Spike, a novel BH3-only protein, regulates apoptosis at the endoplasmic reticulum. FASEB J. *17,* 696-698.

Munro, S. (2003). Lipid rafts: elusive or illusive? Cell *115,* 377-388.

Nagata, S. (1999). Fas ligand-induced apoptosis. Annu. Rev. Genet. *33,* 29-55.

Nakamura-Lopez, Y., Sarmiento-Silva, R.E., Moran-Andrade, J., and Gomez-Garcia, B. (2009). Staurosporine-induced apoptosis in P388D1 macrophages involves both extrinsic and intrinsic pathways. Cell Biol. Int. *33,* 1026-1031.

Nicolier, M., Decrion-Barthod, A.Z., Launay, S., Pretet, J.L., and Mougin, C. (2009). Spatiotemporal activation of caspase-dependent and -independent pathways in staurosporine-induced apoptosis of p53wt and p53mt human cervical carcinoma cells. Biol. Cell. *101,* 455-467.

Nigg, E.A., Cooper, J.A., and Hunter, T. (1983). Immunofluorescent localization of a 39,000-dalton substrate of tyrosine protein kinases to the cytoplasmic surface of the plasma membrane. J. Cell Biol. *96,* 1601-1609.

Oliferenko, S., Paiha, K., Harder, T., Gerke, V., Schwarzler, C., Schwarz, H., Beug, H., Gunthert, U., and Huber, L.A. (1999). Analysis of CD44-containing lipid rafts: Recruitment of annexin II and stabilization by the actin cytoskeleton. J. Cell Biol. *146,* 843-854.

Olsen, C.W., Kehren, J.C., Dybdahl-Sissoko, N.R., and Hinshaw, V.S. (1996). Bcl-2 Alters Influenza Virus Yield, Spread, and Hemagglutinin Glycosylation. J. Virol. *70,* 663-666.

Osborn, M., Johnsson, N., Wehland, J., and Weber, K. (1988). The submembranous location of p11 and its interaction with the p36 substrate of pp60 src kinase in situ. Exp. Cell Res. *175,* 81-96.

Otto, M., Gunther, A., Fan, H., Rick, O., and Huang, R.T. (1994). Identification of annexin 33 kDa in cultured cells as a binding protein of influenza viruses. FEBS Lett. *356,* 125-129.

Padula, M.E., Sydnor, M.L., and Wilson, D.W. (2009). Isolation and preliminary characterization of herpes simplex virus 1 primary enveloped virions from the perinuclear space. J. Virol. *83,* 4757-4765.

Pelengaris, S., Khan, M., and Evan, G. (2002). c-MYC: more than just a matter of life and death. Nat. Rev. Cancer. *2,* 764-776.

Pepinsky, R.B., and Sinclair, L.K. (1986). Epidermal growth factor-dependent phosphorylation of lipocortin. Nature *321,* 81-84.

Perretti, M., and Gavins, F.N. (2003). Annexin 1: an endogenous anti-inflammatory protein. News Physiol. Sci. *18,* 60-64.

Pike, L.J., and Casey, L. (1996). Localization and turnover of phosphatidylinositol 4,5-bisphosphate in caveolin-enriched membrane domains. J. Biol. Chem. *271,* 26453-26456.

Polunovsky, V.A., Wendt, C.H., Ingbar, D.H., Peterson, M.S., and Bitterman, P.B. (1994). Induction of endothelial cell apoptosis by TNF alpha: modulation by inhibitors of protein synthesis. Exp. Cell Res. *214,* 584-594.

Portincasa, P., Conti, G., and Chezzi, C. (1990). Abortive replication of influenza A viruses in HeLa 229 cells. Virus Res. *18,* 29-40.

Powell, M.A., and Glenney, J.R. (1987). Regulation of calpactin I phospholipid binding by calpactin I light-chain binding and phosphorylation by p60v-src. Biochem. J. *247,* 321-328.

Puisieux, A., Ji, J., and Ozturk, M. (1996). Annexin II up-regulates cellular levels of p11 protein by a post-translational mechanisms. Biochem. J. *313 (Pt 1),* 51-55.

Radke, K., Gilmore, T., and Martin, G.S. (1980). Transformation by Rous sarcoma virus: a cellular substrate for transformation-specific protein phosphorylation contains phosphotyrosine. Cell *21,* 821-828.

Raynal, P., and Pollard, H.B. (1994). Annexins: the problem of assessing the biological role for a gene family of multifunctional calcium- and phospholipid-binding proteins. Biochim. Biophys. Acta *1197,* 63-93.

Rescher, U., and Gerke, V. (2004). Annexins--unique membrane binding proteins with diverse functions. J. Cell. Sci. *117,* 2631-2639.

Rescher, U., Ruhe, D., Ludwig, C., Zobiack, N., and Gerke, V. (2004). Annexin 2 is a phosphatidylinositol (4,5)-bisphosphate binding protein recruited to actin assembly sites at cellular membranes. J. Cell. Sci. *117,* 3473-3480.

Rescher, U., Ludwig, C., Konietzko, V., Kharitonenkov, A., and Gerke, V. (2008). Tyrosine phosphorylation of annexin A2 regulates Rho-mediated actin rearrangement and cell adhesion. J. Cell. Sci. *121,* 2177-2185.

Ridley, A.J. (2001). Rho GTPases and cell migration. J. Cell. Sci. *114,* 2713-2722.

Riento, K., and Ridley, A.J. (2003). Rocks: multifunctional kinases in cell behaviour. Nat. Rev. Mol. Cell Biol. *4,* 446-456.

Rintala-Dempsey, A.C., Santamaria-Kisiel, L., Liao, Y., Lajoie, G., and Shaw, G.S. (2006). Insights into S100 target specificity examined by a new interaction between S100A11 and annexin A2. Biochemistry *45,* 14695-14705.

Roseman, B.J., Bollen, A., Hsu, J., Lamborn, K., and Israel, M.A. (1994). Annexin II marks astrocytic brain tumors of high histologic grade. Oncol. Res. *6,* 561-567.

Rosenberger, C.M., Brumell, J.H., and Finlay, B.B. (2000). Microbial pathogenesis: lipid rafts as pathogen portals. Curr. Biol. *10,* R823-5.

Rossignol, P., Ho-Tin-Noe, B., Vranckx, R., Bouton, M.C., Meilhac, O., Lijnen, H.R., Guillin, M.C., Michel, J.B., and Angles-Cano, E. (2004). Protease nexin-1 inhibits plasminogen activation-induced apoptosis of adherent cells. J. Biol. Chem. *279,* 10346-10356.

Ryzhova, E.V., Vos, R.M., Albright, A.V., Harrist, A.V., Harvey, T., and Gonzalez-Scarano, F. (2006). Annexin 2: a novel human immunodeficiency virus type 1 Gag binding protein involved in replication in monocyte-derived macrophages. J. Virol. *80,* 2694-2704.

Saffari, M., Dinehkabodi, O.S., Ghaffari, S.H., Modarressi, M.H., Mansouri, F., and Heidari, M. (2009). Identification of novel p53 target genes by cDNA AFLP in glioblastoma cells. Cancer Lett. *273,* 316-322.

Saiki, R.K., Gelfand, D.H., Stoffel, S., Scharf, S.J., Higuchi, R., Horn, G.T., Mullis, K.B., and Erlich, H.A. (1988). Primer-directed enzymatic amplification of DNA with a thermostable DNA polymerase. Science *239,* 487-491.

Salvesen, G.S., and Dixit, V.M. (1997). Caspases: intracellular signaling by proteolysis. Cell *91,* 443-446.

Sarafian, T., Pradel, L.A., Henry, J.P., Aunis, D., and Bader, M.F. (1991). The participation of annexin II (calpactin I) in calcium-evoked exocytosis requires protein kinase C. J. Cell Biol. *114,* 1135-1147.

Scarlett, J.L., Sheard, P.W., Hughes, G., Ledgerwood, E.C., Ku, H.H., and Murphy, M.P. (2000). Changes in mitochondrial membrane potential during staurosporine-induced apoptosis in Jurkat cells. FEBS Lett. *475,* 267-272.

Schafer, B.W., and Heizmann, C.W. (1996). The S100 family of EF-hand calcium-binding proteins: functions and pathology. Trends Biochem. Sci. *21,* 134-140.

Scheiffele, P., Rietveld, A., Wilk, T., and Simons, K. (1999). Influenza viruses select ordered lipid domains during budding from the plasma membrane. J. Biol. Chem. *274,* 2038-2044.

Scheiffele, P., Roth, M.G., and Simons, K. (1997). Interaction of influenza virus haemagglutinin with sphingolipid-cholesterol membrane domains via its transmembrane domain. EMBO J. *16,* 5501-5508.

Schultz-Cherry, S., Dybdahl-Sissoko, N., Neumann, G., Kawaoka, Y., and Hinshaw, V.S. (2001). Influenza virus ns1 protein induces apoptosis in cultured cells. J. Virol. *75,* 7875-7881.

Schultz-Cherry, S., and Hinshaw, V.S. (1996). Influenza virus neuraminidase activates latent transforming growth factor beta. J. Virol. *70,* 8624-8629.

Semov, A., Moreno, M.J., Onichtchenko, A., Abulrob, A., Ball, M., Ekiel, I., Pietrzynski, G., Stanimirovic, D., and Alakhov, V. (2005). Metastasis-associated protein S100A4 induces angiogenesis through interaction with Annexin II and accelerated plasmin formation. J. Biol. Chem. *280,* 20833-20841.

Sharma, M.R., Koltowski, L., Ownbey, R.T., Tuszynski, G.P., and Sharma, M.C. (2006). Angiogenesis-associated protein annexin II in breast cancer: selective expression in invasive breast cancer and contribution to tumor invasion and progression. Exp. Mol. Pathol. *81,* 146-156.

Shaw, M.L., Stone, K.L., Colangelo, C.M., Gulcicek, E.E., and Palese, P. (2008). Cellular proteins in influenza virus particles. PLoS Pathog. *4,* e1000085.

Shen, Y., Wang, X., Guo, L., Qiu, Y., Li, X., Yu, H., Xiang, H., Tong, G., and Ma, Z. (2009). Influenza A virus induces p53 accumulation in a biphasic pattern. Biochem. Biophys. Res. Commun. *382,* 331-335.

Siever, D.A., and Erickson, H.P. (1997). Extracellular annexin II. Int. J. Biochem. Cell Biol. *29,* 1219-1223.

Simons, K., and Ikonen, E. (1997). Functional rafts in cell membranes. Nature *387,* 569-572.

Simons, K., and Toomre, D. (2000). Lipid rafts and signal transduction. Nat. Rev. Mol. Cell Biol. *1,* 31-39.

Skibbens, J.E., Roth, M.G., and Matlin, K.S. (1989). Differential extractability of influenza virus hemagglutinin during intracellular transport in polarized epithelial cells and nonpolar fibroblasts. J. Cell Biol. *108,* 821-832.

Sun, X., and Whittaker, G.R. (2007). Role of the actin cytoskeleton during influenza virus internalization into polarized epithelial cells. Cell. Microbiol. *9,* 1672-1682.

Sun, X., and Whittaker, G.R. (2003). Role for influenza virus envelope cholesterol in virus entry and infection. J. Virol. *77,* 12543-12551.

Suomalainen, M. (2002). Lipid rafts and assembly of enveloped viruses. Traffic *3,* 705-709.

Swisher, J.F., Khatri, U., and Feldman, G.M. (2007). Annexin A2 is a soluble mediator of macrophage activation. J. Leukoc. Biol. *82,* 1174-1184.

Takeda, M., Leser, G.P., Russell, C.J., and Lamb, R.A. (2003). Influenza virus hemagglutinin concentrates in lipid raft microdomains for efficient viral fusion. Proc. Natl. Acad. Sci. U. S. A. *100,* 14610-14617.

Tanaka, T., Akatsuka, S., Ozeki, M., Shirase, T., Hiai, H., and Toyokuni, S. (2004). Redox regulation of annexin 2 and its implications for oxidative stress-induced renal carcinogenesis and metastasis. Oncogene *23,* 3980-3989.

Thiel, C., Osborn, M., and Gerke, V. (1992). The tight association of the tyrosine kinase substrate annexin II with the submembranous cytoskeleton depends on intact p11- and Ca(2+)-binding sites. J. Cell. Sci. *103 (Pt 3),* 733-742.

Tomas, A., Futter, C., and Moss, S.E. (2004). Annexin 11 is required for midbody formation and completion of the terminal phase of cytokinesis. J. Cell Biol. *165,* 813-822.

Tong, X.B., Kita, K., Karata, K., Zhu, C.L., Sugaya, S., Ichimura, Y., Satoh, M., Tomonaga, T., Nomura, F., Jin, Y.H., and Suzuki, N. (2008). Annexin II, a novel HSP27-interacted protein, is involved in resistance to UVC-induced cell death in human APr-1 cells. Photochem. Photobiol. *84,* 1455-1461.

Tressler, R.J., Updyke, T.V., Yeatman, T., and Nicolson, G.L. (1993). Extracellular annexin II is associated with divalent cation-dependent tumor cell-endothelial cell adhesion of metastatic RAW117 large-cell lymphoma cells. J. Cell. Biochem. *53,* 265-276.

Tuma, P.L., Nyasae, L.K., and Hubbard, A.L. (2002). Nonpolarized cells selectively sort apical proteins from cell surface to a novel compartment, but lack apical retention mechanisms. Mol. Biol. Cell *13,* 3400-3415.

Turpin, E., Luke, K., Jones, J., Tumpey, T., Konan, K., and Schultz-Cherry, S. (2005). Influenza virus infection increases p53 activity: role of p53 in cell death and viral replication. J. Virol. *79,* 8802-8811.

van der Goot, F.G., and Harder, T. (2001). Raft membrane domains: from a liquid-ordered membrane phase to a site of pathogen attack. Semin. Immunol. *13,* 89-97.

Varnai, P., and Balla, T. (1998). Visualization of phosphoinositides that bind pleckstrin homology domains: calcium- and agonist-induced dynamic changes and relationship to myo-[3H]inositol-labeled phosphoinositide pools. J. Cell Biol. *143,* 501-510.

Vedeler, A., and Hollås, H. (2000). Annexin II is associated with mRNAs which may contribute a distinct subpopulation. Biochem. J. *348*, 565-572.

Vishwanatha, J.K., and Kumble, S. (1993). Involvement of annexin II in DNA replication: evidence from cell-free extracts of Xenopus eggs. J. Cell. Sci. *105 (Pt 2),* 533-540.

Waisman, D.M. (1995). Annexin II tetramer: structure and function. Mol. Cell. Biochem. *149-150,* 301-322.

Wang, C., Lin, Y., Su, W., Chen, C., and Lin, C. (2009). Glycogen Synthase Kinase-3 and Omi/HtrA2 Induce Annexin A2 Cleavage followed by Cell Cycle Inhibition and Apoptosis. Mol. Biol. Cell

Wesselborg, S., Engels, I.H., Rossmann, E., Los, M., and Schulze-Osthoff, K. (1999). Anticancer drugs induce caspase-8/FLICE activation and apoptosis in the absence of CD95 receptor/ligand interaction. Blood *93,* 3053-3063.

World Health Organization. (1999). Leading causes of death. Retrieved December 16, 2009, from http://www.who.int/infectious-disease-report/pages/graph1.html

Wright, J.F., Kurosky, A., Pryzdial, E.L., and Wasi, S. (1995). Host cellular annexin II is associated with cytomegalovirus particles isolated from cultured human fibroblasts. J. Virol. *69,* 4784-4791.

Wright, J.F., Kurosky, A., and Wasi, S. (1994). An endothelial cell-surface form of annexin II binds human cytomegalovirus. Biochem. Biophys. Res. Commun. *198,* 983-989.

Wu, Y., Mehew, J.W., Heckman, C.A., Arcinas, M., and Boxer, L.M. (2001). Negative regulation of bcl-2 expression by p53 in hematopoietic cells. Oncogene *20,* 240-251.

Wurzer, W.J., Planz, O., Ehrhardt, C., Giner, M., Silberzahn, T., Pleschka, S., and Ludwig, S. (2003). Caspase 3 activation is essential for efficient influenza virus propagation. EMBO J. *22,* 2717-2728.

Yamada, A., Irie, K., Hirota, T., Ooshio, T., Fukuhara, A., and Takai, Y. (2005). Involvement of the annexin II-S100A10 complex in the formation of E-cadherin-based adherens junctions in Madin-Darby canine kidney cells. J. Biol. Chem. *280,* 6016-6027.

Yang, W., Qu, S., Liu, Q., and Zheng, C. (2009). Avian influenza virus A/chicken/Hubei/489/2004 (H5N1) induces caspase-dependent apoptosis in a cell-specific manner. Mol. Cell. Biochem. *332,* 233-241.

Zeuschner, D., Stoorvogel, W., and Gerke, V. (2001). Association of annexin 2 with recycling endosomes requires either calcium- or cholesterol-stabilized membrane domains. Eur. J. Cell Biol. *80,* 499-507.

Zhang, B.F., Peng, F.F., Zhang, J.Z., and Wu, D.C. (2003). Staurosporine induces apoptosis in NG108-15 cells. Acta Pharmacol. Sin. *24,* 663-669.

Zhang, X.D., Gillespie, S.K., and Hersey, P. (2004). Staurosporine induces apoptosis of melanoma by both caspase-dependent and -independent apoptotic pathways. Mol. Cancer. Ther. *3,* 187-197.

Zhirnov, O.P., Konakova, T.E., Wolff, T., and Klenk, H.D. (2002). NS1 protein of influenza A virus down-regulates apoptosis. J. Virol. *76,* 1617-1625.

Zhu, F.X., Chong, J.M., Wu, L., and Yuan, Y. (2005). Virion proteins of Kaposi's sarcoma-associated herpesvirus. J. Virol. *79,* 800-811.

Zobiack, N., Rescher, U., Laarmann, S., Michgehl, S., Schmidt, M.A., and Gerke, V. (2002). Cell-surface attachment of pedestal-forming enteropathogenic E. coli induces a clustering of raft components and a recruitment of annexin 2. J. Cell. Sci. *115,* 91-98.

Zobiack, N., Rescher, U., Ludwig, C., Zeuschner, D., and Gerke, V. (2003). The annexin 2/S100A10 complex controls the distribution of transferrin receptor-containing recycling endosomes. Mol. Biol. Cell *14,* 4896-4908.

Zokas, L., and Glenney, J.R.,Jr. (1987). The calpactin light chain is tightly linked to the cytoskeletal form of calpactin I: studies using monoclonal antibodies to calpactin subunits. J. Cell Biol. *105,* 2111-2121.

Zong, Z.P., Fujikawa-Yamamoto, K., Li, A.L., Yamaguchi, N., Chang, Y.G., Murakami, M., Odashima, S., and Ishikawa, Y. (1999). Both low and high concentrations of staurosporine induce G1 arrest through down-regulation of cyclin E and cdk2 expression. Cell Struct. Funct. *24,* 457-463.

7 Appendix

7.1 Abbreviations

α	anti or alpha
A	ampere
aa	amino acid
AIF	apoptosis inducing factor
anx	annexin
Apaf-1	apoptotic peptidase activating factor 1
APS	ammonium persulfate
ATP	adenosine-5'-triphosphate
BA	bovine albumin
Bax	Bcl-2–associated X protein
Bcl-2	B-cell lymphoma 2
Bcl-XL	B-cell lymphoma-extra large
BHK	baby hamster kidney
Bid	Bcl-2 interacting domain
BSA	bovine serum albumin
° C	temperature in degree Celsius
C-	carboxyl
c	concentration or cleaved
Ca	calcium
CHX	cycloheximide
CM	calcium minus
CMEC	cardiac microvascular endothelial cells
C(T)	cycle threshold
CtxB	cholera toxin B subunit
Cy	carbocyanine
Da	Dalton
DEAE dextran	diethylaminoethyl dextran
dist. H_2O	distilled water
DICS	death-inducing signal complex
DMEM	Dulbecco's Modified Eagle Medium
DMSO	dimethylsulfoxid
DNA	deoxyribonucleic acid
dNTP	deoxynucleotide triphosphate
DRM	detergent resistant membrane
E. coli	*Escherichia coli*
EDTA	ethylenediaminetetraacetic acid
e.g.	*exempli gratia*, for example
EGF	enhanced growth factor
EGFP	enhanced green fluorescent protein
ER	endoplasmatic reticulum
et al.	*et altera*, and co-workers
EYFP	enhanced yellow fluorescent protein
FA	formaldehyde
FACS	fluorescence assisted cell sorting
FADD	Fas-associated death domain
FCS	fetal calf serum
FITC	fluorescein isothiocyanate
FPV	avian influenza virus A/Bratislava/79
fwd	forward
G	goat
g	gram or acceleration of gravity
GAPDH	glyceraldehyde 3-phosphate dehydrogenase
GFP	green fluorescent protein from *Aequorea victoria*
GM1	monosialotetrahexosylganglioside
GP	Generalised Polarisation

GPI	glycosylphosphatidylinositol
GPMV	giant plasma membrane vesicle
h	hour(s)
HA	hemagglutinin
HBV	hepatitis B virus
HCMV	human cytomegalovirus
HEPES	2-(4-(2-Hydroxyethyl)-1-piperazinyl)ethansulfonsäure
HIV	human immunodeficiency virus
HRP	horse reddish peroxidase
I	intensity
IAP	inhibitors of apoptosis
IAV	influenza A virus
ICT	internal charge transfer
i.e.	*id est*, that is
IF	immunofluorescence
IR	insulin receptor
l	litre
Laurdan	6-Dodecanoyl-2-dimethylaminonaphthalene
LB	Luria Bertani
l_d	liquid disordered
LE	locally excited
l_o	liquid ordered
LSM	laser scanning microscopy
M	molar
m	milli or meter or messenger
µ	micro
M1 / M 2	matrix protein 1 / matrix protein 2
MDCK	Madin Darby canine kidney
MEM	minimum essential medium
MES	2-(N-morpholine)-ethane sulphonic acid
min	minute(s)
MOI	multiplicity of infection
Ms	mouse
mut	mutant
MW	molecular weight
n	nano
N-	amino-
NA	neuraminidase
n.d.	not determined
NEP	nuclear export protein
NFκB	nuclear factor kappa-light-chain-enhancer of activated B cells
NLS	nuclear localisation signal
NP	nucleoprotein
NS-1	non-structural protein 1
OD_{xxxnm}	optical density at xxx nm
p	pico or phospho or plasmid
P	pellet
PA	acidic polymerase protein
PAG	polyacrylamide gel
PAGE	polyacrylamide gel electrophoresis
PARP	poly (ADP-ribose) polymerase
PB1 / 2	basic polymerase protein 1 / 2
PBS	phosphate buffered saline
PCR	polymerase chain reaction
PDGF	platelet derived growth factor
PFA	paraformaldehyde
PFU	plaque forming units
PHD	pleckstrin-homology domain
p.i.	post infection
PIC	protease inhibitor cocktail
$PI(4,5)P_2$	phosphatidylinositol-4,5-bisphosphat
PKC	protein kinase C

PLAP	placental alkaline phosphatise
PLC	phospholipase C
PM	p11 minus
PMS	plasma membrane sphere
POX	peroxidase
PR8	human influenza A/Puerto-Rico/8/34
PVDF	polyvinylidene fluoride
R	receptor
Rb	rabbit
rev	reverse
RNA	ribonucleic acid
RNP	ribonucleoprotein
ROS	reactive oxygen species
rpm	rounds per minute
RT	room temperature
s	second(s)
S	supernatant or state
SD	standard deviation
SDS	sodium dodecyl sulfate
si	small interfering
STS	staurosporine
TAE	Tris-acetate-EDTA
TCA	trichloro acetic acid
TE	Tris-EDTA-Puffer
TEMED	N,N,N',N'-tetramethylethylenediamine
Tet	tetracycline
TN	Tris NaCl
TNF	tumour necrosis factor
Tris	Tris(hydroxymethyl)aminomethan
TxRed	Texas Red
U	unit
v	viral
V	Volt
WB	western blot
wt	wildtype
YFP	yellow fluorescent protein
% (v/v)	volume percent per volume
% (w/v)	weight percent per volume

aa are abbreviated by the international one letter or three letter code.

7.2 Supplementary data

In the following the influenza A virus titres of the different infection experiments are presented.

Data for Figure 4-3:

		virus titre (PFU/ml)		virus titre in XM expressing MDCK
MOI	t (h)	Tet off	Tet on	compared to MDCK (%)
0.01	8	$1.4*10^4$	$1.1*10^4$	127
0.1	8	$1.1*10^5$	$1.1*10^5$	101
0.0001	24	$1.7*10^3$	$5.1*10^3$	33
0.0001	24	$3.4*10^3$	$1.4*10^3$	255
0.0001	24	$1.1*10^3$	$2.1*10^3$	51
0.001	24	$1.1*10^4$	$9.2*10^3$	118
0.001	24	$1.7*10^4$	$1.5*10^4$	117
0.001	24	$1.9*10^4$	$2.7*10^4$	70
0.1	24	$1.3*10^6$	$9.3*10^5$	145
0.1	24	$1.1*10^6$	$1.4*10^6$	79
0.1	24	$7.1*10^5$	$1.3*10^6$	54

Data for Figure 4-5:

		virus titre (PFU/ml)			virus titre in siRNA transfected HeLa compared to untransfected HeLa (%)	
MOI	t (h)	anxA2 siRNA	control siRNA	untransfected	anxA2 siRNA	control siRNA
5	6	$4.5*10^5$	$3.0*10^5$	$2.5*10^5$	180	118
20	6	$6.5*10^6$	$6.5*10^6$	$5.5*10^6$	119	118
20	6	$2.1*10^6$	$1.7*10^6$	$1.4*10^6$	156	122
1	8	$4.3*10^5$	$2.5*10^5$	$4.9*10^5$	89	52
5	8	$2.0*10^6$	$1.5*10^6$	$1.6*10^6$	124	92
5	8	$3.3*10^5$	$3.3*10^5$	$2.5*10^5$	132	130
0.01	16	$1.9*10^4$	$1.6*10^4$	$1.2*10^4$	158	129
0.1	17	$3.1*10^5$	$6.1*10^5$	$6.3*10^5$	48	97
0.1	16	$2.0*10^5$	$8.0*10^4$	$1.2*10^5$	161	64
0.1	16	$2.1*10^5$	$3.5*10^5$	$3.8*10^5$	55	92
0.5	17	$7.9*10^5$	$2.0*10^6$	$2.5*10^6$	32	80
0.5	16	$4.9*10^5$	$5.0*10^5$	$6.1*10^5$	80	82
0.5	16	$4.0*10^6$	$3.3*10^6$	$4.9*10^6$	81	67

Data for Figure 4-7:

		virus titre (PFU/ml)		virus titre in anxA2 siRNA transfected A549 compared to control siRNA transfected A549 (%)
MOI	t (h)	anxA2 siRNA	control siRNA	
1	8	$1.7*10^3$	$1.9*10^3$	92
1	8	$5.0*10^3$	$7.8*10^3$	65
1	8	$2.3*10^4$	$2.2*10^4$	107
5	8	$7.0*10^4$	$7.3*10^4$	97
0.01	24	$8.1*10^2$	$9.4*10^2$	87
0.05	24	$1.9*10^4$	$2.3*10^4$	82
0.1	24	$3.8*10^1$	$3.8*10^1$	100

Data for Figure 4-8:

A) PR8

		virus titre (PFU/ml)		virus titre in $A2^{-/-}$ CMEC compared to $A2^{+/+}$ CMEC (%)
MOI	t (h)	$A2^{+/+}$	$A2^{-/-}$	
0.3	8	$3.5*10^5$	$3.3*10^5$	95.1
0.1	16	$8.5*10^4$	$7.6*10^4$	89.4
0.1	24	$6.6*10^4$	$4.8*10^4$	72.8
0.1	24	$3.0*10^4$	$4.0*10^4$	134.9

B) FPV

		virus titre (PFU/ml)		virus titre in $A2^{-/-}$ CMEC compared to $A2^{+/+}$ CMEC (%)
MOI	t (h)	$A2^{+/+}$	$A2^{-/-}$	
1	8	$2.5*10^6$	$2.5*10^6$	99
1	8	$1.8*10^5$	$1.8*10^5$	99
0.1	16	$5.5*10^6$	$6.6*10^6$	121
0.1	24	$2.9*10^7$	$3.2*10^7$	111

Conference Presentations

09/2009 Annexin Meeting 2009 in Lacanau Océan, France
poster presentation: ”S100A10 regulates annexin A2 - raft association”
Sonja Schäfers, Nina Quiskamp, Michaela Poeter, Ali Reza Nazmi, Volker Gerke, Ursula Rescher

08/2009 EMBO Meeting 2009 in Amsterdam, Netherlands
poster presentation: ”S100A10 regulates annexin A2 - raft association”
Sonja Schäfers, Nina Quiskamp, Michaela Poeter, Ali Reza Nazmi, Volker Gerke, Ursula Rescher

06/2008 Summer School „Pathogen-Host Interactions at Cellular Barriers“, Münster, Germany
poster presentation: “Role of Annexin A2 in Influenza Virus Infection“
Sonja Schäfers, Christina Ehrhardt, Stephan Ludwig, Volker Gerke, Ursula Rescher

03/2008 Joint Meeting with the graduate college 685 in Kleinwalsertal, Austria
oral presentation: ”Role of Annexins in Influenza Virus Infection“

Curriculum Vitae

Acknowledgements

This work would not have been possible without the help of a lot of very special people whom I want to thank here. Many thanks to

- Prof. Dr. Volker Gerke for the opportunity to work in such an interesting field, for his professional advice and helpful discussions and the correction and evaluation of my thesis.
- PD Dr. Ursula Rescher for her excellent professional assistance and helpful ideas, encouragements, discussions and corrections that were indispensible for my work.
- Prof. Dr. Stephan Ludwig for the opportunity to work in cooperation with his lab, for the helpful discussions and advices, for being a member of my triumvirate and for the evaluation of my doctoral thesis.
- Prof. Dr. Berenike Maier for being a member of my triumvirate and for being an examiner of my thesis defence.
- my co-workers at the Institute for Medical Biochemistry, especially my colleagues from lab 0.77 and from Ursula's group - for the good atmosphere, their technical help and a nice time in the lab and outside of the lab.
- the members of the Institute of Molecular Virology for sharing their bench-time with me, for their help and assistance concerning the flu experiments and for a nice working atmosphere in their lab.
- PD Dr. Thomas Grewal for giving me the opportunity to work in his lab at the Faculty of Pharmacy, University of Sydney, for 3 months. I very much appreciate his professional assistance and the helpful discussions. Furthermore, I want to thank Peta Wood for excellent technical help and a great working atmosphere in the lab and a nice time in Sydney.
- Prof. Dr. Katharina Gaus, Cellular Membrane Biology Lab, Centre for Vascular Research, University of New South Wales, and the members of her lab, especially Astrid Magenau and Dr. Carles Rentero. I was able to learn and perform the Laurdan measurements in their lab and am thankful for their technical help and assistance with the evaluation of the data. A special thanks to Carles for the correction of the Laurdan part of this thesis.
- Daniel Lingwood, MPI Dresden, for his help with the PMS experiments.
- Dr. Waltraud Walz-Schmidt and Prof. Dr. Alexander M. Schmidt for the excellent organisation of the graduate school "Molecular Interactions of Pathogens with Biotic and Abiotic Surfaces".
- last but not least my family and friends who always were there for me during my PhD years.